The Development of a Screening Model for the Arthur R. Marshall Loxahatchee National Wildlife Refuge

A Thesis

Presented to the

Graduate Faculty of the

University of Louisiana at Lafayette

In Partial Fulfillment of the

Requirements for the Degree

Master of Science

William B. Roth

Fall 2009

The Development of a Screening Model for the Arthur R. Marshall Loxahatchee National Wildlife Refuge

William B. Roth

APPROVED:

Ehab Meselhe, Chair Professor of Civil Engineering	Jim Lee Professor of Engineering
Don Hayes Professor of Civil Engineering	Michael Waldon U.S. Fish and Wildlife Service Arthur R. Marshall Loxahatchee National Wildlife Refuge
C. E. Palmer Dean of the Graduate School	

Acknowledgments

I would like to express my gratitude to all of those individuals who have contributed to the success of this project. Dr. Ehab Meselhe, my thesis director, provided me with his expertise, guidance, and support throughout my undergraduate and graduate research career. Also, Dr. Michael Waldon, with the Arthur R. Marshall Loxahatchee National Wildlife Refuge, contributed his experience with and knowledge of the Refuge to the data analysis and modeling. Special thanks is also due to the remaining members of my defense committee, Dr. Donald Hayes and Dr. Jim Lee, both of whom provided perspective and constructive criticism during the final stage of my thesis preparation. Additionally, thank you to the other members of the Center for Inland Water Studies, to the employees of the Refuge, to Dr. William Walker, and to Dr. Robert Kadlec. Lastly, I would like to thank my wife, Stephanie, who supported my decision to earn a Master's degree, and her continued encouragement was instrumental to its successful completion.

Financial support for this project is given through the United States Fish and Wildlife Service (DOI). All data for this project were obtained from the South Florida Water Management District database DBHYDRO, the United States Geological Survey SOFIA website, the University of Florida IFAS program, and the Village of Wellington – ACME Drainage District. The findings and conclusions in this document are those of the author and do not necessarily represent the views of the U.S. Fish and Wildlife Service.

Table of Contents

List of Figures

List of Tables

1 Introduction

As a result of restoration efforts, the Everglades wetlands have become a focal point for advancing the hydrological, ecological, and environmental sciences. Specifically, many studies have been aimed at modeling hydrologic processes and the fate and transport of nutrients. These tools are developed to supplement the trends that can be observed from historical data. Additionally, they provide an opportunity to forecast a system's response to certain physical, hydrologic, or water quality alterations. Modeling also provides further analysis of observed data by indicating the weaknesses of sample timing and spatial resolution. Lastly, for systems subject to water management schedules, a model can help optimize pumping and water delivery schemes necessary to meet demands.

Regional models (Fitz et al., 2002; MacVicar et al., 1984; Munson et al., 2002; Raghunathan et al., 2001) of the Everglades are usually of considerable scale, and resulting from coarse model grid resolution, the dynamics of a particular region may not be fully represented. Therefore, other smaller scale models have been developed for water conservation areas (WCAs) (Arceneaux et al., 2007; Lin, 1979; Richardson et al., 1990; Wang et al., 2009; Welter, 2002), stormwater treatment areas (STAs) (Walker, 1995; Walker and Kadlec, 2008), coastal mangrove forests (Twilley and Chen, 1998), or other areas of interest. Whatever the focus, the models have traditionally been implemented in a closed source fashion, where development could not extend beyond pre-established solution methods, parameter sets, governing equations, and water quality modules.

In its Collaborative Planning Toolkit, the United States Army Corps of Engineers (USACE) cites a group of modeling software that is appropriate for analyzing system response, studying alternatives, and optimizing decision making strategies (USACE, 2008). These proprietary software packages (STELLA[1], Berkeley Madonna[2], and others) offer tested finite difference solution methods (e.g., Euler, Rosenbrock, Runge-Kutta) for ordinary differential equations (ODEs). The computational engine of these programs is paired with a graphical user interface, allowing for immediate post-processing of a simulation. Additionally, some packages provide algorithms for optimization and curve fitting. This combination of resources simplifies the process of model development, calibration, revision, and validation.

These software packages have been used in many wetlands-based hydrological modeling efforts. Zhang and Mitsch (2005) successfully applied the STELLA 7.0 software package to produce an integrated systems model of the Olentangy River Wetland Research Park in Columbus, Ohio, which utilized the software's interactive tools to control flows and other components throughout a simulation. Similarly, Twilley and Chen (1998) modeled a mangrove forest in Rookery Bay, Florida using STELLA II software. Their results were verified by a separate model code written in C. Such a comparison between a closed source solution method and an independent open source code reinforced the validity of the software. Moreover, in an effort to quantify the differences between popular systems-based modeling environments, four packages (STELLA, Berkeley Madonna, GoldSim[3],

[1] www.iseesystems.com
[2] www.berkeleymadonna.com
[3] www.goldsim.com

and Simulink[4]) were tested and verified by Rizzo et al. (2006). This effort sought to recreate, with each software, a Surface Wetness Energy Balance (SWEB) model that was initially formulated in Microsoft Excel[5]. Performance for each software package was measured based upon its root mean square error (RMSE) from the original simulation. The results from each model were within a reasonable error range for this and other tests. Lastly, in an effort to expand the applicability of the ODE solvers, Holzbecher and Horner (2003) quantifies the ability of these products to approximate partial differential equation (PDE) solutions.

The modeling effort presented here is a continuation of the work done by Arceneaux et al. (2007), who presented a 2-compartment approach to modeling the hydrology of the Arthur R. Marshall Loxahatchee National Wildlife Refuge (Refuge). This model was programmed into a Microsoft Excel spreadsheet, and simulated a 10-year period from January 1, 1995 to December 31, 2004. The compartments are based on the two unique features of the Refuge, rim canal and interior marsh. Each compartment is defined with an average soil elevation and assumes a flat bottom. The difference in scale between the marsh and canal forced Arceneaux et al. (2007) to implement an ad-hoc method to transfer water between the compartments during periods of high exchange flow. Additionally, results from this model were used to drive a water quality model for chloride and total phosphorus assembled in the U.S. Environmental Protection Agency software WASP 7.0[6], where

[4] www.mathworks.com/products/simulink
[5] office.microsoft.com/en-us/excel
[6] http://www.epa.gov/athens/wwqtsc/html/wasp.html

chloride and total phosphorus were modeled as a conservative constituent and with apparent settling, respectively.

Now termed the Simple Refuge Screening Model (SRSM), version four represents an initial use tool for Refuge management. Its development beyond previous versions has allowed for (1) definition of a stage-discharge relationship for calculated outflow, (2) implementation of the P-Cycling equations per Walker and Kadlec (2008), and (3) implementation of a Monod relationship to approximate Sulfate dynamics (Waldon et al., 2009). Water budget model sensitivity remains for those parameters discussed by Arceneaux et al. (2007) in the documentation for the first version of the SRSM. Additionally, further development of SRSM has allowed for a single, suitable modeling environment to be developed. The Microsoft Excel model was limited in its ability to be expanded beyond the 10-year period of simulation, and the WASP model only allowed for pre-programmed constituent modules to describe nutrient cycling. The initial iteration of the SRSM water budget was developed in STELLA, and while the software was capable of reproducing the results from the previous version, it imposed a restriction on the amount of time steps available for each model run. With the time step value required to run the SRSM, only a half-year model simulation could be performed. This software limitation prevented the SRSM from easily performing long term analyses, and thus required re-investigation of a new modeling platform.

The current version has both the hydrodynamic and constituent transport models programmed into Berkeley Madonna (Macey et al., 2004). This software allows for users to implement models in either a graphical, object-based, environment or an equations

editing window, the SRSM uses the latter. The equations editor of Madonna allows users to self-document model code and to have full control over all state variables, their parameters and solution method, imported datasets, pre-programmed functions, etc. Additionally, the flexibility of the Madonna environment allowed multiple kinetic formulations for constituent fate and transport to be programmed and tested. Such applications would not have been convenient or possible with the previous setup of the SRSM.

1.1 Background

The Arthur R. Marshall Loxahatchee National Wildlife Refuge (Refuge) is a soft-water remnant of the Northern Everglades ecosystem. Located in Palm Beach County, this wetland system is roughly 143,238 acres and is one of the many areas under the umbrella of restoration proposed in the Comprehensive Everglades Restoration Plan (CERP). This effort strives to restore areas damaged by drainage and reclamation started over 150 years ago, and is specifically aimed at regulating the quantity, quality, and timing of flows through the Everglades ecosystem; the progression of overland flow through the Everglades over time is given in Figure 1. Management, maintenance, and monitoring for the Refuge are spread across the public and private sector. The cooperation of all concerned is paramount to the success of Everglades restoration.

The Swampland Act of 1845 and the 1907 Everglades Drainage Act began an extensive effort to utilize the Everglades for development. Such tremendous man-made changes to the system have altered what once was a ridge and slough landscape flooded by sheet flow from Lake Okeechobee (Fling et al., 1994). Then in the 1940s the U.S. Army Corps of

Engineers (USACE) continued by creating 3 water storage areas to meet the demands of the agriculture industry and to set the stage for further urban development (USFWS, 2000). These areas are called Water Conservation Areas (WCA) and have become central to what is one of the most comprehensive wetlands restoration projects in history (Fling et al., 1994 and Dineen and Light, 1994).

The WCAs were initially placed under the control of the Central and Southern Florida Flood Control District (C&SF FCD), now the South Florida Water Management District (SFWMD). An agreement between the SFWMD and the U.S. Fish and Wildlife Service (USFWS) in 1951 under the Migratory Bird Act saw the creation of the Refuge on the land overlaying WCA-1. This area, along with the other two, is part of the larger Kissimmee-Okeechobee-Everglades watershed. However, with the construction of levees, an interior borrow canal, and water regulation and diversion structures, WCA-1 is now hydraulically isolated from this watershed (Richardson et al., 1990).

1.2 Site description

There are two major landscape features of the Refuge, marsh and rim canal. These two sections are vastly different in terms of habitat and geometry, but each depends upon the health of the other, making the Refuge a unique ecosystem. According to the USFWS (2000), the Refuge's vegetation includes six distinct areas: sloughs, wet prairies, saw grass areas, tree islands, cattail stands, and cypress swamps. Those parts of the Refuge with sloughs and wet prairies represent the areas contributing to the natural sheet-flow, as they are typically inundated; sloughs, however, are the deeper of the two. Saw grass areas and tree islands are, by contrast, those not prone to inundation; typically, tree islands are

surrounded by patches of saw grass. Additionally, dense stands of cattail occur in those areas with high nutrient concentration (e.g., wading bird habitats or canal inflow sites). Lastly, the areas of cypress swamp are localized to the east side of the Refuge and represent the last remnant of a prolific vegetative community extending from Lake Okeechobee in north Palm Beach County to Fort Lauderdale in Broward County (Lodge, 1994).

The overall Refuge topography is flat with an average interior marsh elevation of 4.62 m (NGVD 29). The natural flow pattern of water through the Refuge is north to south, owing to the mild ground slope of roughly 1.58 cm per km; additionally, the east to west marsh bathymetric profile is nearly flat (Meselhe et al., 2005). Three canals (L-7, L-39, and L-40) border the Refuge, isolating it from the surrounding areas (Figure 2). Taken as a single entity, the perimeter canal is roughly 100 km long, has a cross section that varies along its length, and has an average depth of 3.24 m (NGVD 29).

The hydrologic cycle of the Refuge depends on regulated water flows and natural processes. There are 19 structures (both inflow and outflow) along the perimeter canal of the Refuge, and their locations are shown in Figure 2. The operation of outflow or release structures is based on an idealized regulation schedule (Figure 3) developed by the USACE (1994). This plan for the water control structures attempts to regulate stage in the Refuge so as to maximize the benefits of flood control, water delivery, fish and wildlife, and saltwater intrusion prevention (USFWS, 2000). USACE (1994) and USFWS (2000) provide further descriptions of the regulation schedule and its implementation for the Refuge.

Precipitation in the Everglades region helps drive all other hydrologic processes. The rainfall is a result of frontal, convective, and tropical system-driven events (Abtew et al., 2005). Additionally, Abtew et al. (2005) performed a long-term precipitation study in south Florida, a "high-rainfall region," and found that the annual average is 134.1 cm. Typically, June is the wettest month and December is the driest, with the wet season (June to October) accounting for 66% of the annual rainfall; Palm Beach county also has the highest rainfall amount of all south Florida regions (Abtew et al., 2002 and Abtew et al., 2005). Meselhe et al. (2005) performed a 10-year analysis for the Refuge (1995-2004), and found June to be the wettest month with an average of 19.6 cm and December to be the driest month with an average of 4.6 cm.

Throughout the Everglades region, evapotranspiration (ET) is another significant component of the hydrologic cycle. German (2000) conducted a comprehensive regional analysis of ET in the Everglades. The yearly average value of ET in the Everglades is usually greater than 101.6 cm. Also, German (2000) found the mean annual ET to be dependent on the median water depth of the gage site. Lastly, ET was found to be subject to seasonal variation, with the lowest values occuring from December to February and the highest values occurring from May to August.

1.3 Site data assessment

A wealth of observed data is available throughout the Refuge. A heavily monitored area such as this can be termed "data rich" (Arceneaux et al., 2007). With so much available information, there comes the ability to increase the knowledgebase through data analysis and numerical modeling. The analysis presented by Meselhe et al. (2005) sought to

provide an overview of all available data for the Refuge and cite those organizations responsible for its collection and dissemination. This document was consulted exclusively in the data acquisition process for the SRSM.

1.3.1 Boundary data

The period of study for this project is 14-years and 6-months (January 1, 1995 to June 30, 2009), which is a multiyear extension from the previous modeling effort done by Arceneaux et al. (2007). The data required for model simulation are outflow (m^3/day), inflow (m^3/day), constituent concentrations (mg/L), precipitation (m/day), and ET (m/day). Unless expressly stated, all data are downloaded from the SFWMD's DBHYDRO[7] database. Meselhe et al. (2005) specifies the particular time series available for both surface water (hydraulic structure flow, precipitation, ET, etc.) and water quality from this database. Also, this document specifies which surface water datasets have been quality assured by the SFWMD; these time series are denoted "PREF" in the Recorder field of the database and should be used for model calibration and validation. Also, each time series from a gage is given a unique identifier called a DBKEY. Only one will be PREF data, but data from other DBKEYs can be used to fill missing days from the PREF time series. Meselhe et al. (2005) evaluates each data set from DBHYDRO and describes how to fill gaps in a time series.

[7] http://my.sfwmd.gov/dbhydroplsq

1.3.1.1 Hydraulic structure flow

There are four types of flow data used in the SRSM. One set represents all historic inflow to the system; whereas, the rest are outflow. The three different types of outflow in the SRSM are: historical, water supply (S-39), and emergency hurricane release (S-10ACD). Table 1 gives the operational period, flow direction, and total flow for each structure. The cumulative values for historic inflow and outflow are 8912.4 hm^3 and 8528.1 hm^3, respectively; their difference is 4.3% of the inflow. Cumulative values for each year are given in Figure 4. Lastly, G-338 is officially labeled as an outflow structure; however, a value for cumulative inflow is given in Table 1. This inflow volume is insignificant and is assumed to be the result of necessary maintenance to the structure.

The only dataset not directly downloaded from DBHYDRO is the water supply release from the S-39 structure; this time series is approximated based on the stage measurement at the 1-8C gage and Regulation Schedule. The difference between the measured stage and the A-1 Floor of the regulation schedule is calculated; those days with a difference less than -8.53 cm (Zone B) are deemed water supply releases. The total number of water releases from the S-39 during this period is 2552. Based on the tolerance set above, 52% of these releases were in accordance with the schedule; the remaining 48% were for water supply. However, the amount of water differs. A total of 1,800 hm^3 was released for the entire period, with 67% resulting from scheduled releases and the remaining 33% for water supply. Additionally, data for emergency releases are needed for the 2004 and 2006 hurricane seasons, as the model cannot approximate these values.

1.3.1.2 Hydraulic structure constituent load

Dynamics for three constituents are approximated by the SRSM, chloride (CL), total phosphorus (TP), and sulfate (SO4). Therefore, it is necessary to calculate the loading rate for each constituent at each inflow site. In the model each flow control structure, inflow and bidirectional, has a water quality monitoring site paired with it. Different measurement types are available from DBHYDRO; those used for this project are grab and auto-composite samples. Grab samples are available for all three constituents, whereas auto-composite samples are only available for TP. Both methods of sampling give concentration measured in mg/L (g/m^3). When available, composite values are preferred, as the sample value is assumed constant for an entire 14-day period preceding a measurement. Grab samples differ in that they occur on an irregular basis. Table 2 provides a summary of the flow and concentration measurement sites used for load calculation; also provided are average values for the period of study. As evinced by the table, some flow sites do not always have a water quality station directly paired with it. In this case a nearby station is used. Additionally, sulfate measurements are not available from the G-301 water quality site; therefore, S-5A values are substituted as needed. Meselhe et al. (2005) performed a comprehensive analysis of available chloride and total phosphorus data for 1995-2004; this document is considered when evaluating boundary data for sulfate as well.

Time series are built based on coincidence of constituent measurements and inflow events. Those days having both constituent measurement and inflow event will use those exact values to calculate the loading rate into the Refuge. For those days where flow occurs

without a concentration measurement, a linear interpolation from the nearest constituent values gives the concentration necessary to calculate the load such that

$$L = cQ \tag{1}$$

where L is constituent load (g/d), c is constituent concentration (g/m^3), and Q is flow rate (m^3/d). In this way, time series made with grab and composite samples are the same; however, composite sample values, as stated above, are held constant for 14 days. Therefore, any flows taking place during this window will be assigned the same concentration value.

Using the above methods, loads for each constituent are calculated on a yearly basis. Such values provide a global understanding of the constituent transport to and from the Refuge. Additionally, the percentage of mass retained in the Refuge is calculated by dividing the difference of the inflow and outflow loads by the total inflow load. The average yearly net mass loads for CL, TP, and SO4 are 23,503 MT, 25 MT, and 7,819 MT, respectively, where MT stands for metric tons (10^3 kilograms). The average percent mass retained for CL, TP, and SO4 is 33%, 42%, and 35%, respectively. The previous values are calculated using 1995-2008 values, as only six months of 2009 are used in this analysis. The following set of figures (Figures 5, 6, and 7) and tables (Tables 3, 4, and 5) outline the yearly loads for all three constituents.

1.3.1.3 Precipitation

Precipitation data are downloaded from the Meteorological Data section of the DBHYDRO database. These data are also subject to the QA/QC "PREF" labeling stated above;

Meselhe et al. (2005) provides research on which DBKEY data should be used for analysis. There are 9 gages used to estimate daily average precipitation for the Refuge S-5A, STA1W, S-6, WCA1ME, LOXWS, S-39, Gage 6, Gage 8, and Gage 10 (Figure 8).

The latter three stations are located outside the eastern border adjacent to the Refuge in the Village of Wellington in ACME drainage basin B. The STA1W gage is located on the western side in the former Everglades Nutrient Removal Program (ENRP) area. The remaining stations are located within or on the boundary of the Refuge. Table 6 gives the available precipitation data for the period of study in the Refuge.

Time series for the SRSM represent area-averaged precipitation for each event and are constructed using the Thiessen Polygon Method, which weights the precipitation from each gage based upon its area of influence and assumes that the rainfall received at any point in the watershed is equal to that of the nearest gage (Chow et al., 1988). Missing data for precipitation events prompted Arceneaux et al. (2007) to use 17 different Thiessen Polygon scenarios generated with ArcGIS 9.0 to complete the area-average time series for the 1995-2004 period. Figure 8 shows an example Thiessen Polygon scenario. This method is used to extend the period of study to the middle of 2009. Figures 9 and 10 visualize yearly and monthly averages, respectively, of area-averaged precipitation for the Refuge.

1.3.1.4 Evapotranspiration

ET data are downloaded from the Meteorological Data section of the DBHYDRO database. There is one gage used to estimate daily ET for the Refuge: STA1W, formerly the Everglades Nutrient Removal Program (ENRP) area. This site directly measures ET using

a lysimeter. German (2000) concludes that ET does not vary considerably across the entirety of the Everglades; therefore, it is reasonable to use a single gage reading for the Refuge. However, local effects of ET, such as vegetation type and water depth, are present across the Refuge. Both are described in the Model Development section. Yearly and monthly averaged ET values are plotted in Figures 9 and 10, respectively.

1.3.2 Water levels

The previous sections discuss those parameters directly affecting the water level in the Refuge. Daily variation in the water surface elevation is measured within the marsh interior and rim canal by six continuous recording gages. Five of these gages are spread throughout the marsh (North, South, 1-7, 1-8T, and 1-9); the remaining gage (1-8C) is located on the east side of the Refuge in the L-40 canal (Figure 11).

The latter four devices measure the stage (ft) with respect to the National Geodetic Vertical Datum of 1929 (NGVD 29), and all data are available from DBHYDRO. The first two, North and South, are referenced to the North American Vertical Datum of 1988 (NAVD 88). Meselhe et al. (2005) should be consulted when aggregating these data, as multiple time series are available for most gages. Table 7 summarizes the data record for each gage. The average measured values for the marsh and canal are 4.86 and 4.96, respectively.

1.3.3 Water quality monitoring sites

Data for model assessment are available from water quality monitoring sites within the Refuge. Meselhe et al. (2005) placed these sites into five categories: (1) Everglades protection area (EVPA), (2) “enhanced,” (3) District Transect (XYZ), (4) hydraulic

structure, and (5) independent monitoring. The first four types will be discussed in this report. Table 8 displays the periods of availability for these monitoring sites. The Enhanced, EVPA, and Structures types may all be downloaded from DBHYDRO; the XYZ sites are available upon special request to the SFWMD. Additionally, Table 9 displays the maximum, minimum, and average values for chloride (CL), total phosphorus (TP), and sulfate (SO4). Figures 12 and 13 plot monthly and yearly averages of canal concentration for all three constituents; similarly, Figures 14 and 15 plot monthly and yearly averages of marsh concentration for all three constituents.

For some months a single station could have more than one measurement value. The arithmetic average of these values is taken and is used to represent the whole month. Table 24 in the appendix of this document cites canal structures where coincident measurements are present. Additionally, several high values are removed from the data and declared outliers based on visual observation of station time series. Arceneaux et al. (2007) compared these extreme values with the conductivity measurements reported on the same day to assure that each value is indeed an outlier. Those values that are removed from the data set are given, along with the method used for comparison, in the appendix.

The data downloaded from DBHYDRO also include days where the concentration is below the minimum detection limit (MDL). When the constituent concentration falls below the limit, the database reports the negative value of the MDL; these values vary by site. For analysis purposes, half of the absolute value of the MDL is taken when necessary. During the data period, there are 53 and 477 days with negative values for total phosphorus and

sulfate, respectively. There are no chloride values falling below the MDL for the data period.

1.3.3.1 EVPA stations

There are fourteen EVPA gages spread throughout the Refuge (Figure 16) interior marsh; all were operational for the period of study. These monitoring sites were established to monitor the physical, chemical, and biological quality of the marsh. For CL, TP, and SO4 sampling is done on a near-monthly basis; however, four months during the period of study do not have measurements for CL or SO4. All other months have at least one station reporting a measurement. The average number of measurements per site for TP, CL, and SO4 is 143, 125, and 126, respectively.

1.3.3.2 Enhanced stations

The monitoring sites in the Enhanced program do not begin reporting until mid-2004. There are thirty-nine stations spread throughout the Refuge, four of which (A104, A115, A129, and A135) measure concentrations in the rim canal. As can be seen in Figure 16, the Enhanced program contribution nearly doubles the amount of measurements taken previously in the Refuge. The average number of measurements per site for TP, CL, and SO4 is 40, 40, and 38, respectively.

1.3.3.3 XYZ transect stations

The eleven XYZ stations were set up by the SFWMD along what was believed to be a nutrient gradient and are displayed in Figure 16 (Meselhe et al., 2005). The average numbers of samples per site are 145, 130, and 129 for TP, CL, and SO4, respectively. Two

of these stations (X0 and Z0) are in the perimeter canal, while the remaining nine step gradually into the marsh. All samples taken at these sites are Grab type samples. Table 10 gives a summary of the averages for the period of study of each gage; it is clear that there is a reduction in concentration with increasing distance from the rim canal. Figure 17 shows the gradient of the arithmetic average of constituent concentration.

1.3.3.4 Hydraulic structure stations

Those hydraulic structures in Table 1 labeled as Outflow, with the exception of G-94A, are used for assessing model predictions in the canal. The maximum, minimum, and average values are given for each constituent in Table 9 under the "Structure" heading. All samples from these sites are of the Grab type. Additionally, these measurements, along with those from the EVPA sites in the marsh, provide the most complete set of water quality data for the canal. However, since the majority of these sites are in the southern portion of the Refuge, the measurements prior to the start dates of the XYZ and Enhanced programs may introduce some bias.

2 SRSM (v 4) method and implementation

The conceptual framework of version 4 of the SRSM remains unchanged since version 1 which was implemented by Arceneaux et al. (2007). However, the computational method differs, as do the kinetic formulations for sulfate and phosphorus. Comparisons between the original version and version 4 one are provided here.

2.1 Water budget model development

The water budget model component of the SRSM aggregates the Refuge into its two distinct areas, rim canal and interior marsh. The canal is roughly 100 km long and has a surface area of 4.03 km^2; additionally, the surface area for the entire marsh is 560 km^2. A schematic for the 2-compartment water budget is given in Figure 18.

The only connection between the canal and marsh compartments is through exchange flow, Q_{mc}. A model such as this is similar to the level pool routing technique described by Chow et al. (1988). Other model assumptions include that (1) the marsh and canal both have a flat water surface, (2) the marsh and canal compartments are characterized by average soil elevations (NGVD 29) 4.62 m (15.16 ft) and 3.24 m (10.63 ft), respectively, and (3) the surface area of each compartment is constant. The average soil elevations were used by Arceneaux et al. (2007) in the first version of the SRSM. These values are obtained from bathymetric data of the Refuge collected by Daroub et al. (2002) for canal cross sections and Desmond (2003) for the marsh.

Initial conditions for water budget simulation represent measured values on the start day, January 1, 1995. The initial canal stage is obtained from gage 1-8C on the eastern side of

the Refuge and has a value of 5.24 m (17.19 ft). The initial marsh stage is given by the arithmetic average of gages 1-7 and 1-9; the initial value for the marsh is 5.23 m (17.16 ft).

The SRSM water budget two state variables account for compartment volume (m^3) as a result of the change in storage caused by various hydrologic abstractions seen in Figure 18. The governing equations for canal and marsh rate of volume change are given in 2 and 3, respectively. The ordinary differential equations are solved with the Berkeley Madonna software using the fourth order Runge-Kutta solution technique. A time step of 0.005 day, or 7.2 minutes, was found to be adequate to obtain reliable simulations. The rate of change of volume in the canal and marsh compartments is given by

$$\frac{dV_c}{dt} = Q_{in} - Q_{out} - Q_{mc} + A_c \cdot \left(P - ET_c - G_c\right) \quad (2)$$

where t is time (day), V_c is volume of the canal compartment (m^3), Q_{in} is structure inflow into the Refuge (m^3/day), Q_{out} is structure outflow from the Refuge (m^3/day), Q_{mc} is exchange flow from the canal to marsh (m^3/day), A_c is canal surface area (m2), P is precipitation (m/day), ET_c is evapotranspiration from the canal compartment (m/day), and G_c is the groundwater seepage rate for the canal compartment (m/day) and

$$\frac{dV_m}{dt} = Q_{mc} + A_m \cdot \left(P - ET_m - G_m\right) \quad (3)$$

where t is time (day), V_m is volume of the marsh compartment (m^3), Q_{mc} is exchange flow from the canal to marsh (m^3/day), A_m is marsh surface area (m^2), P is precipitation (m/day),

ET_m is evapotranspiration from the marsh compartment (m/day), and G_m is the groundwater seepage rate for the marsh compartment (m/day).

2.1.1 Boundary time series

Inflow data, as described in the above section, are used directly from DBHYDRO, and are input to the SRSM separated by structure. The outflow can either be historic data similar to the aforementioned inflow or calculated based upon the stage in the canal; the latter is described in the section concerning calculated model parameters. Observed precipitation values are aggregated from the nine gages listed above by using the Thiessen Scenarios compiled by Arceneaux et al. (2007). Lastly, ET measurements from STA1W are used to directly remove water from the canal compartment (ET_c); whereas, ET is reduced with depth in the marsh compartment such that

$$ET_m = f_{ET} \cdot ET_{obs} \tag{3}$$

where f_{ET} is a reduction factor and ET_{obs} is observed data from STA1W. The reduction parameter f_{ET} is given as

$$f_{ET} = MAX\left[f_{ET\_min}, MIN\left(1, \frac{H}{H_{ET}}\right)\right] \tag{4}$$

where f_{ET_min} is the minimum allowable reduction of ET with depth (20%), H is marsh water depth (m), and H_{ET} is the threshold depth for ET reduction (0.82 m). In the event that the marsh stage drops below the average soil elevation, H is assigned a value of 0. This method was calibrated by Arceneaux et al. (2007) in version 1 of the SRSM.

2.1.2 Calculated model parameters

Calculated model outflow for the S-10A, S-10C, S-10D, and S-39 structures is based upon the regulation schedule described above. A rating curve was derived from observed outflow at the S-10 structures and the distance of the observed stage measurements at the 1-8C gage from the A-1 floor of the regulation schedule. Figure 19 shows the rating curve as a relationship of stage distance to outflow. The SRSM uses this rating curve as a lookup function to estimate the combined regulatory outflow for the S-10 structures. A scaling factor, based upon a long-term average, is used to increase this value to incorporate the regulatory release from S-39.

The exchange flow between the two model compartments is calculated using a stage difference equation similar to a weir equation. This relationship is based upon the Power Law described by Kadlec and Knight (1996) and is taken directly from the first version of the SRSM. The equation calculates a flow exchange such that

$$Q_{mc} = CH^3\left(E_c - E_m\right) \tag{5}$$

where Q_{mc} is the exchange in water volume from the marsh to the canal (m3/day),

$$C = \frac{BW \cdot 10^7}{R}, \tag{6}$$

B is a calibrated transport coefficient (30/m/d), W is the average marsh width (81,500 m), R is the length of exchange (13,000 m), E_c is the calculated canal stage (m), and E_m is the calculated marsh stage (m).

Groundwater seepage from the rim canal and from the interior marsh compartments is described by a seepage coefficient multiplied by the difference between the calculated stage (marsh or canal) minus an assumed static exterior boundary stage

$$G_i = seep_i \left(E_i - E_b \right) \quad (1)$$

where i is the marsh or canal compartment, G_i is the calculated seepage rate (m/day), $seep_i$ is the seepage rate coefficient (1/day), and E_b is the boundary stage (3.5 m). The seepage rate coefficient was estimated to be 0.0001315 (d^{-1}) and 0.042 (d^{-1}) for the marsh and canal compartments, respectively, in the SRSM version 1 calibrated by Arceneaux et al. (2007). Further calibration of the SRSM resulted in an alteration in the marsh seepage constant to a value of 0.00025 (d^{-1}). This re-calibration is discussed in section 2.3.

2.2 Model performance measures

The SRSM's capability, both for calibration and validation, is based upon 7 statistical performance measures: bias, standard deviation, root mean squared error (RMSE), correlation coefficient (R), coefficient of determination (R^2), variance reduction, and Nash Sutcliffe efficiency (E). Each measure compares an aspect of the model predictions to observed data for the period of study. Each of these performance measures must be calculated using values with commensurable units; however, the latter four (R, R^2, variance reduction, and E) are dimensionless.

Bias is the difference of the average values of modeled and observed data (Montgomery et al., 2001). This value is given by

$$Bias = M_{avg} - O_{avg} \tag{8}$$

where M_{avg} is the average modeled value and O_{avg} is the average modeled value.

Standard deviation (σ) is calculated for the observed values (σ_o), modeled values (σ_m), and error (σ_r). Error, also called the residual (r), is calculated by subtracting the observed value from the modeled value. The general form of the standard deviation is given by

$$\sigma = \sqrt{\frac{\sum_{i=1}^{n}\left(X_i - X_{avg}\right)}{n-1}} \tag{9}$$

where X_i is the ith value of observed, model or error data, X_{avg} is the average value of observed, model, or error data, and n is the total number of observations.

Berry and Lindgren (1996) state that the root mean square error (RMSE) is the "typical" or "average" error to be expected. The RMSE from Legates and McCabe (1999) is calculated such that

$$RMSE = \sqrt{\frac{\sum_{i=1}^{n}\left(M_i - O_i\right)^2}{n}} \tag{10}$$

where M_i is the ith value of modeled data and O_i is the ith value of observed data.

Variance reduction is commonly reported as a percent, and in this case, gives a quantitative representation of how well the model output data follow the variations in the observed data. This statistic is calculated by

$$\text{Variance Reduction } = 1 - \left(\frac{\sigma_r}{\sigma_o} \right)^2 \tag{11}$$

σ_r = standard deviation of error (residual) and

σ_o = standard deviation of the observed data.

The correlation coefficient (R) is a dimensionless representation of the linear relationship between the observed and modeled data. Legates and McCabe (1999) calculate this value by

$$R = \frac{\sum_{i=1}^{n} \left[\left(O_i - O_{avg} \right) \left(M_i - M_{avg} \right) \right]}{\sqrt{\sum_{i=1}^{n} \left(O_i - O_{avg} \right)^2 \sum_{i=1}^{n} \left(M_i - M_{avg} \right)^2}}. \tag{12}$$

The coefficient of determination (R^2) gives a parameter that quantifies the goodness of fit between the observed data and modeled values to a best fit line, commonly used in linear regression. The value of the dimensionless parameter R falls in the range -1 to 1, with a value of 1 when there is a perfect positive linear dependence between modeled and observed values. The value of R^2 falls between 0 and 1. It is noted that R and R^2 are not affected by bias or scaling errors, and may therefore provide misleading measures of calibration if used alone.

Lastly, the Nash Sutcliffe Efficiency (E) gives a quantitative measure of the model's ability to predict the observed data; moreover, it is reflective of both the bias and the variance reduction. The upper bound of E is positive 1, indicating a perfect fit between modeled and observed data. A value of 0 indicates the model and the average value of the observed data are equal in their ability as predictors. E is bounded by negative infinity on the lower end; negative values suggest the model is an unreliable predictor. Legates and McCabe (1999) calculate efficiency by

$$E = 1.0 - \frac{\sum_{i=1}^{n}\left(M_i - O_i\right)}{\sum_{i=1}^{n}\left(O_i - O_{avg}\right)}. \qquad (13)$$

In addition to these performance measure statistics, diagnostic plots were used to evaluate model performance. Three types of diagnostic plots are presented in later sections: scatter, percent distribution, and residual.

2.3 Water budget model recalibration

The calibration parameters outlined by Arceneaux et al. (2007) for the SRSM version 1 are: transport coefficient (B), seepage rate constants for both compartments ($seep_i$), and the ET reduction factor (f_{ET_min}). Using historical outflow, these parameters were calibrated for SRSM version 1 for a 5-year period (Jan-95 to Jan-99), and validated using the 5-year period (Jan-99 to Jan-04). It is assumed with version 4 of the SRSM that the calibrations set by Arceneaux et al. (2007) still hold true for historical outflow; however, the

implementation of a regulated outflow model the model's ability to predict outflow as an added performance measure.

A comparison of annual cumulative historic and calculated outflow for the S-10 structures was used as an additional calibration measure. Figure 20 gives a bar chart with annual outflow totals plotted for the entire data period. From Figure 21, it is observed that the model has a positive bias in 8 out of 15 years, over-predicting the historical cumulative annual outflows. The average cumulative outflows for historical and calculated outflow are 6854 hm^3 and 7107 hm^3, respectively. The cumulative bias is 253 hm^3, or 17.4 hm^3/yr, or 3.7% of historic outflow. This bias is within the error typically associated with structure discharge estimation using rating curves (Ansar and Chen, 2009). This positive bias value represents 73% of the initial volume of the Refuge.

It was determined that more seepage loss in the marsh would, in addition, draw down the canal stage and decrease the amount of water leaving by calculated outflow. Results of the calibration can be seen in Figure 21; the original marsh seepage and new marsh seepage are denoted by (1) and (2), respectively. Cumulative calculated outflow is now 6777 hm^3, giving an error (-77 hm^3) that represents 22% of initial Refuge volume, or -1.1% of observed cumulative outflow. Lastly, the R and R^2 values for pre and post-calibration remained the same, 0.98 and 0.96, respectively.

2.4 Constituent models

Water quality has been of major concern for the maintenance and restoration of the Refuge. Historically, this was an area low in nutrient concentration and allowed indigenous flora

and fauna to thrive. However, changes in water quality have seen such communities suffer with exotic, invasive species beginning to upset the ecosystem.

Loading of phosphorus in surface water runoff, primarily from agriculture, enters the Refuge through stormwater pump stations (S-6 and S-5A, among others). Pumped discharges have caused increased levels of TP in the Water Conservation Areas; the amount of phosphorus deposited in rainfall and dry deposition has also increased near the EAA as a result of agricultural activities (e.g., burning cane fields, dust from agricultural operations) (Davis, 1994). Additionally, the Everglades Nutrient Removal Project (ENRP) completed in 1993 and subsequent completion of stormwater treatment areas (STAs), along with best management farming practices, has resulted in the reduction of surface water phosphorus concentration (USFWS, 2000). Regardless, the areas surrounding anthropogenic input sites have seen an increase in species indicative of elevated nutrients, particularly cattail, which invades areas originally populated with natural low-nutrient plant communities (Davis, 1994; Mitsch and Gosselink, 2007). Data analysis and modeling efforts are targeted at supporting the reduction of eutrophication.

Increases of SO4 in Refuge waters have allowed for increases in the production of methylmercury, which is the most bioaccumulative form of mercury (Krabbenhoft, 1996). Organisms ingest methylmercury much faster than they eliminate it. As a result, methylmercury accumulates in plants and travels upward through the food-chain. Sulfate-reducing obligate anaerobes, such as *Desulfovibrio* bacteria, are responsible for the methylation of mercury, which is an initial step toward water and organism contamination; moreover, the rate of sulfate reduction is highest in areas with low pH (Krabbenhoft, 1996

and Mitsch and Gosselink, 2007). Therefore, understanding the dynamics of sulfate over time in the Refuge affords managers the opportunity to test scenarios that reduce it and other contaminants.

The development and implementation of simple constituent models for the SRSM provides an assessment tool for Refuge managers that predicts the spatially aggregated impact of alternative scenarios on water quality. Moreover, these constituent models pave the way for developing more spatially complex models, because parameter testing and verification can be done quickly in the SRSM.

Each constituent model is based on a 4-compartment approach that aggregates the Refuge into concentric areas (Figure 22). This arrangement allows for constituent concentration to decrease with distance from the canal; a similar approach, but defining a different spatial aggregation, was used in the Refuge by Harwell et al. (2008) and Surratt et al. (2008) to analyze data showing the propagation of water from the canal to the marsh interior. The canal in the constituent model corresponds to the canal compartment defined in the water budget model. It is the most exterior compartment, and is designated as compartment 4. The remaining three areas comprise the marsh, and in aggregate correspond to the marsh compartment in the water budget model. The marsh compartments are numbered in ascending order moving toward the center of the Refuge. The widths of compartments 1 and 2 are 1 km and 3 km, respectively. Arceneaux et al. (2007) used the same approach to implement version 1 in WASP 7.0.

The marsh and canal compartments are defined with the same average soil elevations given above for the water budget model, 4.62 m and 3.24 m, respectively. This characteristic of the model gives each marsh compartment the same stage value (i.e. a flat pool assumption) and depth. Additionally, the canal surface area is independent of stage, and remains constant, 4.03 km^2; the surface areas for compartments 1, 2, and 3 are 89.36 km^2, 224.1 km^2, and 246.6 km^2, respectively. Exchange between marsh compartments is similar to a tidal prism calculation, where the exchange flow term (Q_{mc}) is weighted based upon the affected area. The flow weight for a compartment is the fraction of the exchange flow that enters the outer boundary of the compartment. The flow weights for the three marsh compartments are found with the respective compartment areas in Table 11. Fickian dispersion, as implemented in version 1, is not present in this version. Further description of this method can be found in Arceneaux et al. (2007).

Waldon et al. (2009) describes the general rate equations used for constituent reduction in the Refuge. Equation 14 outlines basic constituent transport in the Refuge compartments. The general equation for constituent fate and transport is similar to the water budget equations (Equations 1 and 2), as it is based upon a daily mass balance, with losses resulting from reaction or sediment interaction programmed as necessary.

$$\frac{dM_{i,j,k}}{dt} = qnet_{i,j,k} + a_{i,j,k} - g_{i,j,k} - r_{i,j,k} \qquad (14)$$

where *i* is the constituent (CL, SO4, TP), *j* is the compartment (1...4), *k* is the DMSTA calibration set (EM or PEW) TP only, *M* is the mass (g), *qnet* is the net mass loading by surface flow (g/day), *a* is the wet and dry aerial deposition (g/day), *g* is the seepage and

evapotranspiration loss (g/day), and *r* is the loss to reaction (Monod: SO4) or sediment interaction (DMSTA: TP) (g/day).

The water quality model is linked dynamically with the water budget model, which was not the case in version 1. The simulation time step of 0.005 day (7.2 minutes) gives reliable simulation of both the water budget and constituents. All parameters for model initialization and rate equations are given in Table 12.

The fraction of ET representing transpiration (35%) is a mechanism that removes constituent mass from the system. This method was previously used as a calibration parameter by Arceneaux et al. (2007); however, this ratio is not recalibrated for version 4 of the SRSM. A similar methodology of splitting ET into evaporation and transpiration is found in Andersen et al. (2001) and Zhang et al. (2002).

2.4.1 Chloride

Chloride is modeled as a conservative throughout the Refuge. However, chloride mass is lost to seepage and transpiration as described above. Arceneaux et al. (2007) used wet and dry deposition values (2.00 mg/L and 500 mg/m^2/yr, respectively) for calibrating version 1 of the SRSM. However, upon model reevaluation, it was deemed necessary to increase the dry deposition parameter from 500 mg/m^2/yr to 1136 mg/m^2/yr. However, this increase has very little affect on the overall model performance, as it results in a 0.45% change (5600 MT) to the total mass of CL entering the Refuge. Additionally, the time series for each compartment is largely unaffected; the marsh interior saw the greatest affect. The

maximum error is 2.1 mg/L and this represents 3% of the average concentration range for this compartment (67 mg/L).

Initial conditions for the concentration in each compartment represent the monthly average of all water quality sites within that compartment; values for January 1, 1995 in compartments 1, 2, 3, and 4 are: 71.5 mg/L, 30.0 mg/L, 12.19 mg/L, and 89.55 mg/L, respectively. Chloride mass transport is described such that

$$\frac{dM}{dt} = qnet + a - g \tag{15}$$

where M is the mass (g), $qnet$ is the net mass loading by surface flow (g/day), a is the wet and dry aerial deposition (g/day), and g is the seepage and transpiration loss (g/day).

2.4.2 Sulfate

Wang et al. (2009) applied the WASP model structure from Arceneaux et al. (2007) to estimate SO4 dynamics using an apparent settling model with a first order removal rate. This approach is similar to the TP modeling done by Arceneaux et al. (2007). Version 4 of the SRSM implements a Monod relationship to approximate SO4 dynamics (Waldon et al. 2009); the values for wet and dry deposition are consistent with those found in Wang et al. (2009), 1.0 mg/L and 138.2 mg/m^2/yr, respectively.

The Monod relationship introduces a maximum removal term R_{max}, which bounds SO4 mass leaving the system at high concentrations (zero order reaction rate); at intermediate concentrations, removal is reduced and subject to a half-saturation constant (k_{half}); at low

concentrations the removal rate becomes first order with a first order rate equal to R_{max}/k_{half}. R_{max} was estimated by Wang et al. (2009) based upon calibrated first-order apparent settling coefficients and the long-term average concentration for the entire marsh to be 14.4 g/m^2/yr. Based on limited calibration runs, the half-saturation value used here is 1 mg/L. The initial conditions for SO4 in compartments 1 to 4 are 19.55 mg/L, 6.18 mg/L, 1.21 mg/L, and 35.68 mg/L, respectively. The sulfate model is described such that

$$\frac{dM}{dt} = L - QC - \left[\frac{R_{Max} CA}{k_{half} + C} \right] \quad (16)$$

where M is the mass in the water column (g), L is the loading rate in the cell (g/day), C is the concentration of surface water (g/m^3), Q is the outflow (m^3/day), A is the area (m^2), R_{Max} is the maximum sulfate removal (g/m^2/yr), and k_{half} is the half saturation constant (g/m^3).

2.4.3 Total phosphorus

The DMSTA P-cycling model kinetic equations and parameterizations are used to simulate TP dynamics in the Refuge (Walker and Kadlec, 2008). Some processes other than the TP kinetics that are simulated in the DMSTA are not implemented identically in the SRSM (e.g., wetting/drying, ET reduction at shallow depth), and therefore the SRSM should not be considered simply an alternative implementation of the entire DMSTA model. Two calibration parameter sets (parameterizations) are used for comparison to observed values, pre-existent wetland (PEW) and emergent marsh (EMG). As defined by Walker and Kadlec (2008) PEW describes a constructed wetland with pre-established vegetation and

calcitic waters; additionally, EMG represents a marsh containing emergent vegetation that has established itself on disturbed (e.g., farmed) soil.

The P-cycling model consists of two state variables, one representing the mass of TP in biomass storage such that

$$\frac{dS}{dt} = F_C F_z k_1 SC - k_2 S^2 - k_3 S \tag{17}$$

where S is the temporary storage in biomass (mg/m^2), C is the concentration of surface water (mg/m^3), F_c is the concentration multiplier, F_z is the depth multiplier, k_1 is the maximum uptake rate (m^3/mg-yr), k_2 is the recycle rate (m^2/mg-yr), and k_3 is the burial rate (1/yr). The second state variable is reserved for TP mass in the water column, and is given by

$$\frac{dhC}{dt} = L - QC - F_C F_z k_1 SC + k_2 S^2 \tag{18}$$

where h is the water depth (m), L is the loading rate in the cell (mg/m^2-yr), and Q is the outflow (m/yr). These two variables interact via the uptake and release terms, which are part of the pre-calibrated coefficients used for PEW and EMG. These equations, as implemented in the SRSM, are given in greater detail by Waldon et al. (2009). A schematic of these equations in the SRSM is given in Figure 23.

Initial values on January 1, 1995 for TP concentration (µg/L) in compartments 1 to 4 are 6.5, 14.3, 13.3, and 50, respectively. Additionally, initial storage is set to 0.5 g/m^2 in

compartment 1 and 0.1 g/m^2 in compartments 2 and 3. The steady state equation for storage can be solved and used to approximate these initial conditions. Table 12 above outlines the values for PEW and EMG calibration sets. Lastly, wet and dry deposition values for TP are 0.01 mg/L and 10 $mg/m^2/yr$. These numbers are less than those quoted by Davis (1994), which he noted represent over-estimations to these two parameter values (0.029 mg/L and 36 $mg/m^2/yr$).

3 SRSM results

3.1 Water budget model results

The SRSM stage calculations for the simulation period, 1/1/1995 to 6/30/2009, are in good agreement with the observed data. Canal simulation values are compared with the daily average stage at the 1-8C gage in the L-40 canal on the eastern side of the Refuge. Marsh stage, however, is based upon the average of gages 1-7 and 1-9; both of these measurement devices are located in the Refuge interior marsh.

According to Arceneaux et al. (2007) the SRSM is not intended to predict values at low canal stage. Any observed or modeled value below 4.267 m (14 ft) NAVD 29 is given a constant value of 4.267 m for the time series and performance measure analysis. Total days falling at or below this threshold depth for the observed data at 1-8C and model simulation are 108 and 162, respectively. Additionally, the observed sample number (n) in Table 13 for the canal compartment is missing 88 days as a result of damage incurred during the 2004 hurricane season. Stage results for the canal and marsh compartments are plotted in Figures 24 and 25, respectively.

In addition to the stage analysis, a model budget of daily average values is developed for all water entering or leaving the Refuge. Cumulative yearly values for all hydrologic parameters are given in Figures 26, 27, and 28. As stated previously, the year 2009 includes only six months of simulation data and should not be considered representative of the entire year. Table 14 presents the simulation ending values for each parameter along with the respective yearly average values. Additionally, from the “% of Cumulative” value

given in Table 15, it is clear that the model budget is closed. This value is obtained by calculating the overall difference in water volume as a percentage with respect to the cumulative inflowing water volume. The budget value is calculated by

$$\text{Budget} = V_{init} + Q_{in\_total} - V_{final} - Q_{out\_total} \quad (19)$$

where V_{init} is the initial Refuge water volume (m^3), Q_{in_total} is the total inflow volume (m^3), V_{final} is the final Refuge water volume (m^3), and Q_{out_total} is the total outflow volume (m^3).

As previously described in section 2.2, several types of diagnostic plots are also used to evaluate the capability of the SRSM. These six figures are given in the appendix of this document. These graphs support the information given by the statistics in Table 13. On average, the marsh stage predicted by the model is an underestimation of the observed value, as seen by the negative bias value, the percent distribution curve (Figure 51), and the stage scatter plot (Figure 53). Additionally, these graphs point out the weakness of the SRSM to capture low stage in the canal compartment. As seen in the residual plot (Figure 54) for the canal, the variability increases with a decrease in stage.

3.2 Water quality model results

The following sections will outline the performance of each constituent model of the SRSM. Observed and model values are averaged on a monthly basis for this analysis. Moreover, when calculating the statistics for the marsh the observed and model values are not separated by compartment; rather these values are aggregated into one marsh comparison analysis. Because the model affords no spatial disaggregation beyond the

concentric compartment arrangement (e.g., north/south or east/west separation), Arceneaux et al. (2007) found the aforementioned method appropriate. In this way the observed and model values still retain the property of their location; whereas, if all values for the marsh were averaged, those areas with disparate monitoring schemes would be ill-represented and the analysis would lose what little spatial variance the model imposes on the observed data.

In general, all comparisons of the constituent models are in good agreement with the observed data for the period of study. Performance is very high for the canal (compartment 4); this result, though, is not unexpected. Because the volume of the canal is small in comparison with the marsh and because it is often effluent dominated, the canal concentration is subject to peaks approximating the inflow concentration during inflow events. Moreover, it is assumed that no constituent kinetics should be implemented for the canal compartment; therefore, all canal constituent model results are based upon mass transport in and out through pumps and structures, and overbank flow in and out of the marsh. This assumption can be verified by comparing the median residence times of the canal and marsh, 11.7 and 472.9 days, respectively. The difference between these two values validates the assumption that canal water does not remain in the compartment long enough to be influenced by the constituent kinetics.

As previously described, Wang et al. (2009) modeled sulfate with apparent settling in the Refuge using the scheme set forth by Arceneaux et al. (2007). The results of implementing a Monod relationship for sulfate dynamics improved model performance and allowed sulfate-related parameters to be spatially invariant. Finally, of particular note are the results of the DMSTA P-cycling model. While the Refuge is not precisely characterized by

the conditions describing wetland systems used in developing either of the calibration sets (Walker and Kadlec, 2008), model performance suggests that the Refuge is better represented with the emergent marsh (EMG) calibration values.

3.2.1 Chloride simulation

The following graphs (Figures 29, 30, 31, and 32) and table (Table 16) provide an analysis of SRSM chloride simulation on a monthly average basis; the observed averages (black dots) are plotted with standard deviation bars. Canal results, compartment 4, are given first; followed by compartments 1, 2, and 3.

Additional diagnostic graphs are given to supplement the traditional time series graphs. These figures (Figures 68 to 75) visualize the calibration performance. The scatter and residual plots both indicate that the SRSM canal and marsh predictions are generally underestimations of observed chloride concentration. The marsh percent distribution (Figure 72) also indicates an underestimation of chloride; however, the pattern is clearly representative of the observed data.

3.2.2 Sulfate simulation

As seen in the time series graphs (Figures 33, 34, 35, and 36) of sulfate observed and simulated values, monthly average concentrations are subject to considerable variation. Table 17 gives a brief analysis of the ranges displayed by both sets of values. As discrete daily observed values and daily model averages are used, the values presented in this analysis are slightly different from those in the sulfate performance measures (Table 18). The values displayed in the performance measure table and the diagnostic plots (Figures 76

to 83) all indicate a consistent under prediction of the observation; nonetheless, the performance remains in good agreement with these values. However, the wide range of values seen in the marsh scatter plots indicates that long-term and trend averages (Figures 76 and 78) are more appropriately plotted as a log-log relationship; visualized as such, the relationship between simulated and observed data is much more apparent.

3.2.3 Total phosphorus simulation

As mentioned above, two calibration sets from DMSTA are implemented in the SRSM. All calibration performance statistics were superior for the emergent marsh (EMG) parameter set when compared to the pre-existent wetland (PEW) set. To better visualize the variation between these two simulations (Figures 37, 38, 39, and 40), an envelope is plotted for the monthly time series, where the space between the two simulations is hatched with upward diagonal lines. The performance measures (Table 19) all indicate good agreement between simulated and observed data. Additionally, time series graphs of biomass storage are given in Figures 41 and 42.

3.2.4 Constituent mass accumulation and budget

An identical analysis of yearly accumulations and total overall model budget is given above in the water budget model results section. Here, an accounting of daily inflow and outflow values is used to determine the success of the SRSM to accurately calculate constituent mass transport. All values representing mass are given in metric tons (MT) unless otherwise stated. Total and average accumulation over the 14.5 year simulation period is given in Tables 20 and 21, respectively.

To minimize the space utilized by graphs in the text, cumulative yearly constituent values for mechanisms driving constituent transport are given in a series of bar-graphs in the appendix. Table 22 outlines the values used for calculating the budget for each simulated constituent; the value designated as the closing value is a mass and is also given as a percent of the cumulative inflowing mass. The budget equation for the mass balance models is given by

$$\text{Budget} = M_{init} + L_{in\_total} - M_{final} - L_{out\_total} \tag{20}$$

where M_{init} is the initial Refuge constituent mass (MT), L_{in_total} is the total constituent mass flowing into the Refuge (MT), M_{final} is the final Refuge constituent mass (MT), and L_{out_total} is the total constituent mass flowing out of the Refuge (MT).

The resultant values given by Equation 20 indicate model budgets close for each constituent. However, an additional comparison is made between the model cumulative outflow constituent mass loads with those given in the data section of this document (Figures 43, 44, and 45). With the exception of one data point in the sulfate comparison, all outflow loads are in good agreement with those presented in the site data analysis section. This value occurs for the year 1995 and is considered extreme. Such a high value of observed outflow can be attributed to the insufficient boundary concentration data available for sulfate in 1995.

3.3 Scenario analysis

The SRSM presents Refuge managers with the opportunity to test and assess management scenarios based on area-averaged applications. While this model does not disaggregate the marsh into north, south, east, or west compartments, it still can be used to evaluate management proposals based on a Refuge-wide response. Two such applications of the SRSM are presented here.

3.3.1 Inflow concentration reduction

The first scenario investigates the marsh response to reduction in inflow concentration. Specifically, water entering the Refuge will have a static concentration equivalent to the wet deposition value of each constituent (CL=2 mg/L, SO4=1 mg/L, and TP=0.01 mg/L). The pre-drainage Everglades ecosystem was rainfall and sheet-flow driven (USFWS, 2000). Pulses of high nutrient loads from anthropogenic sources were not present. Even today the Refuge interior may appear to be guarded from some of this loading. However, this investigation determines the time and extent of the interior marsh's response to this concentration reduction. Since it has been established in the previous section that the EMG calibration set outperforms PEW, the results from the former set are used for scenario analysis.

This analysis compares the typical model results in compartment 3, marsh interior, with those from the scenario simulation. Figures 46, 47, and 48 display graphs of the simulation results for each constituent. The series labeled "Base SRSM" corresponds to the results presented above. As with the time series given in previous sections, this presentation uses

monthly average model output for graphical analysis. Additionally, the response of biomass storage for the interior marsh compartment is visualized in Figure 49.

The model results demonstrate that the response of the interior is near immediate for surface water concentrations of chloride and sulfate. The storage component of the P-cycling model also responds quickly to the change in inflow concentration. The concentrations of chloride and sulfate under this scenario begin to deviate from those of the base values in mid to late 1995. For chloride, of the 174 months of simulation, 26 months (15%) have a difference less than or equal to 2 mg/L, and for sulfate 119 months (68%) have a difference less than or equal to 1 mg/L. These results suggest that the interior concentrations will be lowered under less intense loading conditions from the perimeter control structures.

However, the concentration of Total Phosphorus is very similar to the base run SRSM values, with all of the difference values being less than the constant inflow concentration (0.01 mg/L). These results, paired with the reduction in the overall storage values, are appropriate given the structure of the P-cycling storage equation (17), as there is less TP mass loading and the coefficients for the first and second order storage loss terms do not change. Therefore, in areas of low concentration the same amount of storage continues to be removed regardless of the mass entering the system at the perimeter. Finally, these results validate that the perimeter marsh areas near canal inflow sites act as buffers to high TP inflow concentrations.

3.3.2 Model response to inflow data resolution

Hourly mean flow values for each structure along the perimeter canal are available to the public from DBHYDRO; however, upon special request, flow data with finer resolution (e.g., 60-min and 30-min intervals) can be obtained. This scenario investigates modeled concentration sensitivity, to inflow data resolution. These results will also be used to infer whether the day to day operations of perimeter canal structures should remain of the 6 to 8 hour "pulse" type or whether this window should be lengthened to reduce the impact.

Two simulations are performed, one with mean daily inflow values (AVG), as in the model results previously presented, and the other with hourly flow measurements (HOURLY). Just as in the previous section, all three water column concentrations and TP biomass storage values are used for the assessment of this scenario. Difference values are calculated for each day of model output by subtracting the HOURLY result from the AVG result. The comparison indicates that the resolution of inflow data does indeed influence the constituents' concentrations, particularly in compartments 1 and 4. Table 23 outlines the maximum, minimum, average, and standard deviation of the difference values for water column concentration and TP storage. When the average difference is negative, the results indicate that HOURLY flow data cause more constituent mass to be transported from the boundary to the marsh. In the case of chloride and sulfate, all marsh compartments have negative average differences and the canal compartment has a positive average difference. Therefore, the variation of inflow seen in the hourly data not only causes more mass to be transported to and retained in the marsh, but also causes the canal to become diluted. In the case of total phosphorus concentration, the first marsh compartment is the only one to be affected by the hourly flow data; this result can be attributed to the P-cycling storage

uptake and burial mechanisms. The average difference for all storage values is negative. However, compartment 1 is substantially larger than the other two, indicating that this compartment, according to the model, effectively reduces the water column concentration and helps to protect the interior from intrusion events.

4 Conclusions

With considerable ease of model setup and assurance of computational efficiency, the benefits of the Berkeley Madonna programming environment are readily apparent. Despite the short time step required for model simulation, the software provides results much faster than previous models. The ability to freely manipulate the solution method and time step allowed for easy testing and calibration of parameters and kinetics formulations. This fact leads to one of the main benefits of the SRSM. Since this model is part of a suite of models aimed at testing management scenarios for Refuge restoration efforts, the ability to efficiently test various parameter schemes affords the opportunity to pre-calibrate values of various kinetics relationships for more computationally expensive models.

Further scrutiny of the model structure and presented results leads to an understanding of the applicability of the SRSM. Although it is intended to be used as a management scenario testing model, there are applications for which it is not appropriate. For example, scenarios that propose to significantly alter the flow patterns through structural changes in the Refuge landscape (e.g., construction of berms or removal of levees) cannot be analyzed. Additionally, results are limited in their ability to capture the dynamics of a specific site within the Refuge. Understanding the limitations of the SRSM allows for appropriate application and interpretation of results.

The stage prediction for the period of study is in good agreement with the observed values. Scenarios and exercises concerned with flow regulation can be implemented and analyzed with little effort. However, such analysis is limited by the model's inability to properly

capture the stage below 4.2672 m (14 ft). This limitation is, in part, caused by the SRSM assumption of a rectangular canal cross-section. Moreover, since there is no variation in cross-section, the results from this compartment are representative of an idealized canal. Canal stage predictions, therefore, should be considered as an average value and not representative of a particular canal site. Similarly, the SRSM prediction of marsh stage should be considered an average value for the entire marsh. The assessment of any given scenario should be viewed in a global sense for each computational compartment. Therefore, management decisions can be screened based on the "spatially averaged" results that the SRSM provides. However, the ability of the two compartment hydrodynamic model to capture the recession in stage seen yearly in the marsh interior gives credence to the model's ability to accurately simulate the aggregate marsh behavior.

The outflow calculated for the S-10 and S-39 structures compares well with yearly historic outflow values. Because regulation schedule calculations performed in the SRSM occur for each time-step, every 7.2 minutes, there is a discrepancy with the actual operation of these structures in the Refuge. Regulatory releases from these structures are manually performed and do not occur with the precision assumed in the SRSM. Future versions of this and other models created for the Refuge should consider evaluating model performance based on an idealized weekly schedule, where outflows do not adjust on weekends and are held constant over the entire day. For accurate model predictions, refinement of these calculations to this degree for the SRSM is not ultimately necessary. Daily average values for stage in both the marsh and canal compartments agree well with the observed data. Moreover, the purpose of the SRSM is to provide a tool for long-term management scenarios; therefore, capturing the dynamics within modeled days as a result

of these calculated regulatory releases is not a primary goal of this particular modeling effort. However, this is an important exercise which should be implemented in the SRSM to observe the affects on stage and water quality predictions.

Additionally, improvement can be made to the model's calculation of stage in the marsh and canal compartments. Currently, the stage/volume relationship is linear and does not consider the reduction of water surface area with depth, therefore; the canal is assumed to be a rectangular channel. Implementation of such relationships should allow for a more realistic approximation of stage during the periods of drawdown in both the canal and marsh.

The constituent models implemented in the SRSM perform adequately under the assumption of a spatially aggregated marsh and singular canal compartment; therefore, making inferences of site-specific events based on the compartment arrangement of the SRSM is not appropriate. Additionally, chloride transport as a conservative tracer does not appear to suffer in the absence of Fickian dispersion mechanisms. It can be assumed that the model, resulting from the coarse spatial characteristics and solution method, has high numerical dispersion. This fact works in favor of this version's success. However, future compartment models that disaggregate the marsh into more compartments should consider dispersion mechanisms as part of constituent mass transport. However, despite the inherent dispersion, the results indicate that the canal and marsh predictions underestimate the observed chloride concentration. This bias can be explained by the increase in marsh seepage used to calibrate the calculated outflow.

Sulfate dynamics approximated by the Monod relationship are in good agreement with the observed data for long term simulation periods. However, the availability of inflow concentration data is infrequent, particularly for early simulation years. Increased frequency of monitoring of sulfate in the Refuge inflows and outflows would enhance the development of water quality modeling for this and other projects.

The P-cycling method performs well for the emergent (EMG) calibration set from DMSTA, and this set should represent primary values for TP model simulations. Additionally, collaboration with DMSTA developers should continue, as updates or recalibration may necessitate changes in these values. However, the residual plot for the marsh, Figure 90, visualizes the negative bias of the model, and it appears that the bias increases in a near-linear fashion with increasing concentration. This indicates that for increasing water column concentration the uptake and burial terms of the storage equation dominate, which can be resolved with recalibration of the k_1 and k_3 terms for the Refuge. Regardless, uncertainty remains for the values calculated by the storage equation. While the initial condition is within an order of magnitude of the steady state value on the start date (1/1/1995), little else can be determined from the storage dynamics seen during the simulation period. As data become available for soil P concentration, values for the marsh areas should be compared with those output from the SRSM.

From the results presented herein, it is clear that the SRSM version 4 capitalizes on the strengths of previous versions and utilizes a new interface to become more flexible both in water budget and constituent modeling. The interface provided by the Berkeley Madonna software allows for easy expansion/integration of this model. Lastly, with a 14.5 year

period of study, this version will allow Refuge managers to have a considerable amount of data available for model simulation and assessment.

References

Abtew, W., Huebner, R. S., Ciuca., V., 2005. Hydrology of the South Florida Environment. In: Redfield, G., (Ed.), 2006 South Florida Environmental Report. South Florida Water Management District , West Palm Beach, FL, pp. 1-46.

Abtew, W., Huebner, R. S., Sunderland, S., 2002. Hydrological Analysis of the 2000–2001 Drought in South Florida. South Florida Water Management District , West Palm Beach, FL, pp. 1-100.

Andersen, J., Refsgaard, J. C., Jensen, K. H., 2001. Distributed hydrological modeling of the Senegal river basin—model construction and validation. Journal of Hydrology 247 (3-4), 200-214.

Ansar, M., Chen, Z., 2009. Generalized flow rating equations at prototype gated spillways. Journal of Hydraulic Engineering 135 (7), 602-608.

Arceneaux, J., 2007. The Arthur R. Marshall Loxahatchee National Wildlife Refuge Water Budget and Water Quality Models, MS. Thesis. University of Louisiana at Lafayette, Lafayette, LA.

Arceneaux, J., Meselhe, E. A., Griborio, A., Waldon, M. G., 2007. The Arthur R. Marshall Loxahatchee National Wildlife Refuge Water Budget and Water Quality Models." Report No. LOXA-07-004. University of Louisiana at Lafayette in cooperation with the U.S. Fish and Wildlife Service, Lafayette, LA. <http://loxmodel.mwaldon.com>

Berry, D. A., Lindgren, B. W., 1996. Statistics: Theory and Methods. Duxbury Press, New York.

Chow, V. T., Maidment, D. R., Mays, L. W., 1988. Applied Hydrology. McGraw-Hill, New York.

Davis, S. M., 1994. Phosphorus Inputs and Vegetation Sensitivity in the Everglades. In: Davis, S. M. and Ogden, J. C., (Eds.), Everglades: The Ecosystem and Its Restoration. St. Lucie Press, Delray Beach, FL, pp. 357-78.

Desmond, G., 2003. South Florida high-accuracy elevation data collection project. FS-162-96. U.S. Department of the Interior, U.S. Geological Survey, Reston, VA. <http://sofia.usgs.gov/publications/fs/162-96/>

Daroub, S., Stuck, J. D., Rice, R. W., Lang, T. A., Diaz, O. A., 2002. Implementation and verification of BMPs for reducing loading in the EAA and Everglades Agricultural Area BMPs for reducing particulate phosphorus transport. Phase 10 Annual Report, WM 754. Everglades Research and Education Center, Institute of Food and Agricultural Sciences, University of Florida, Belle Glade.

Harwell, M. C., Surratt, D. D., Barone, D. M., Aumen, N. G., 2008. Conductivity as a tracer of agricultural and urban runoff to delineate water quality impacts in the northern Everglades. Environmental Monitoring and Assessment 147 (1-3), 445-462.

Holzbecher, E., Horner, C., 2003. A Reactive Transport Model for Redox Components. In: Hadeler, A., Schulz, H.D., (Eds.), Geochemical Processes in Soil and Groundwater, Wiley-VCH: Weinheim, Germany, pp. 413-44.

Kadlec, R. H., Knight, R. L., 1996. Treatment Wetlands. CRC Press, Inc., Boca Raton, FL.

Krabbenhoft, D. P., 1996, Mercury Studies in the Florida Everglades. U.S. Geological Survey Fact Sheet, FS-166-96.

Legates, D. R., McCabe Jr., G. J., 1999. Evaluating the use of "goodness-of-fit" measures in hydrologic and hydroclimatic model validation. Water Resources Research 35 (1), 233-42.

Light, S. S., Dineen, J. W., 1994. Water Control in the Everglades: A Historical Perspective. In: Davis, S. M. and Ogden, J. C., (Eds.), Everglades: The Ecosystem and Its Restoration. St. Lucie Press, Delray Beach, FL, pp. 47-84.

Lin, S., 1979. The application of the Receiving Water Quantity Model to the Conservation Areas of South Florida. DRE-91, South Florida Water Management District, West Palm Beach, FL.

Lodge, T. E., 1994. The Everglades Handbook: Understanding the Ecosystem. CRC Press, Inc., Boca Raton, FL.

Macey, R., Oster, G., Zahnley, T., 2000. Berkeley Madonna User's Guide Version 8.0. University of California, Department of Molecular and Cellular Biology, Berkeley, CA.

MacVicar, T. K., Van Lent, T., Castro, A., 1984. South Florida Water Management Model Documentation Report. Technical Publication 84-3, South Florida Water Management District, West Palm Beach, FL.

Meselhe, E., Arceneaux, J., Waldon, M.G., 2007. Mass Balance Model Version 1.01. Report No. LOXA-07-002, University of Louisiana at Lafayette in cooperation with the U.S. Fish and Wildlife Service, Lafayette, LA. <http://loxmodel.mwaldon.com>

Meselhe, E. A., Griborio, A. G., Gautam, S., Arceneaux, J. C., Chunfang, C. X., 2005. Hydrodynamic And Water Quality Modeling For The A.R.M. Loxahatchee National Wildlife Refuge, Phase 1: Preparation Of Data, Task 1: Data Acquisition and Processing. Report No. LOXA05-014, University of Louisiana at Lafayette, prepared for the Arthur R. Marshall Loxahatchee National Wildlife Refuge, USFWS, Lafayette, LA. <http://sofia.usgs.gov/lox_monitor_model/advisorypanel/ data_acq_report.html>

Meselhe, E. A., Waldon, M. G., Roth, W., 2009. A.R.M. Loxahatchee National Wildlife Refuge Simple Refuge Screening Model Version 4.00 User's Manual. Lafayette, LA: University of Louisiana at Lafayette, (draft, in review).

Mitsch, W. J., Gosselink, J. G., 2007. Wetlands. John Wiley and Sons, Inc., Hoboken, New Jersey.

Montgomery, D. C., Runger, G. C., Hubele, N. F, 2001. Engineering Statistics. John Wiley and Sons, Inc., New York.

Munson, R., Roy, S., Gherini, S., McNeill, A., Hudson, R., Blette, V., 2002. Model Predication of the Effects of Changing Phosphorus Loads on the Everglades Protection Area. Water, Air, and Soil Pollution, 134 (1/4), 255-273.

Raghunathan, R., Slawecki, T., Fontaine, T. D., Chen, Z., Dilks, D. W., Bierman, V. J., Jr, Wade, S., 2001. Exploring the dynamics and fate of total phosphorus in the Florida Everglades using a calibrated mass balance model. Ecological Modeling, 142 (3), 247- 259.

Richardson, J. R., Bryant, W. L., Kitchens, W. M., Mattson, J. E., Pope, K. R., 1990. An evaluation of refuge habitats and relationships to water quality, quantity, and hydroperiod: A synthesis report. University of Florida, Florida Cooperative Fish and Wildlife Research Unit, Gainesville, FL.

Rizzo, D. M., Mouser, P. J., Whitney, D. H., Mark, C. D., Magarey, R. D., Voinov, A. A., 2006. The comparison of four dynamic systems-based software packages: Translation and sensitivity analysis. Environmental Modelling and Software, 21 (10), 1491-1502.

South Florida Water Management District (SFWMD), 2003. DBHYDRO Browser User Documentation. South Florida Water Management District, West Palm Beach, FL.

Surratt, D. D., Waldon, M. G., Harwell, M. C., Aumen, N. G., 2008. Time-series and spatial tracking of polluted canal water intrusion into wetlands of a national wildlife refuge in Florida, USA. Wetlands 28 (1), 176-183.

United States Army Corps of Engineers (USACE), 1994. Environmental Assessment: Modification of the Regulation Schedule Water Conservation Area No. 1. U.S. Army Corps of Engineers, Jacksonville, FL. <http://mwaldon.com/Loxahatchee/GrayLiterature/USACE-1995-Lox-Regulation-Schedule.pdf >

United States Army Corps of Engineers (USACE), 2008. Chapter 4: Computer Software for Collaborative Planning. In: The Collaborative Planning Toolkit. <http://www.svp.iwr.usace.army.mil/CPToolkit/>

United States Army Corps of Engineers (USACE), 2009. Comprehensive Everglades Restoration Plan (CERP), The Everglades Water Flow Maps: Past, Present & Future (Combined). <www.evergladesplan.org/education/requested_downloads.aspx>

United States Fish and Wildlife Service, 2000. Arthur R. Marshall Loxahatchee National Wildlife Refuge Comprehensive Conservation Plan. U.S. Fish and Wildlife Service, Boynton Beach, Florida. <http://loxahatchee.fws.gov>

Waldon, M. G., Meselhe, E. A., Roth, W. B., Wang, H., Chen, C. 2009 A.R.M. Loxahatchee National Wildlife Refuge Water Quality Modeling – Rates, Constants, and

Kinetic Formulations. Report No. LOXA009-003, University of Louisiana at Lafayette in cooperation with the U.S. Fish and Wildlife Service, Lafayette, LA.

Walker, W. W., 1995. Design for Everglades Stormwater Treatment Areas. Water Res. Bull., 31 (4), 671-685.

Walker, W. W., Kadlec, R. H., 2008. Dynamic Model for Stormwater Treatments Areas - Version 2. <http://wwwalker.net/dmsta/index.htm>.

Wang, H., Waldon, M. G., Meselhe, E. A., Arceneaux, J. C., Chen, C., and Harwell, M. C., 2009. Surface Water Sulfate Dynamics in the Northern Florida Everglades, USA. Journal of Environmental Quality, 38 (2), 734-741.

Welter, D., 2002. Loxahatchee National Wildlife Refuge HSE model. South Florida Water Management District, West Palm Beach, FL.

Zhang, L., Mitsch, W. J., 2005. Modelling hydrological processes in created freshwater wetlands: an integrated system approach. Environmental Modelling and Software, 20 (7), 935-946.

Zhang, Y., Li, C., Trettin, C. C., Li, H., Sun, G., 2002. An integrated model of soil, hydrology, and vegetation for carbon dynamics in wetland ecosystems. Global Biogeochem. Cycles, 16 (4), 1061.

Appendix

The first two tables display those data points that were amended due to redundancy or extreme values. Table 24 displays the structure, constituent, and number of duplicate measurements. In the event of a duplicate measurement, both values are averaged and used as the boundary concentration on that day. Table 25 displays those days for which concentration of chloride and sulfate are observed to be extreme values. The measurements are confirmed to be artificial if a comparison with conductivity yields a drastically different value. Arceneaux et al. (2007) used the long term average chloride and conductivity values to establish a linear relationship used to predict chloride concentration from measured conductivity. Since the data period has been extended, the chloride to conductivity rations have been adjusted appropriately.

The first series of graphs displays the diagnostic plots used for stage model evaluation. These graphs (Figures 50 to 55) are described within the text and referenced as needed. The figures alternate between canal and marsh results. The first pair is the percent distribution plots (Figures 50 and 51) and is followed by the scatter (Figures 52 and 53) and residual plots (Figures 54 and 55).

The second series of graphs displays the yearly cumulative mass values for each constituent simulated by the SRSM. These figures (Figures 56-67) display the constituents in the following order: chloride, total phosphorus (EMG), total phosphorus (PEW), and sulfate. There are three bar charts for each constituent. These figures are meant to accompany each

constituent simulation by displaying the long term accumulation patterns of mass in the Refuge.

The final series of graphs (Figures 68-91) displays the diagnostic plots used for constituent model evaluation. Results for each constituent are given for the marsh and canal compartments. The graphs are arranged in the following order: yearly average scatter, monthly average scatter, percent distribution, and residual plot.

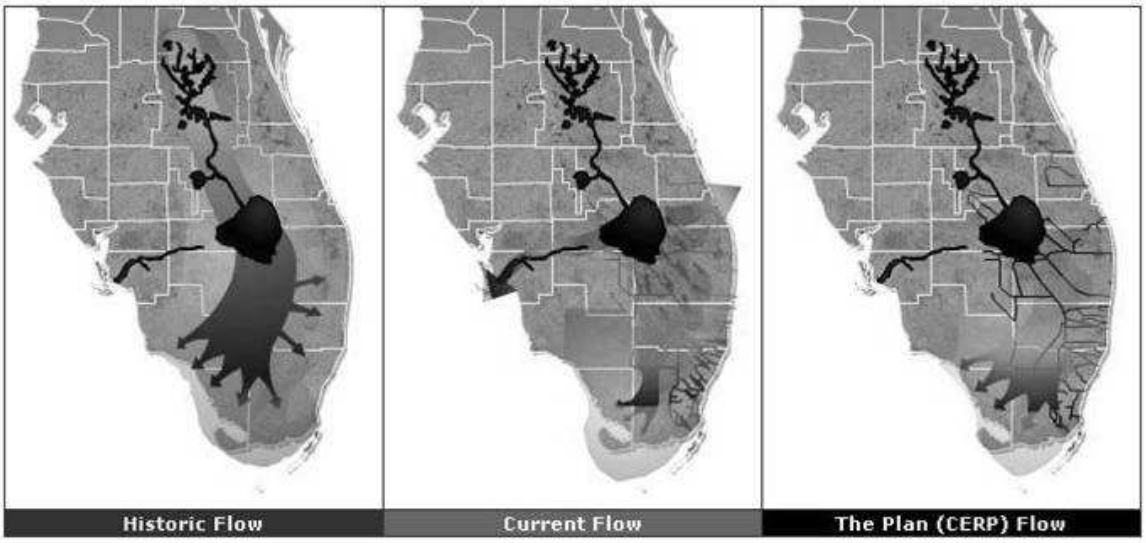

Figure 1 – Past, present, and proposed flow through the Everglades (USACE, 2009).

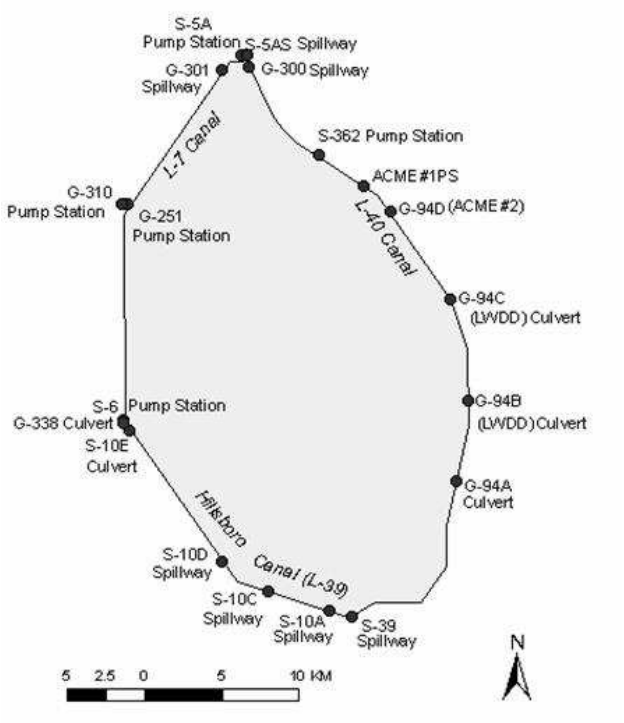

Figure 2 – Locations of all hydraulic structures along the perimeter canal (Meselhe et al., 2005).

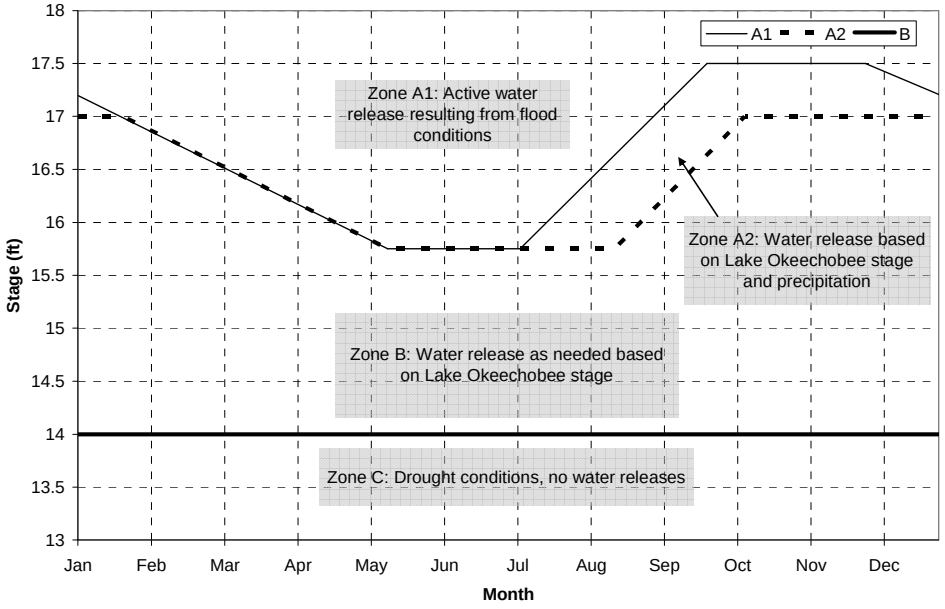

Figure 3 – Regulation schedule for Loxahatchee National Wildlife Refuge; adapted from USFWS (2000).

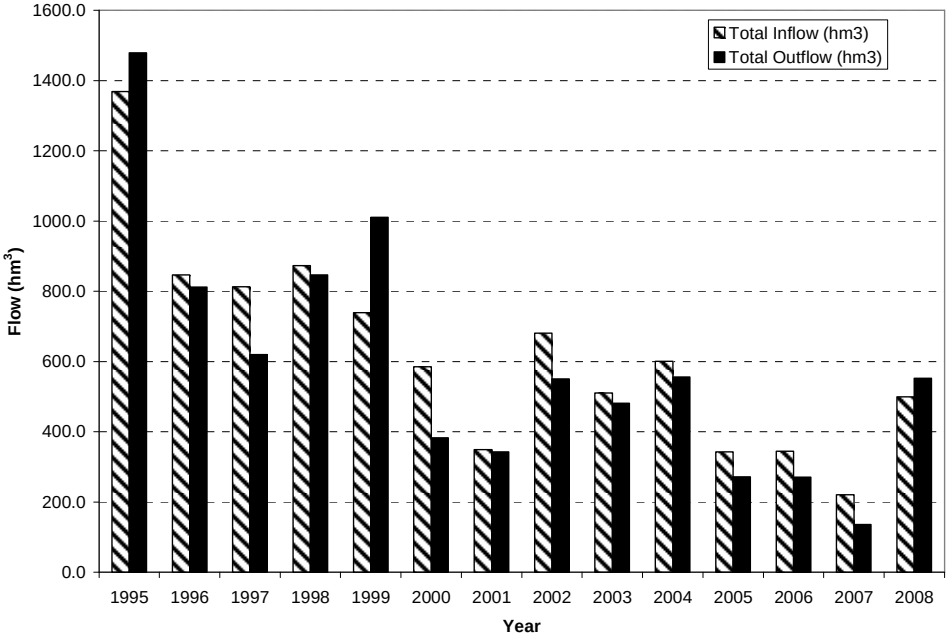

Figure 4 – Cumulative historic flow from hydraulic structures for the data period, with the exception of Jan-09 to Jun-09.

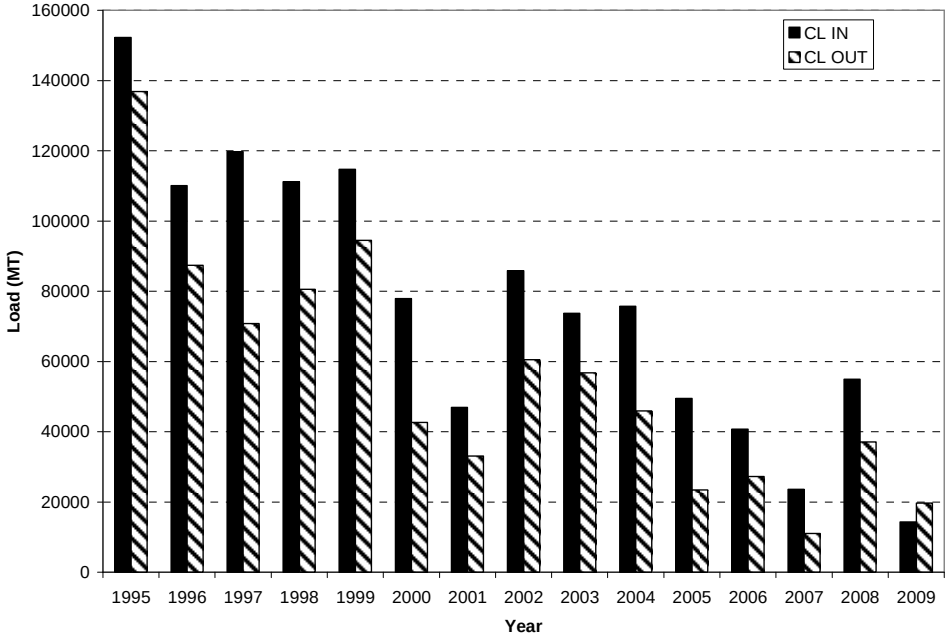

Figure 5 – Chloride inflow and outflow loads (for the perimeter structures) calculated for the data period.

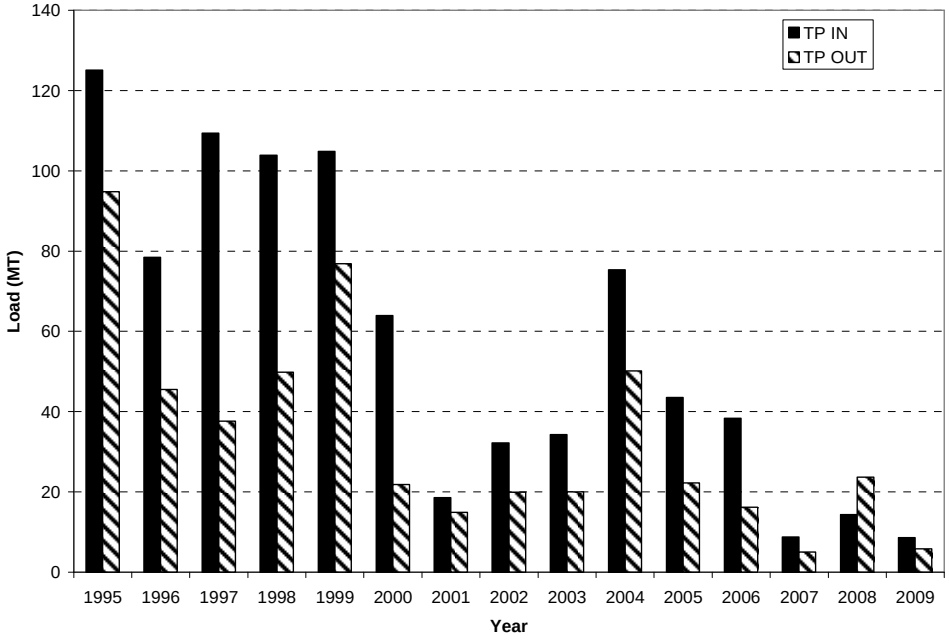

Figure 6 – Total phosphorus inflow and outflow loads (for the perimeter structures) calculated for the data period.

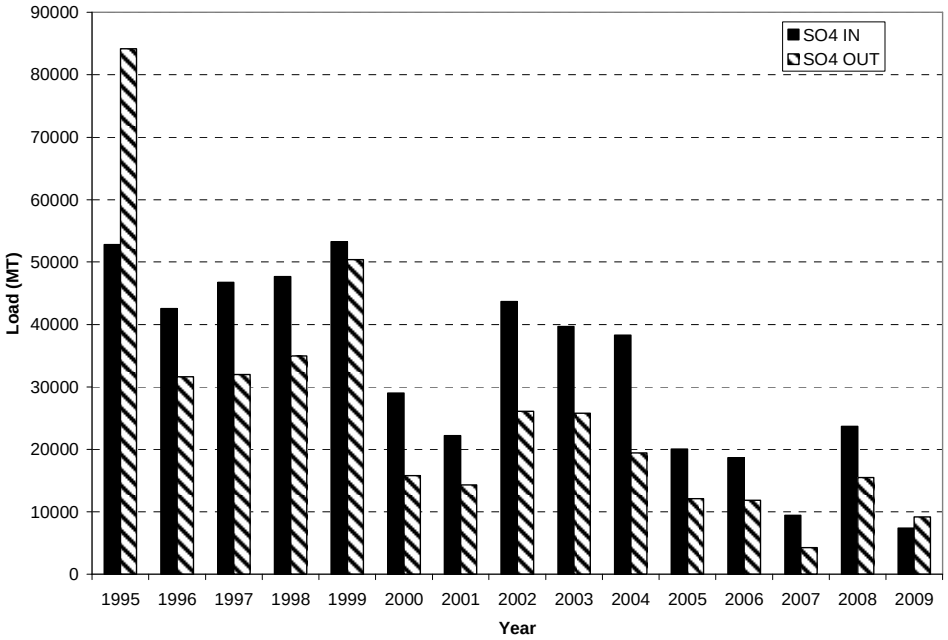

Figure 7 – Sulfate inflow and outflow loads (for the perimeter structures) calculated for the data period.

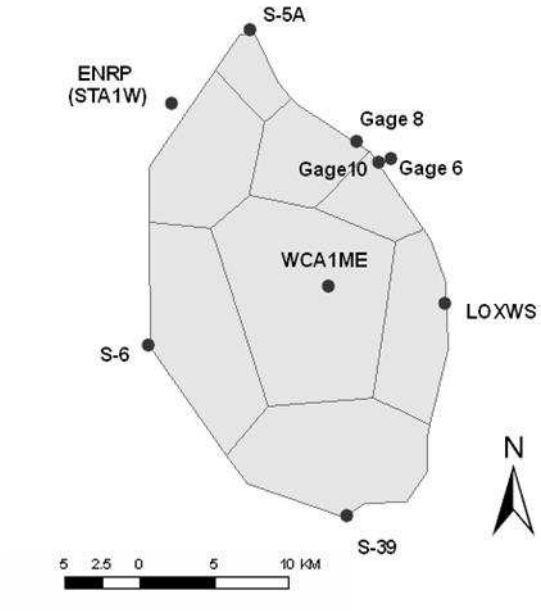

Figure 8 – Thiessen polygon scenario used in calculating area-average precipitation (Arceneaux et al., 2007).

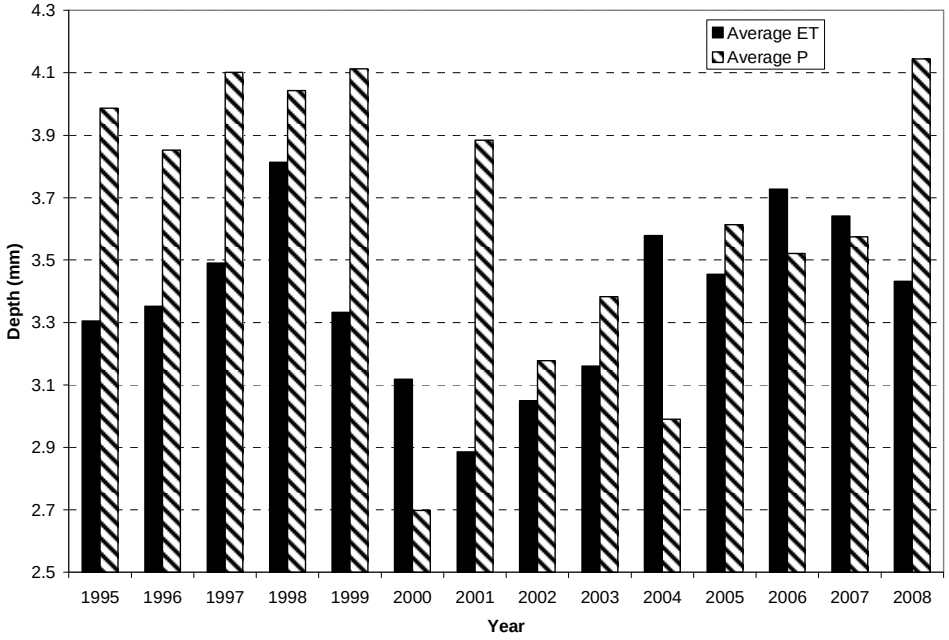

Figure 9 – Yearly average of ET and precipitation for the Refuge.

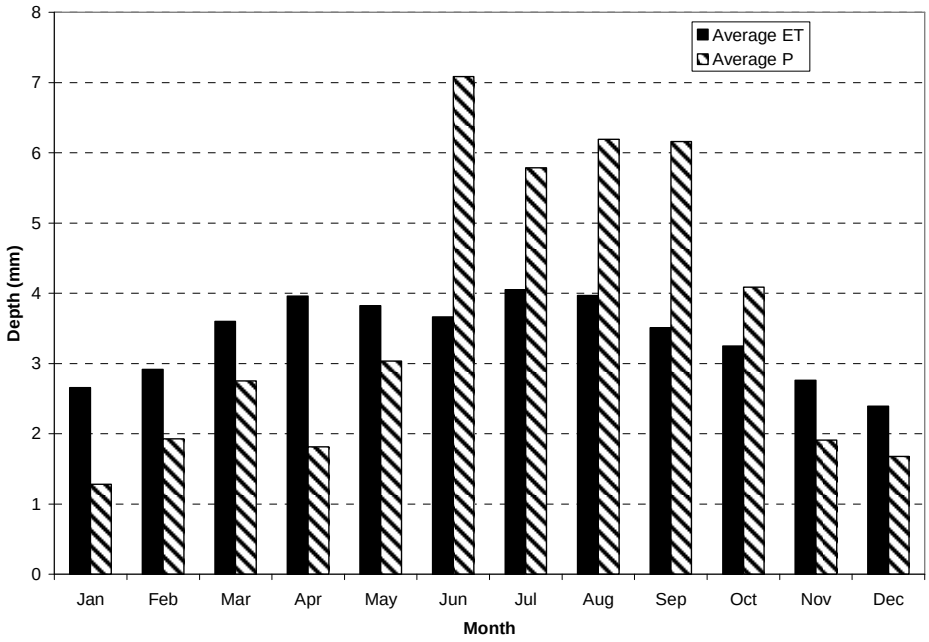

Figure 10 – Monthly average of ET and precipitation for the Refuge.

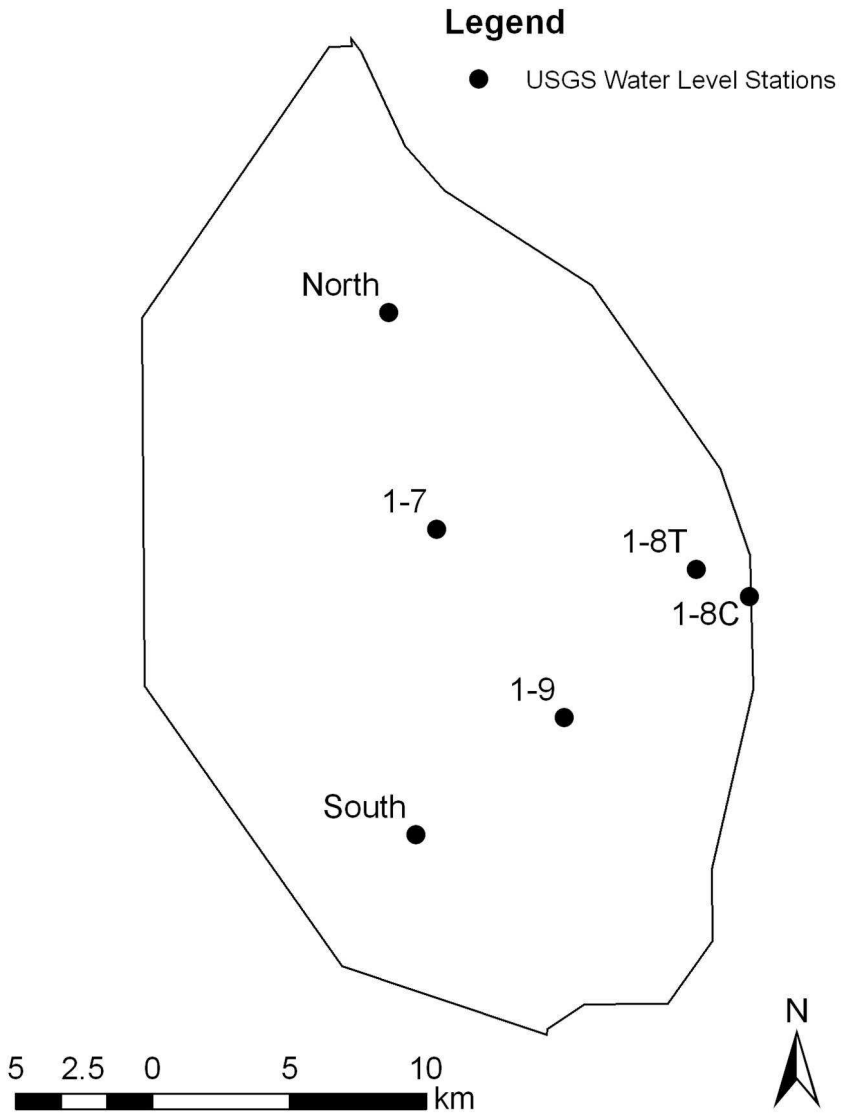

Figure 11 – Water level recording stations in the Refuge; adapted from Meselhe et al. (2005).

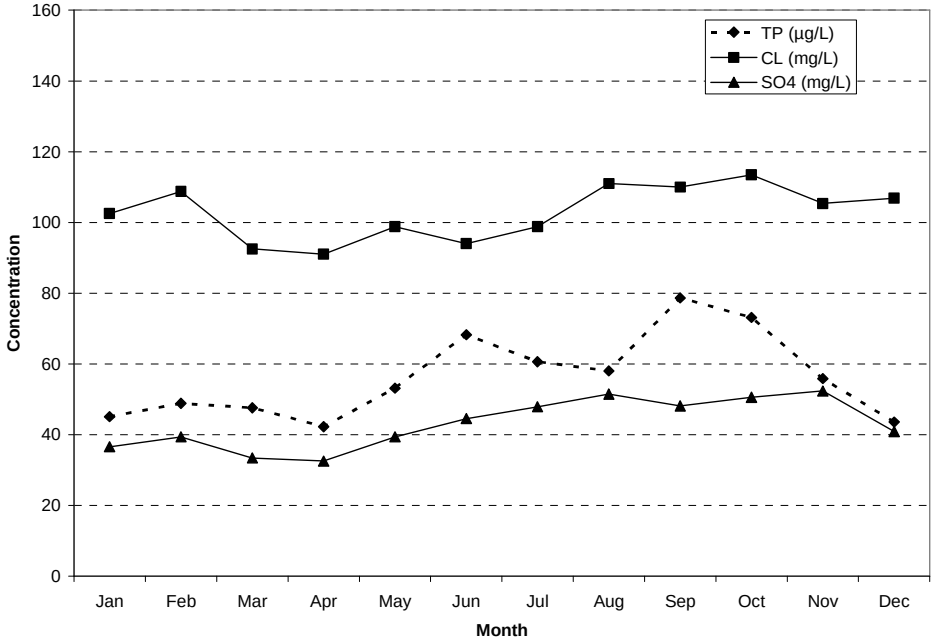

Figure 12 – Monthly average observed concentration in the canal.

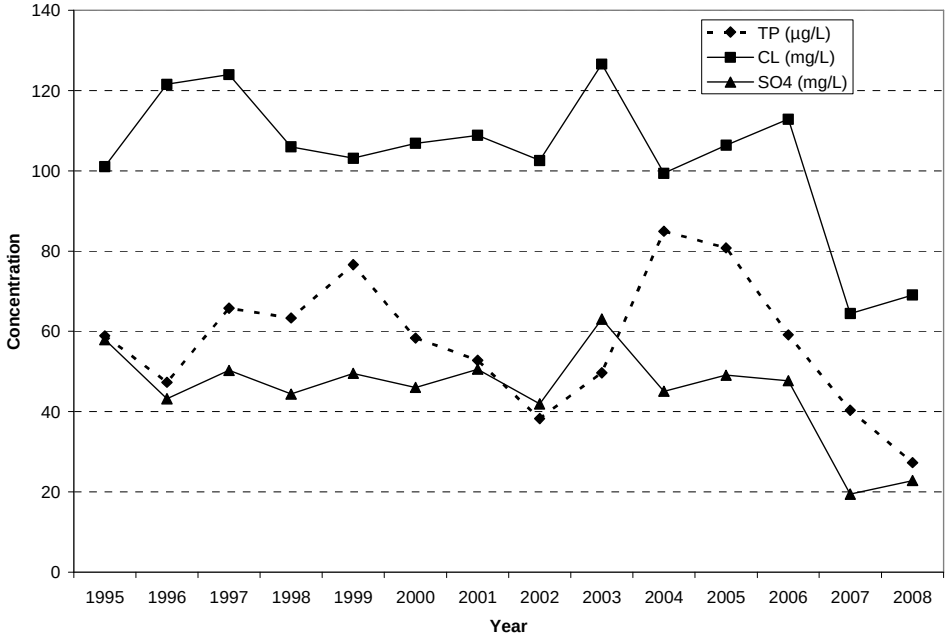

Figure 13 – Yearly average observed concentration in the canal.

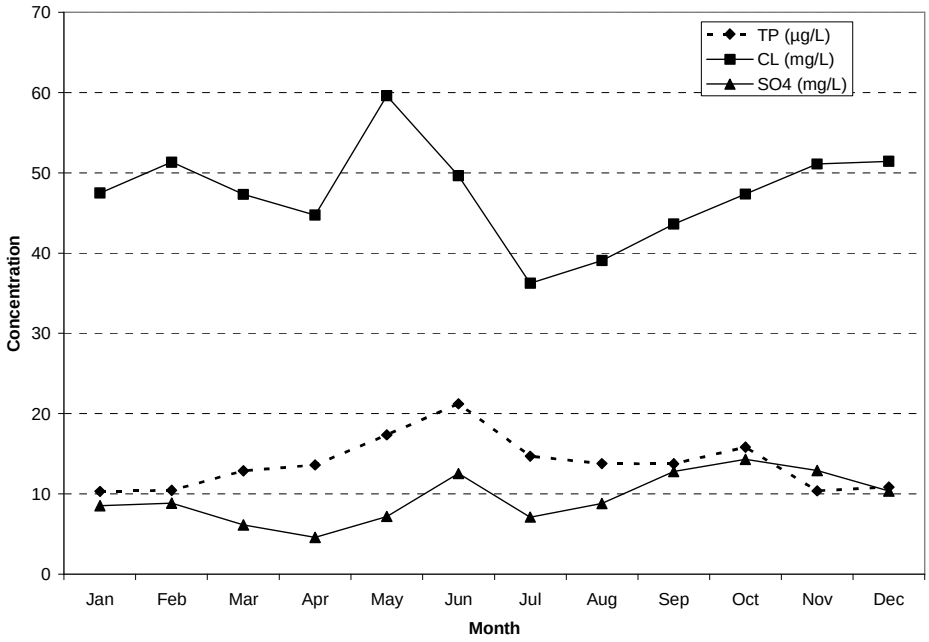

Figure 14 – Monthly average observed concentration in the marsh.

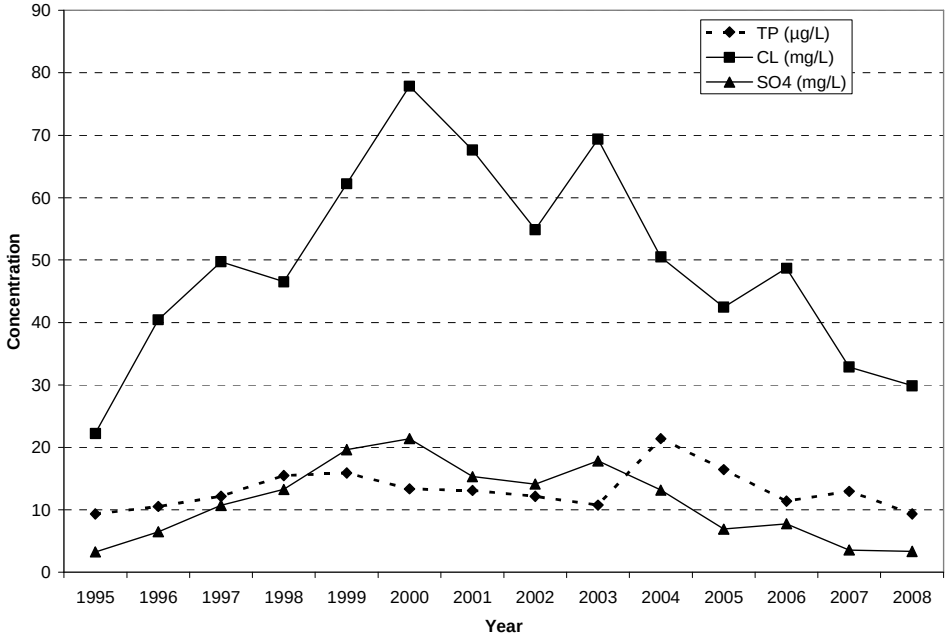

Figure 15 – Yearly average observed concentration in the marsh.

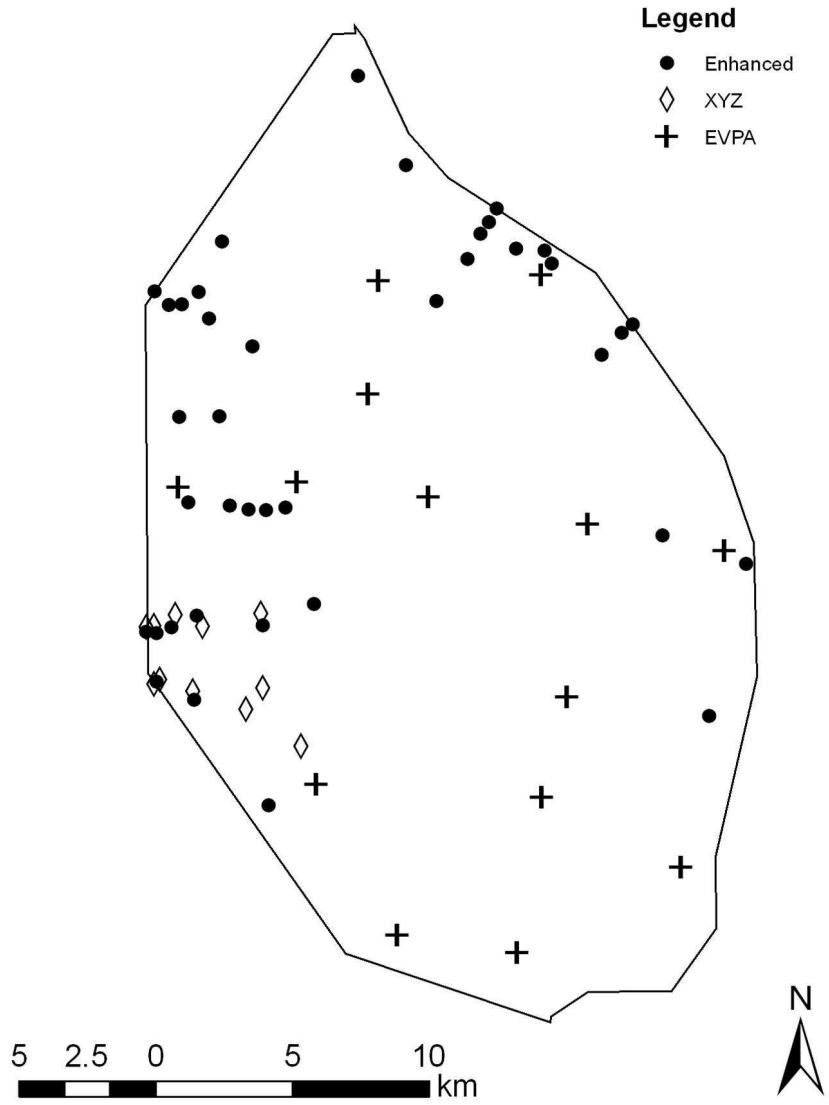

Figure 16 – Location of water quality stations in the Refuge; adapted from Meselhe et al. (2005).

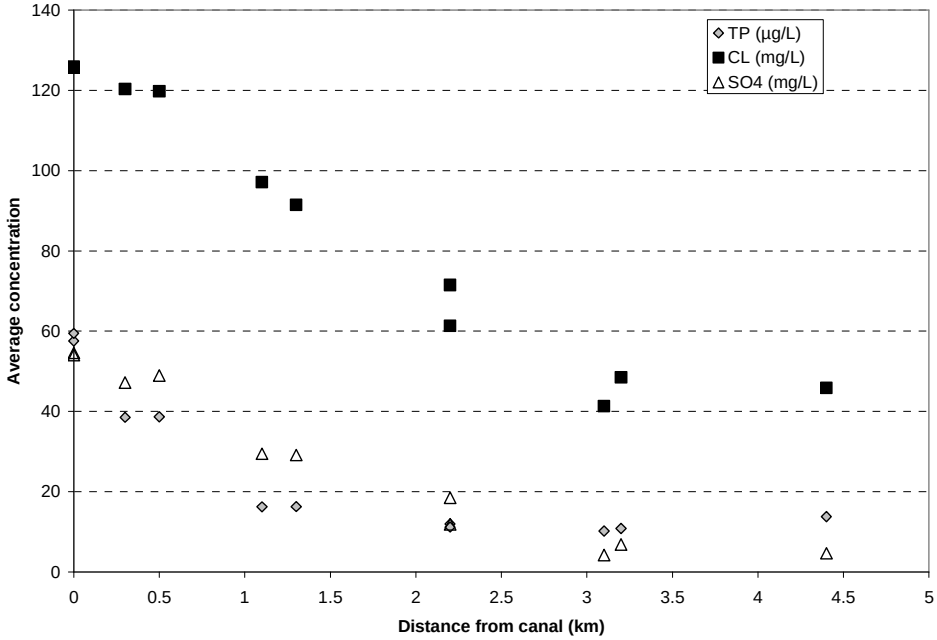

Figure 17 – Gradient of concentration with increasing distance from the rim canal; adapted from Meselhe et al. (2005).

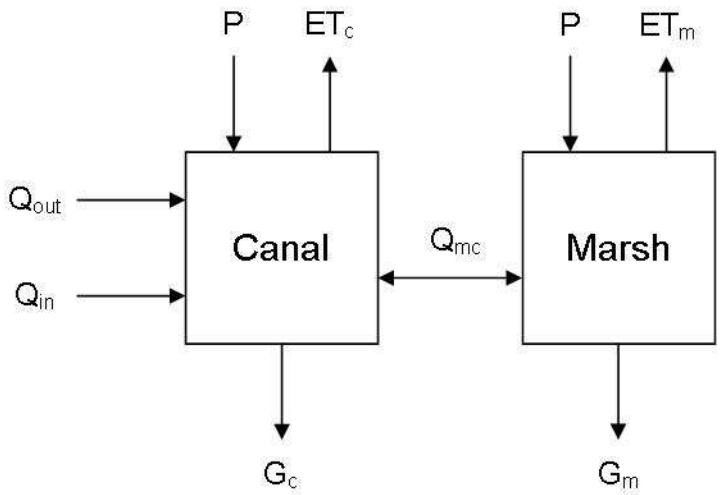

Figure 18 – 2-compartment schematic for the SRSM water budget.

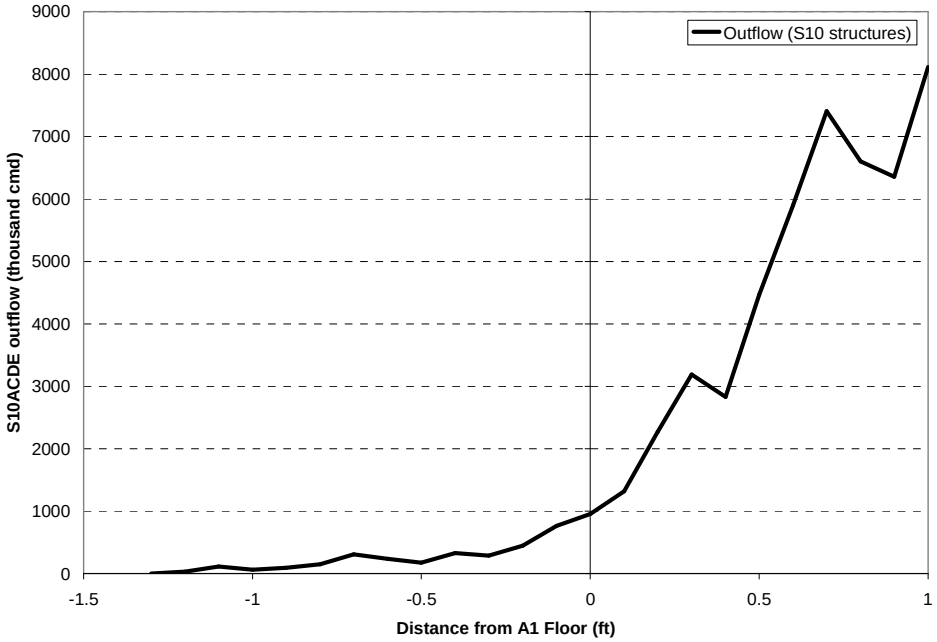

Figure 19 – Rating curve used to calculate outflow in the SRSM.

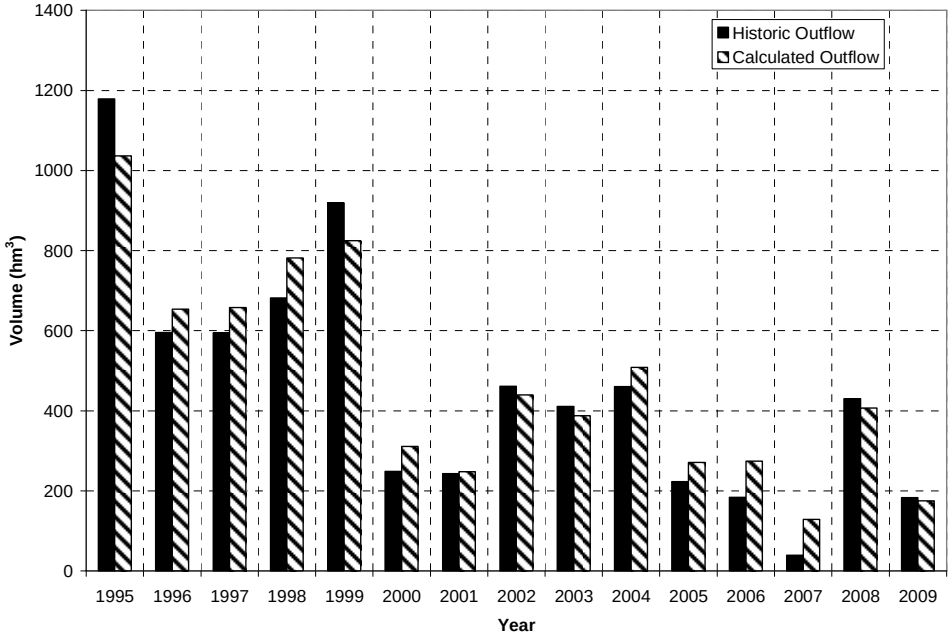

Figure 20 – Annual cumulative outflow volume, observed and calculated, from structures S-10ACD and S-39 prior to model reevaluation.

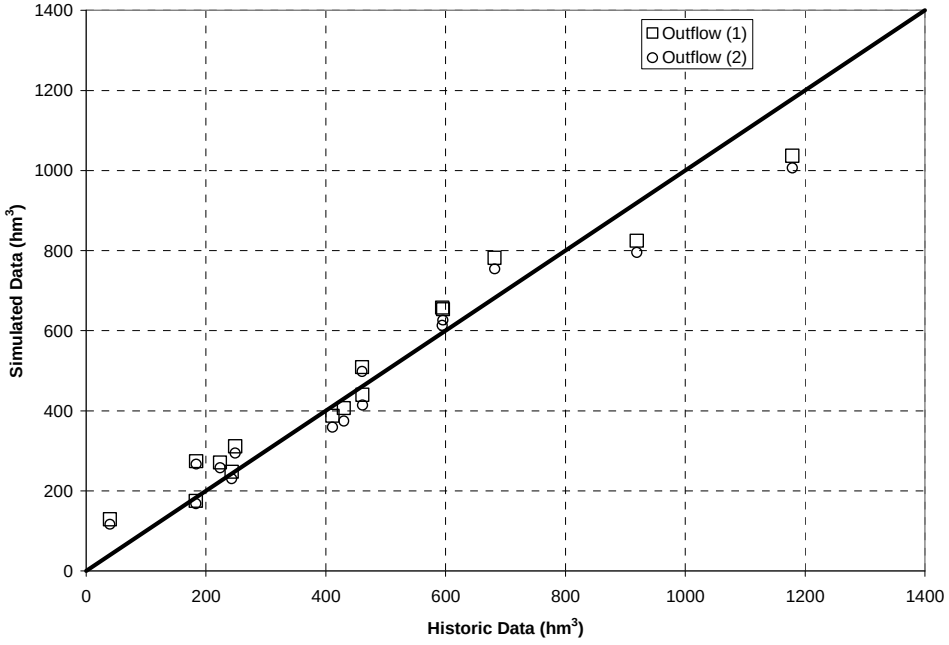

Figure 21 – Scatter plot of yearly cumulative outflow for original (1) and new (2) seepage coefficients versus historical data.

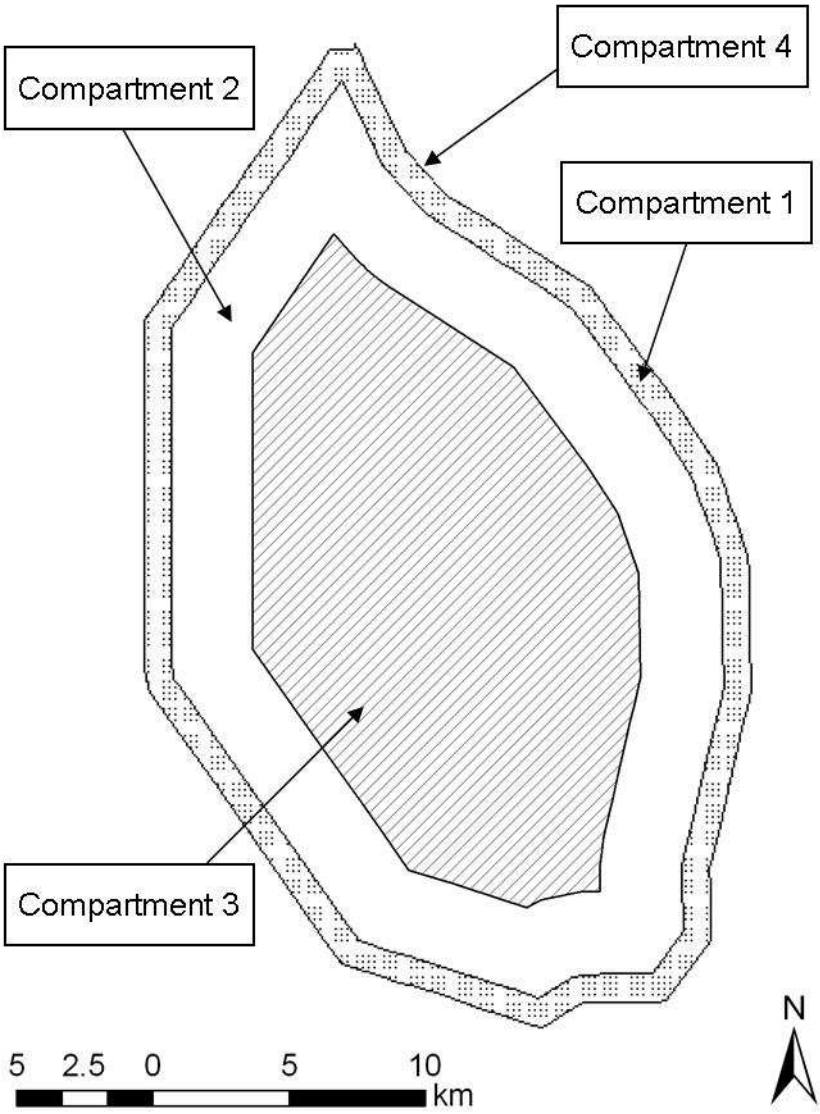

Figure 22 – Compartment arrangement for SRSM constituent models; adapted from Arceneaux et al. (2007).

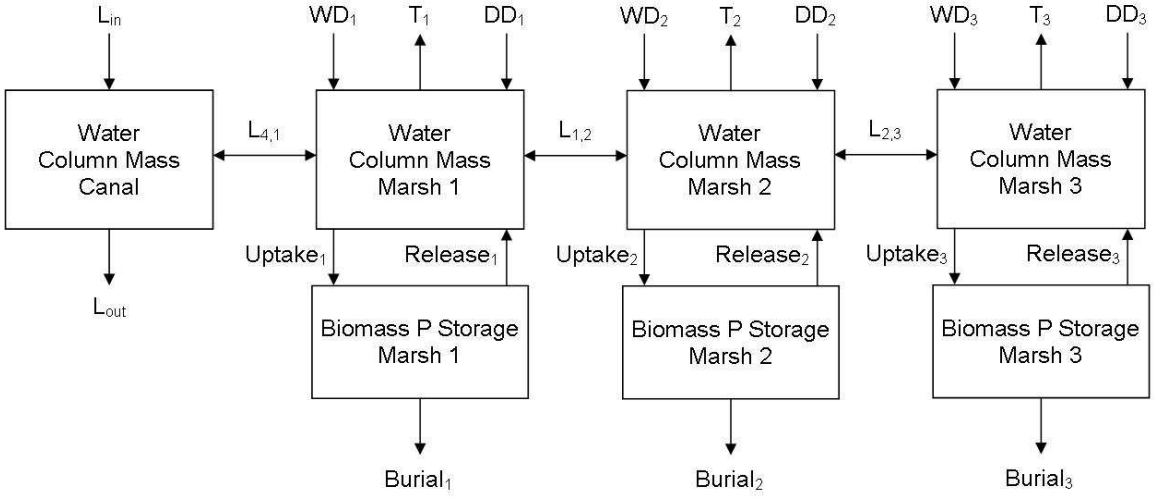

Figure 23 – Adaptation of the P-cycling model to the SRSM compartment layout.

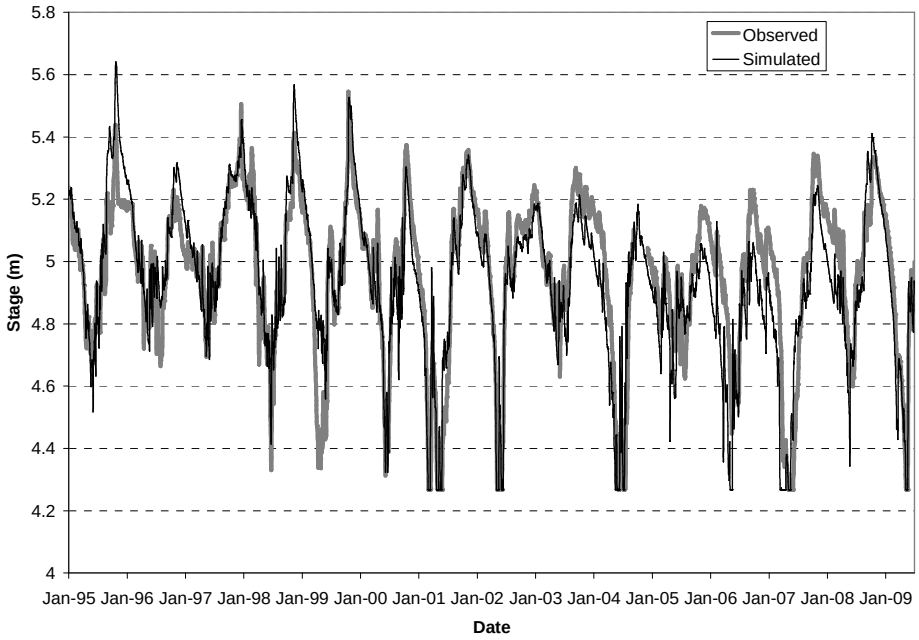

Figure 24 – Canal stage time series for the data period (1/1/1995 to 6/30/2009).

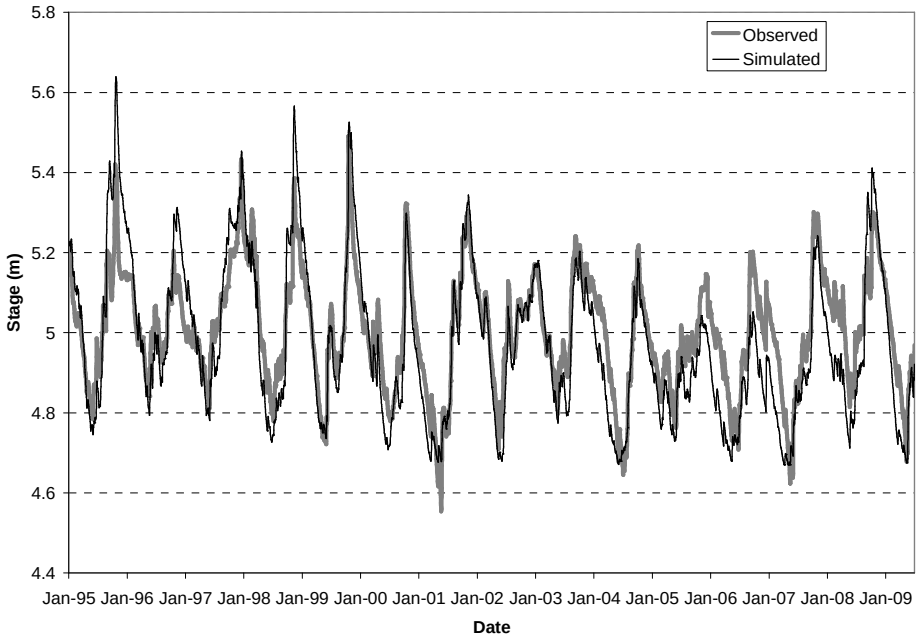

Figure 25 – Marsh stage time series for the data period (1/1/1995 to 6/30/2009).

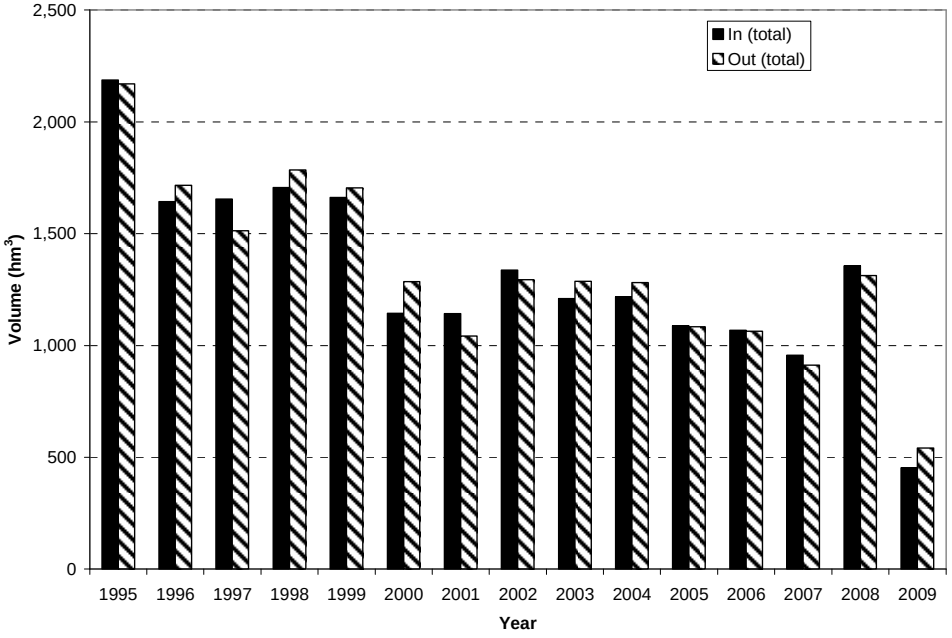

Figure 26 – Cumulative values of total water volume entering and leaving the Refuge on a yearly basis.

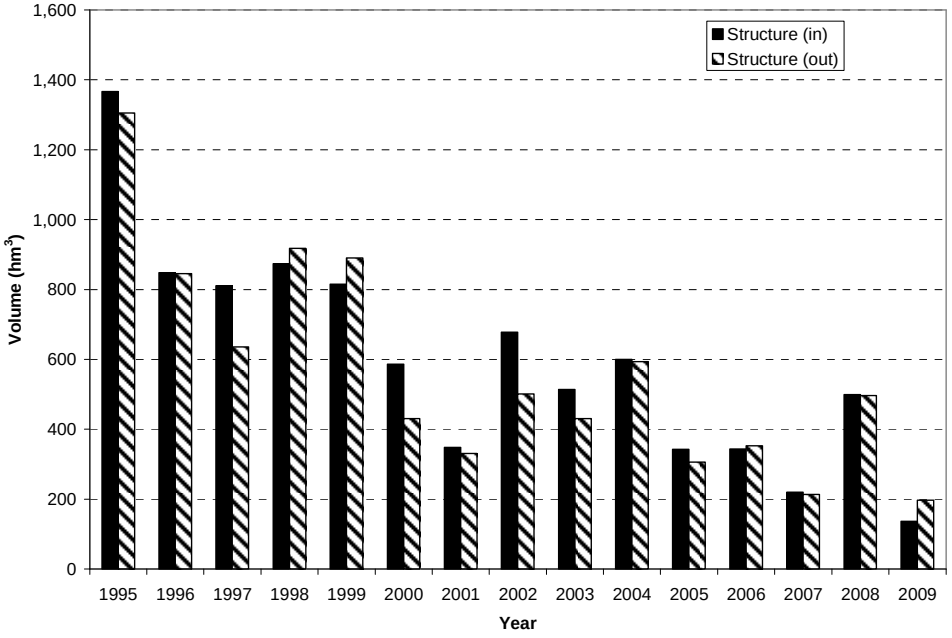

Figure 27 – Cumulative values of water volume entering (data driven) and leaving (estimated by model) the Refuge through perimeter canal structures on a yearly basis.

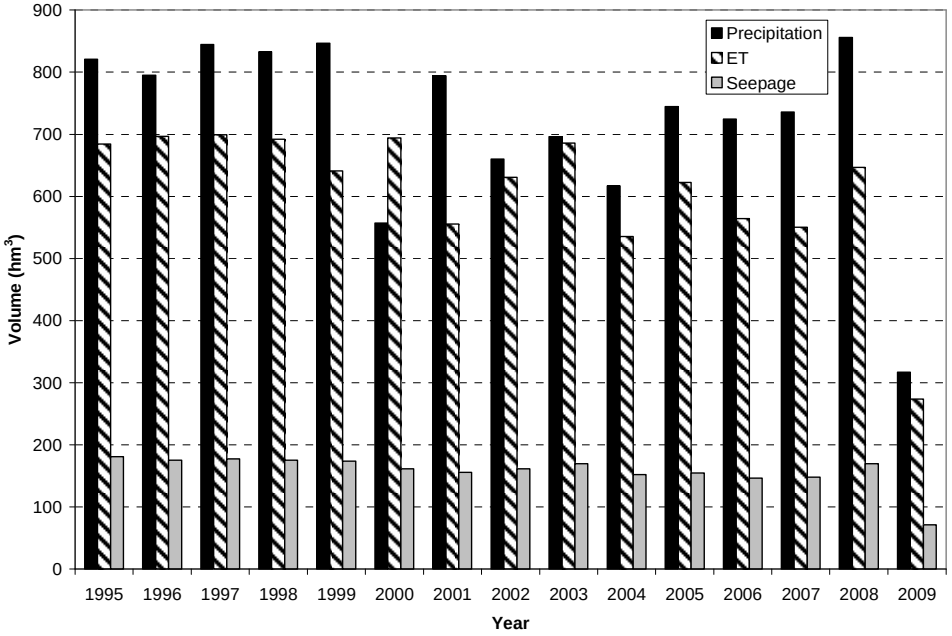

Figure 28 – Cumulative values of water volume entering and leaving the Refuge through precipitation, ET, and seepage on a yearly basis.

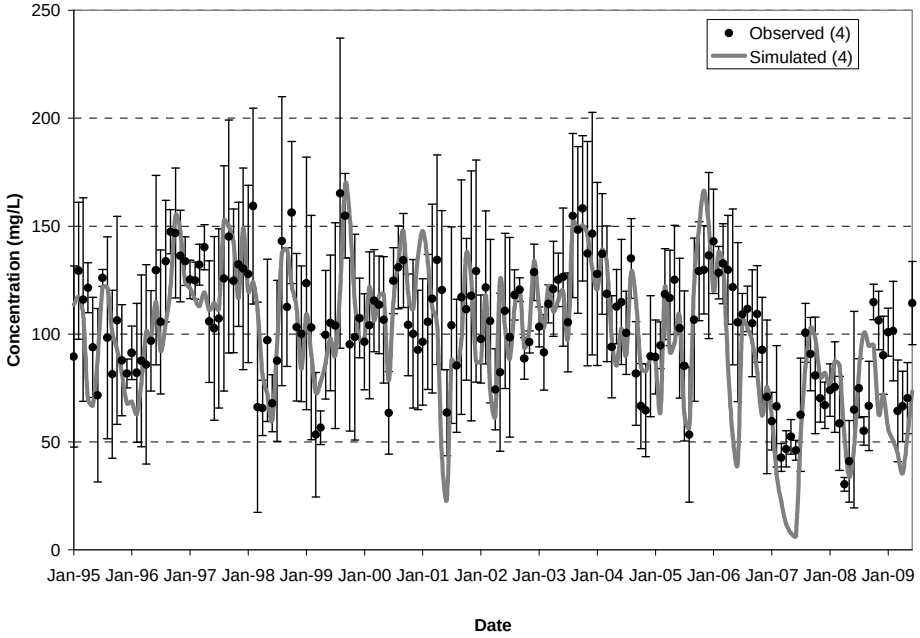

Figure 29 – Monthly time series of canal chloride concentration.

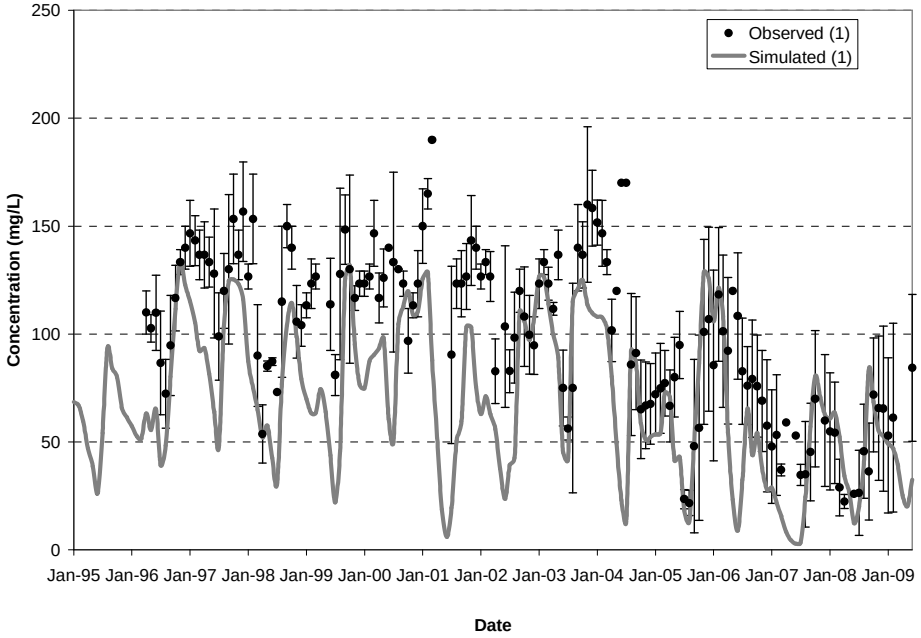

Figure 30 – Monthly time series of compartment 1 chloride concentration.

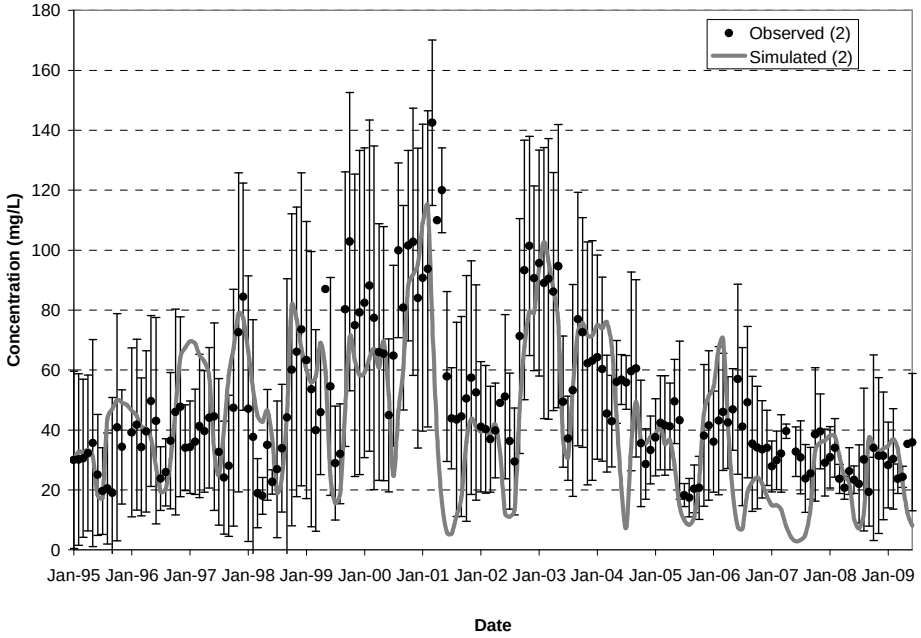

Figure 31 – Monthly time series of compartment 2 chloride concentration.

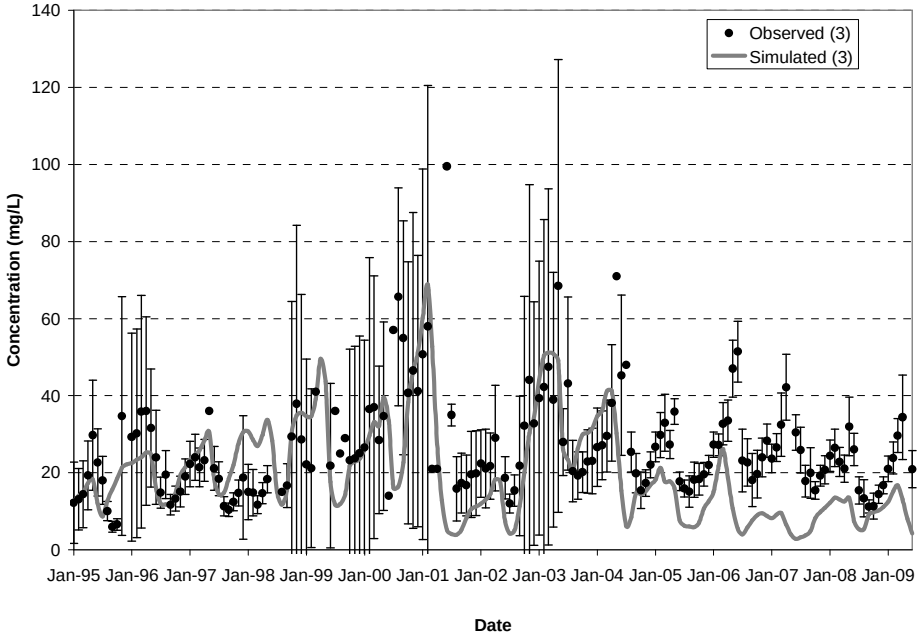

Figure 32 – Monthly time series of compartment 3 chloride concentration.

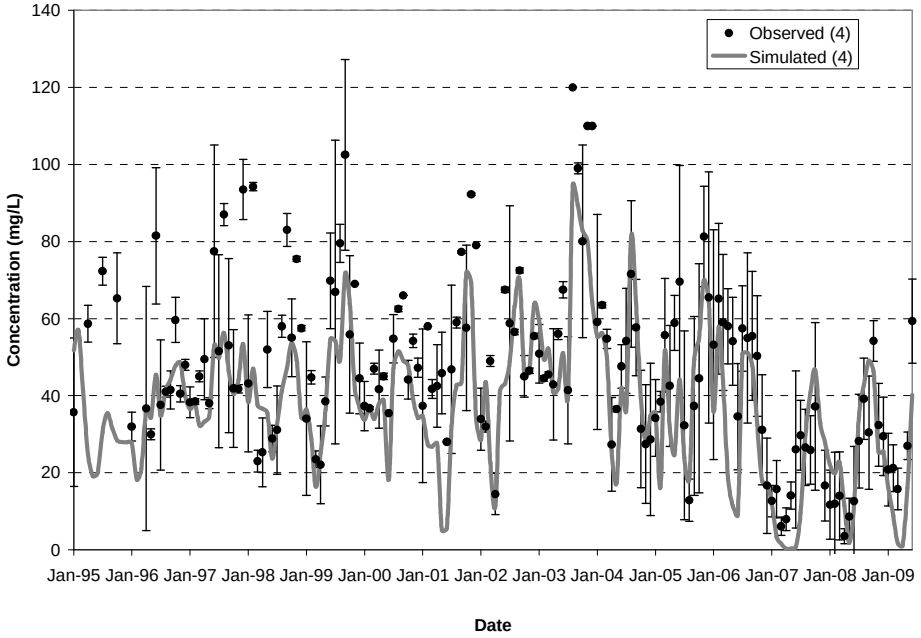

Figure 33 – Monthly time series of canal sulfate concentration.

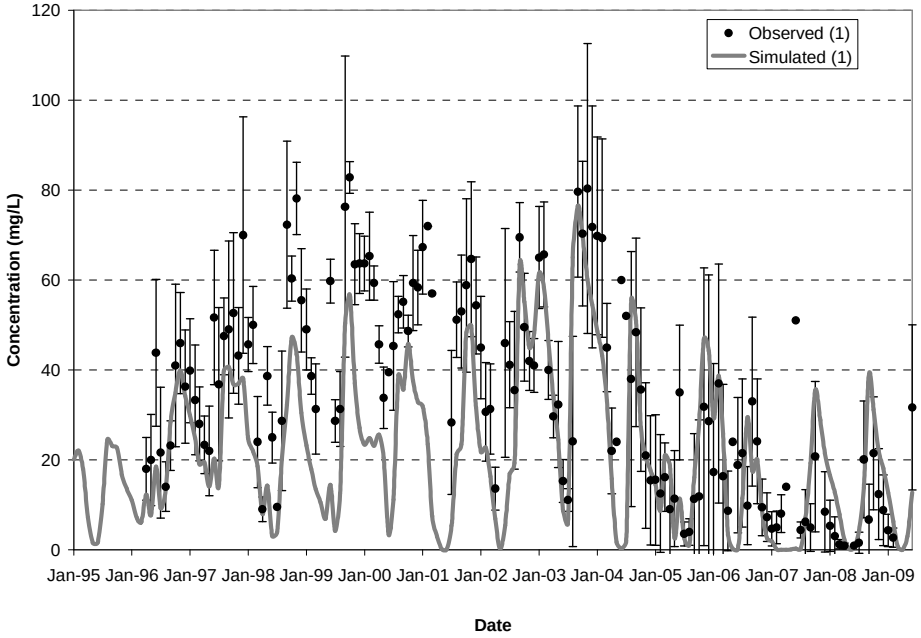

Figure 34 - Monthly time series of compartment 1 sulfate concentration.

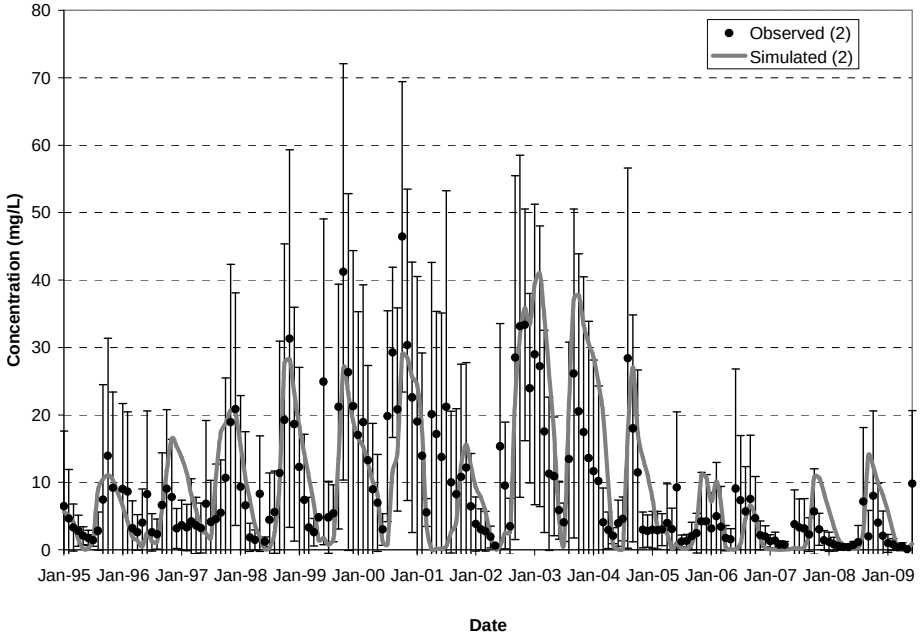

Figure 35 – Monthly time series of compartment 2 sulfate concentration.

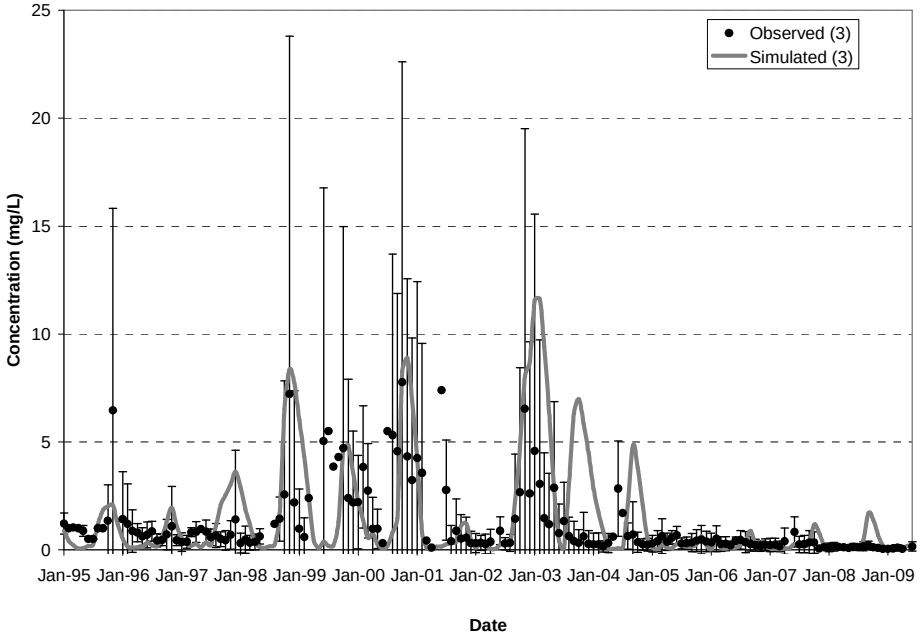

Figure 36 – Monthly time series of compartment 3 sulfate concentration.

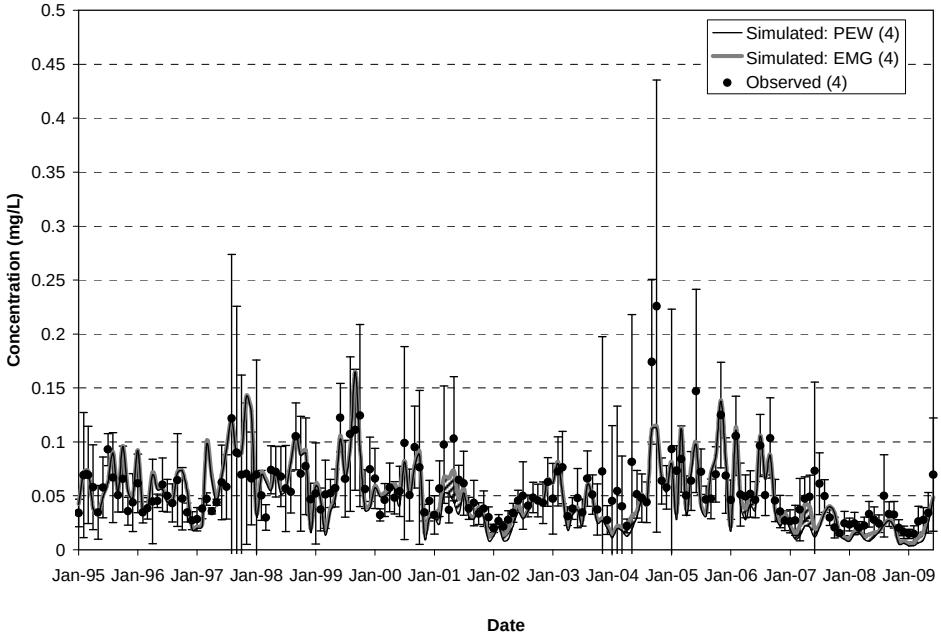

Figure 37 – Monthly envelope time series of canal total phosphorus.

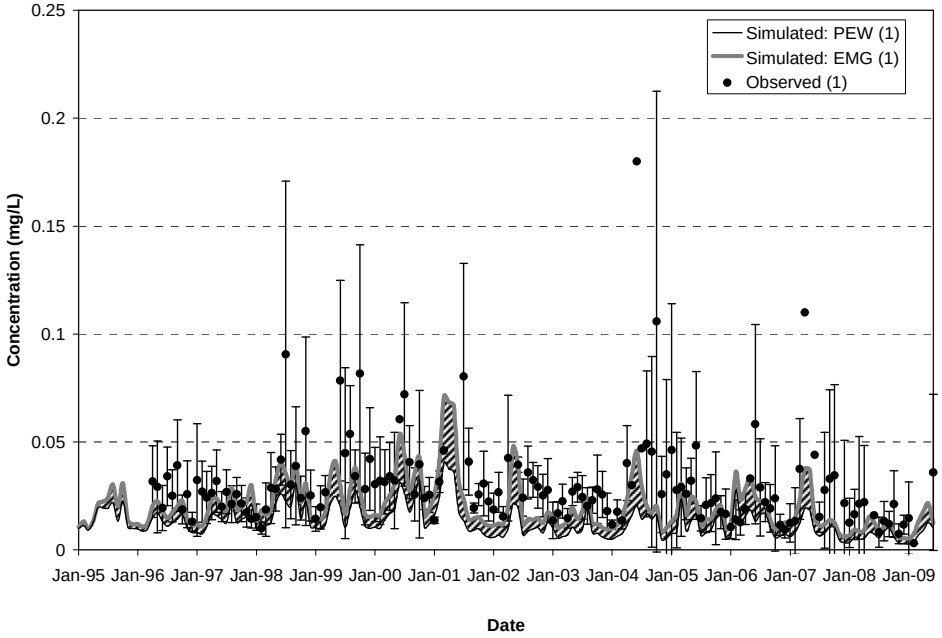

Figure 38 – Monthly envelope time series of compartment 1 total phosphorus.

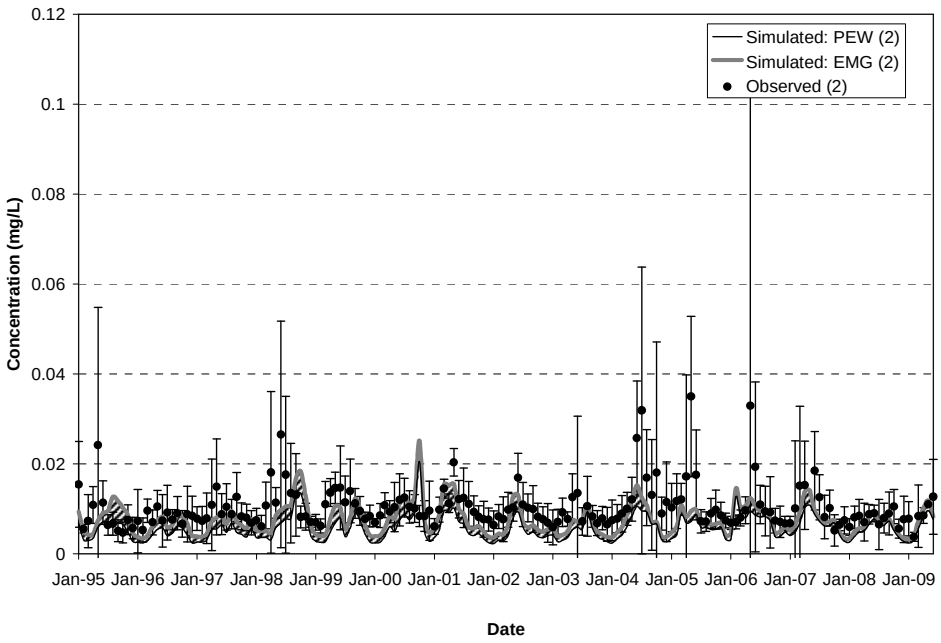

Figure 39 – Monthly envelope time series of compartment 2 total phosphorus.

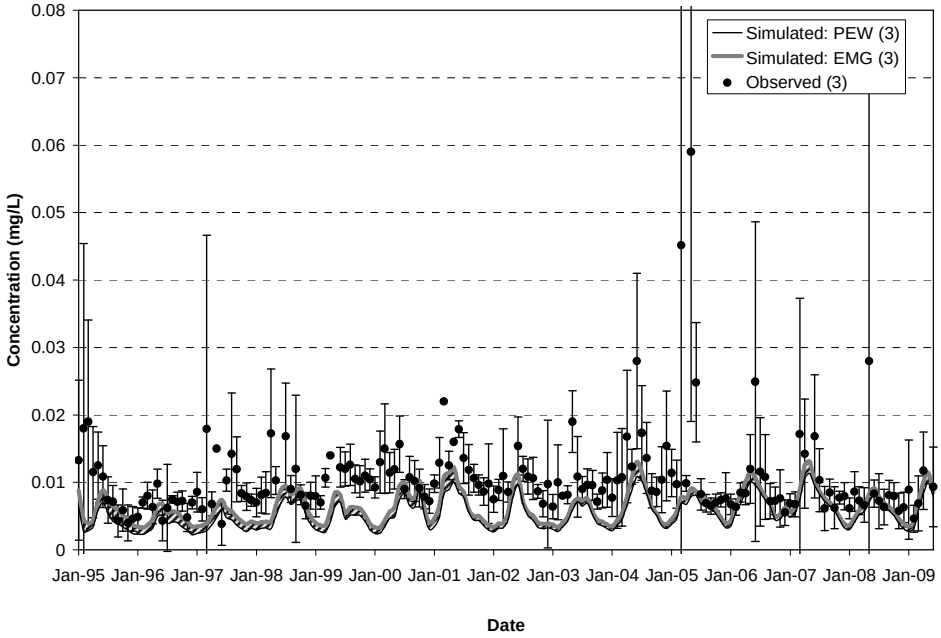

Figure 40 – Monthly envelope time series of compartment 3 total phosphorus.

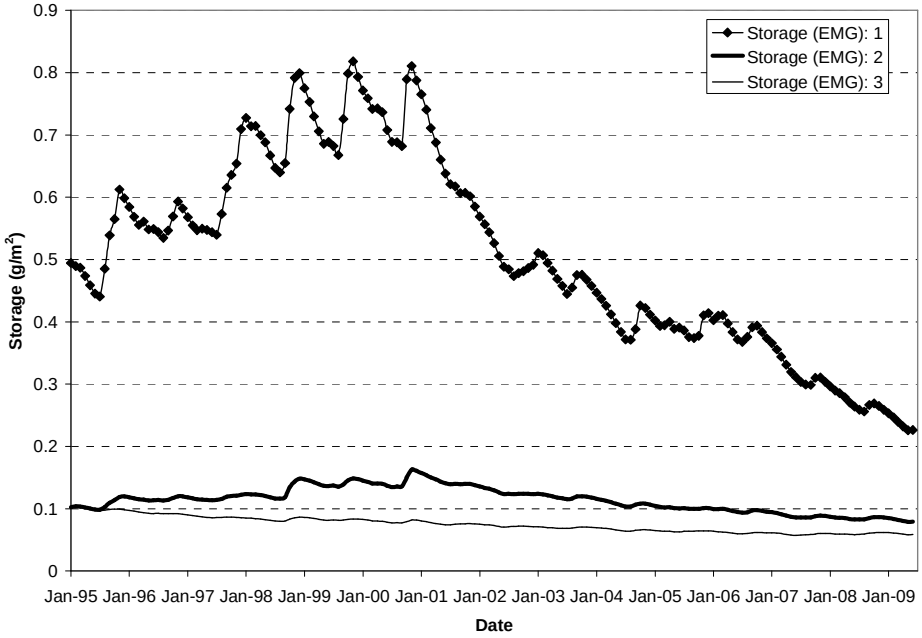

Figure 41 – Monthly storage values from Emergent Marsh simulation.

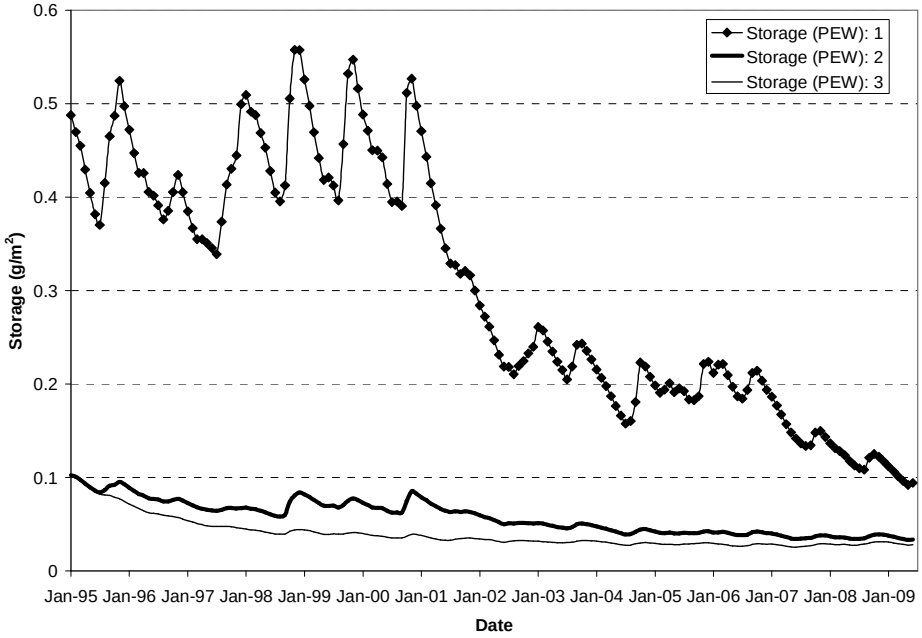

Figure 42 – Monthly storage values from Pre-existent Wetland simulation.

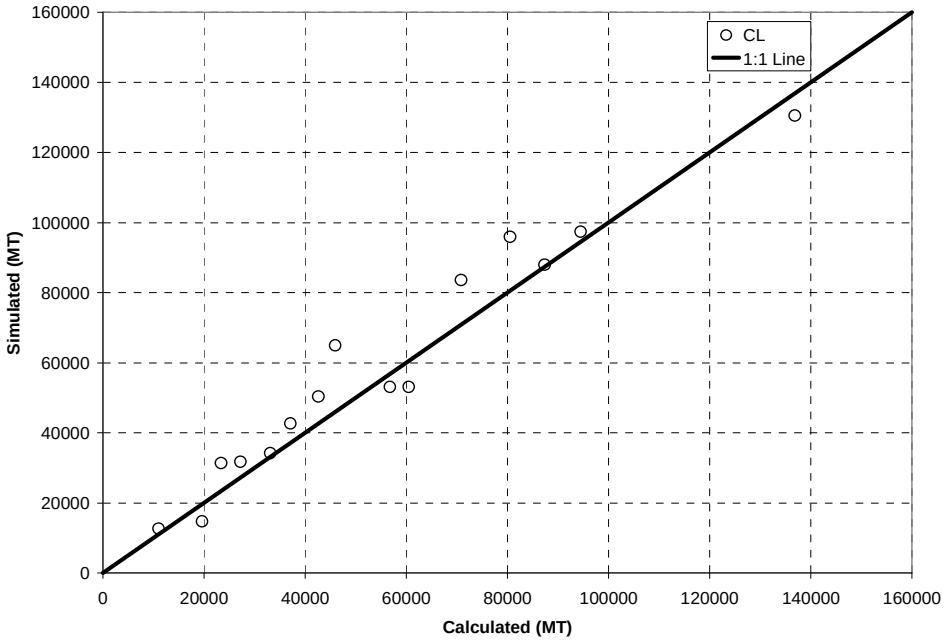

Figure 43 – Cumulative yearly outflow load comparison for chloride.

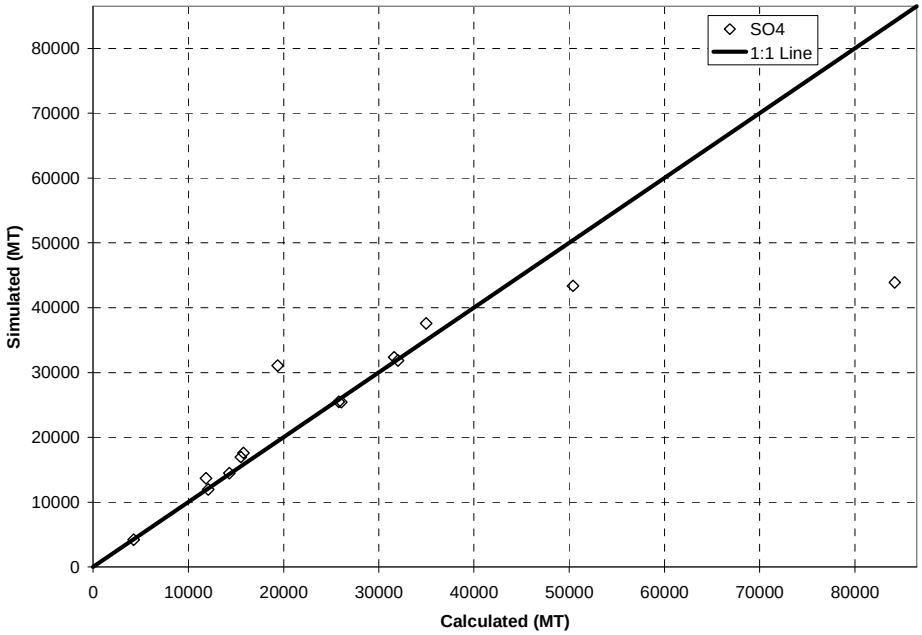

Figure 44 – Cumulative yearly outflow load comparison for sulfate.

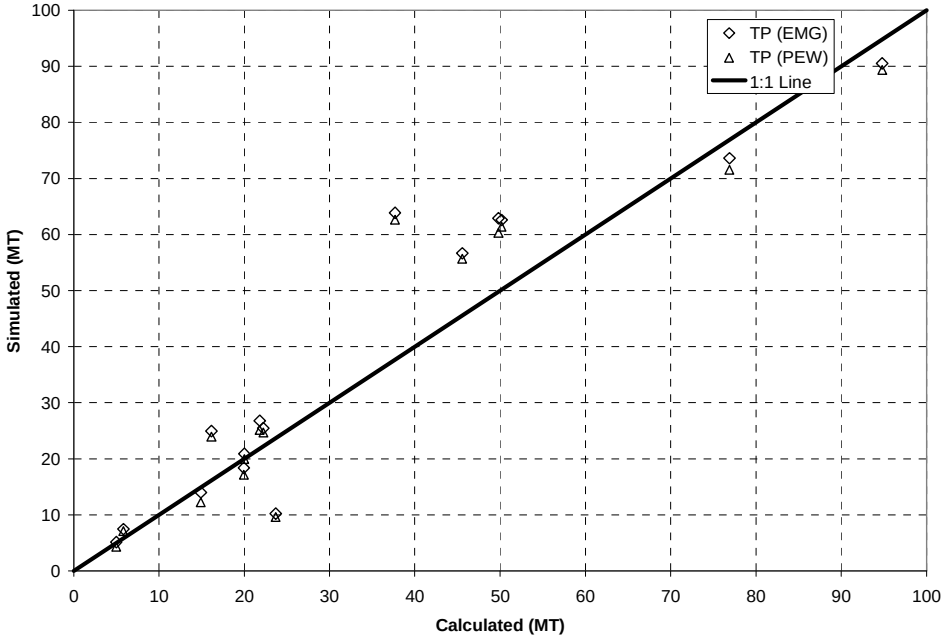

Figure 45 – Cumulative yearly outflow load comparison for total phosphorus.

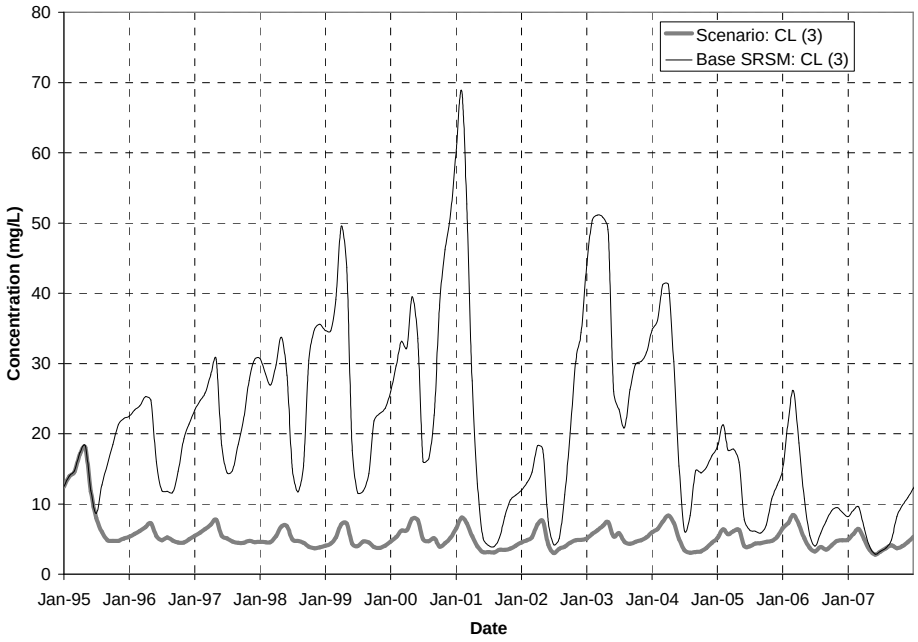

Figure 46 – Interior marsh response to chloride inflow load reduction.

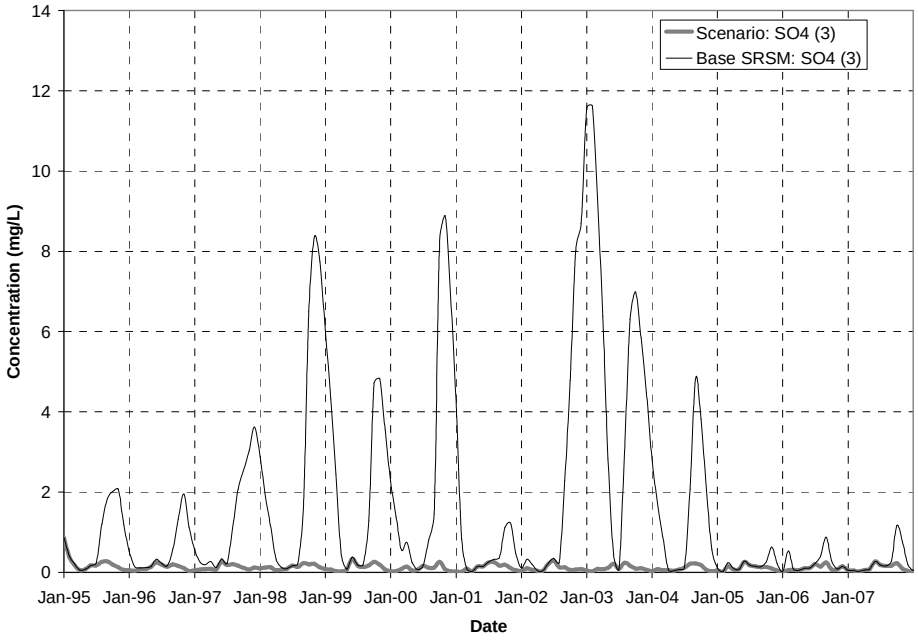

Figure 47 - Interior marsh response to sulfate inflow load reduction.

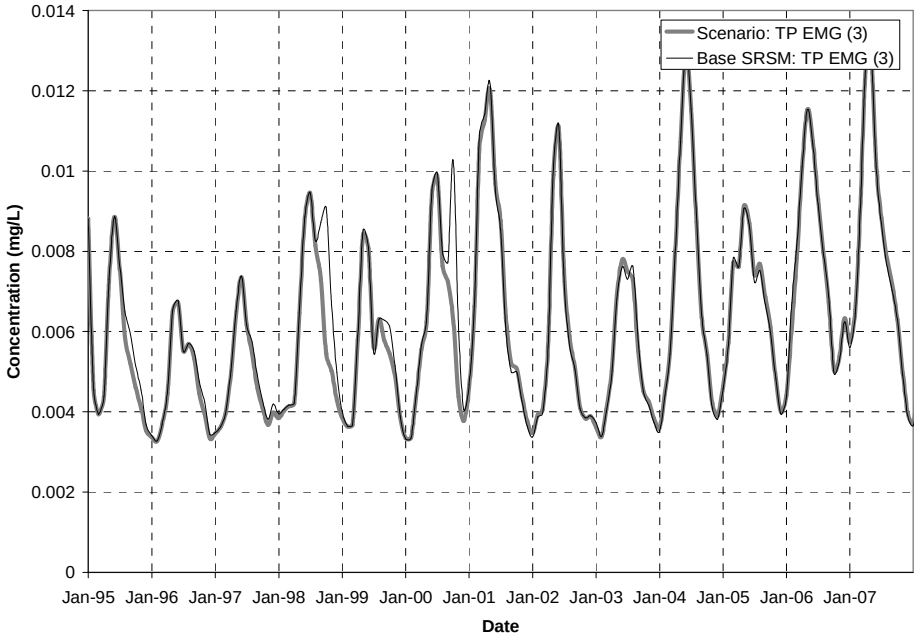

Figure 48 – Interior marsh response to total phosphorus inflow load reduction.

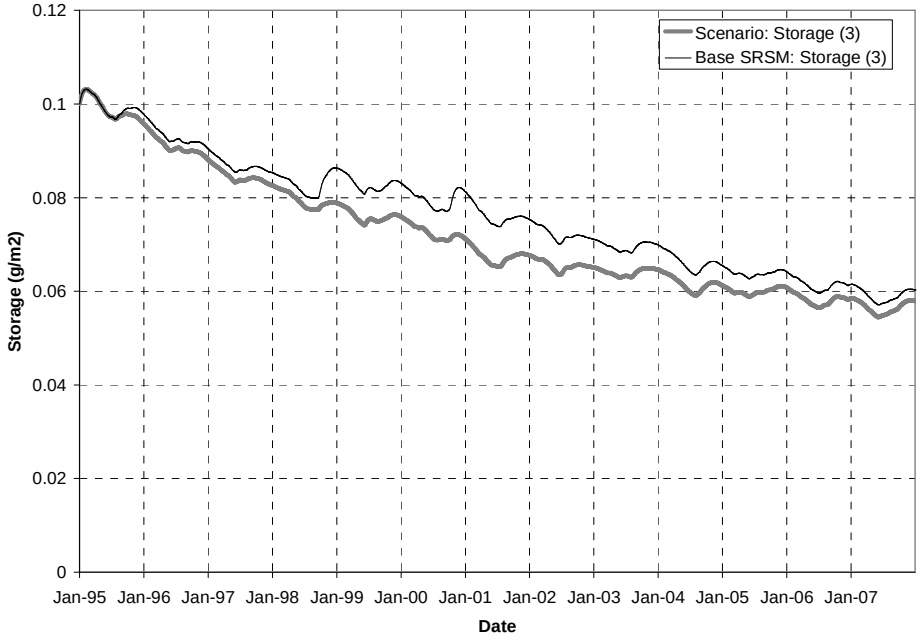

Figure 49 – Interior marsh storage response to total phosphorus inflow load reduction.

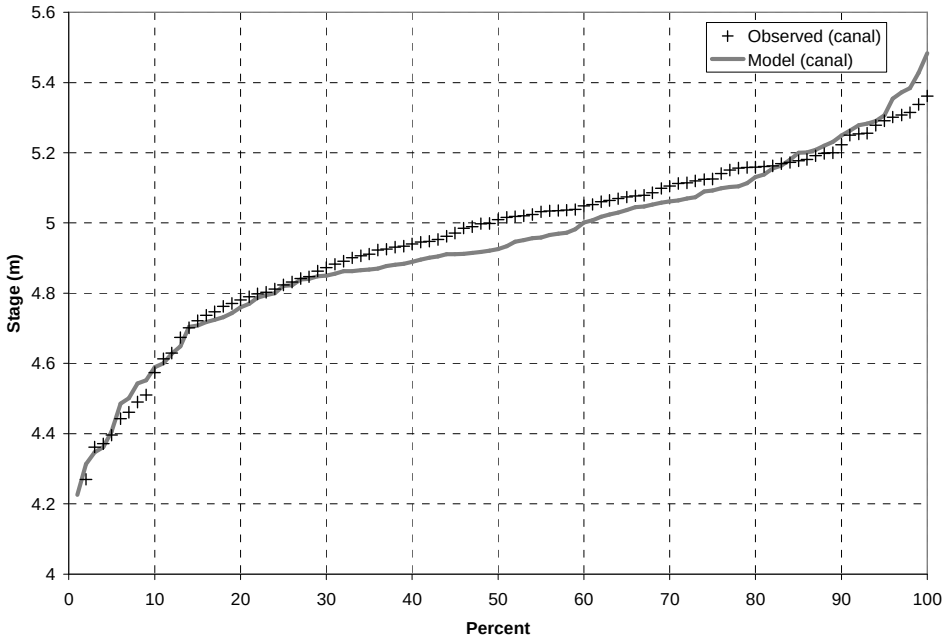

Figure 50 – Canal percent distribution curve.

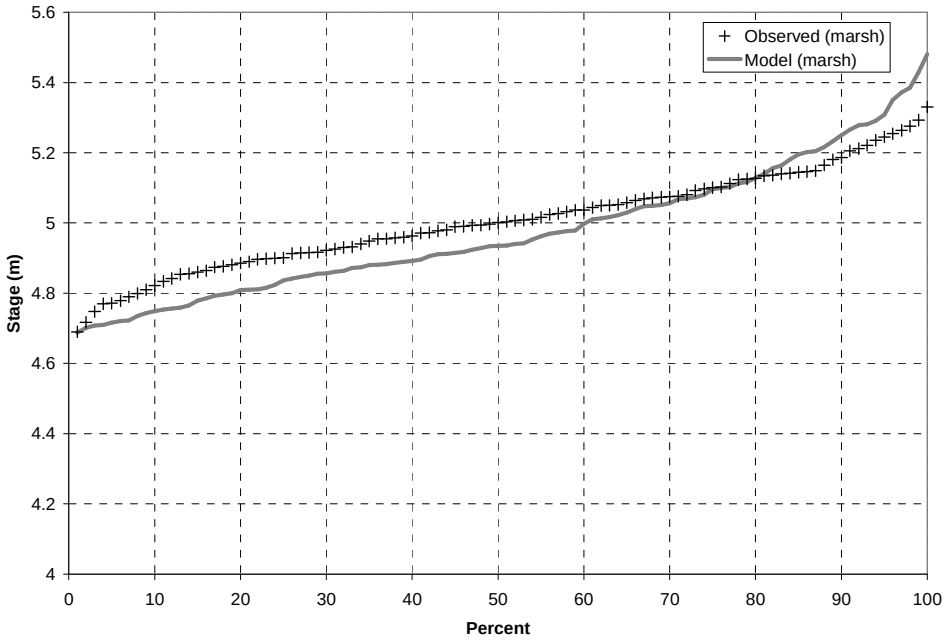

Figure 51 – Marsh percent distribution curve.

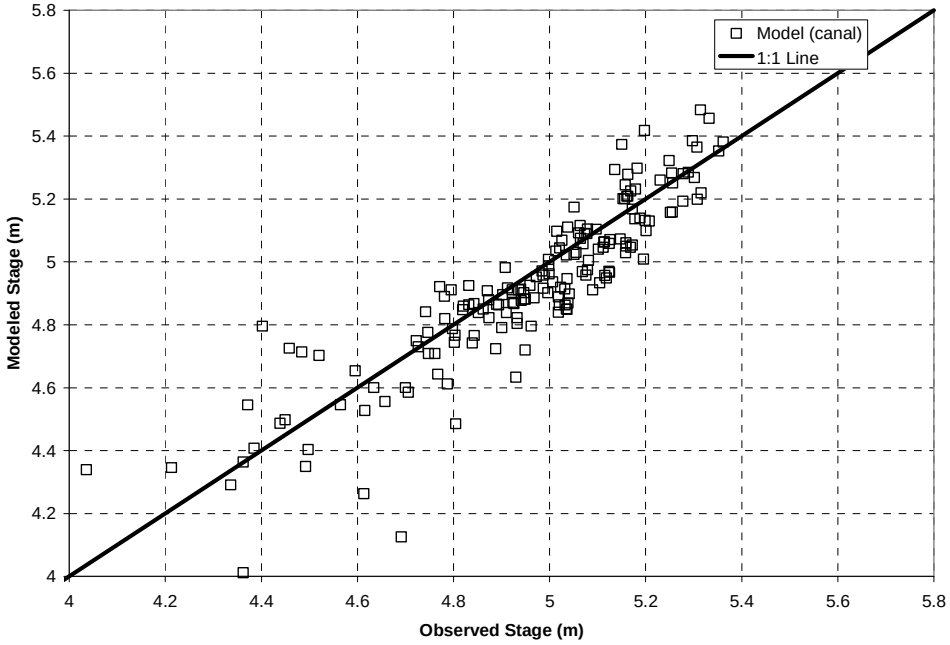

Figure 52 – Canal stage scatter plot.

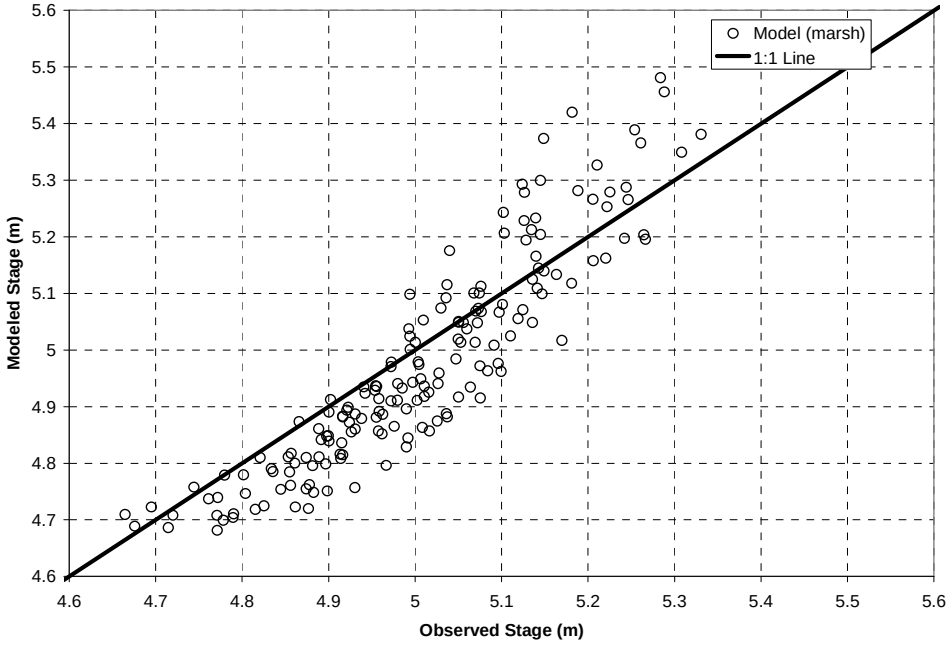

Figure 53 – Marsh stage scatter plot.

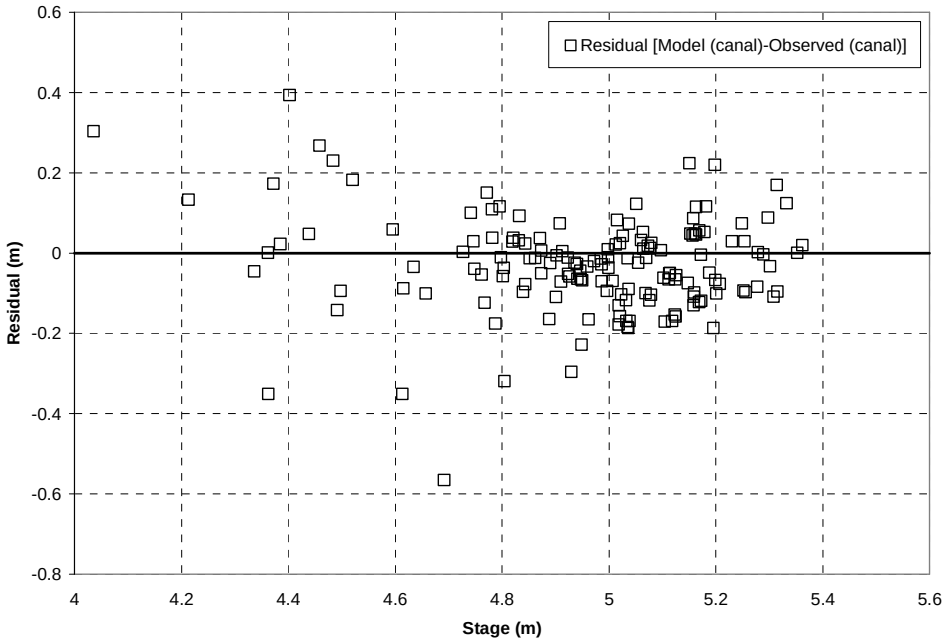

Figure 54 – Canal stage residual.

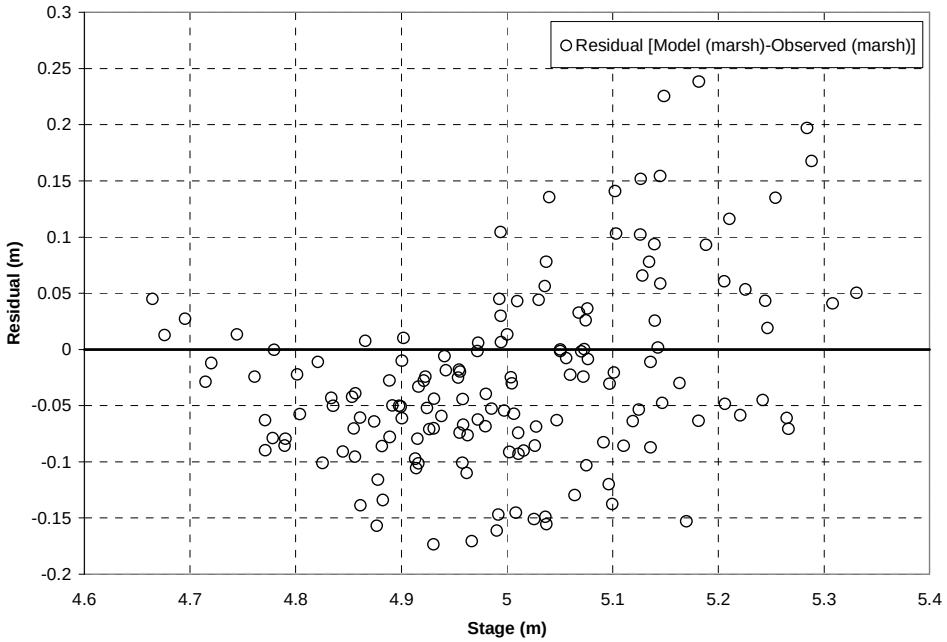

Figure 55 – Marsh stage residual.

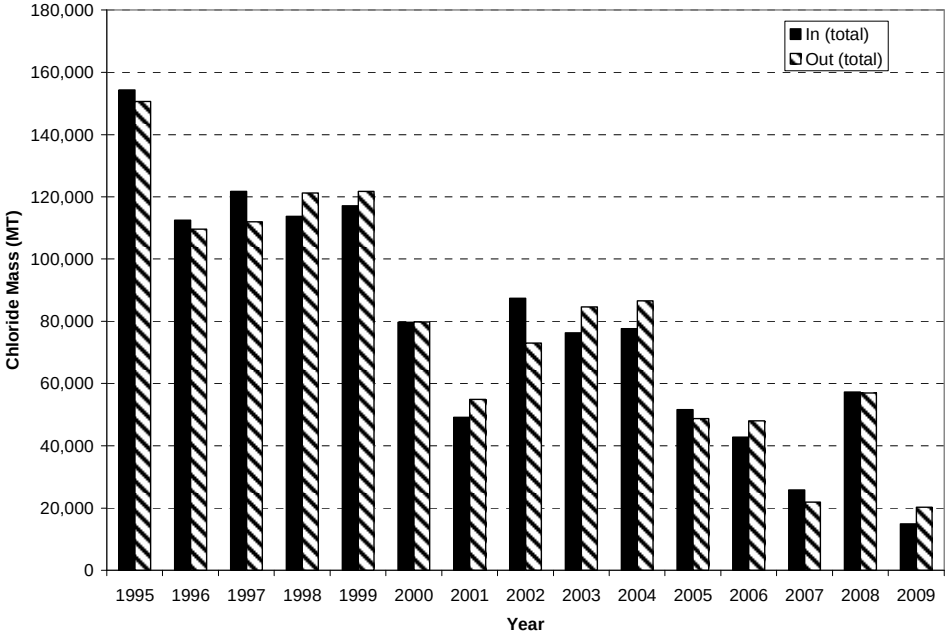

Figure 56 – Total chloride inflow and outflow accumulation for the data period.

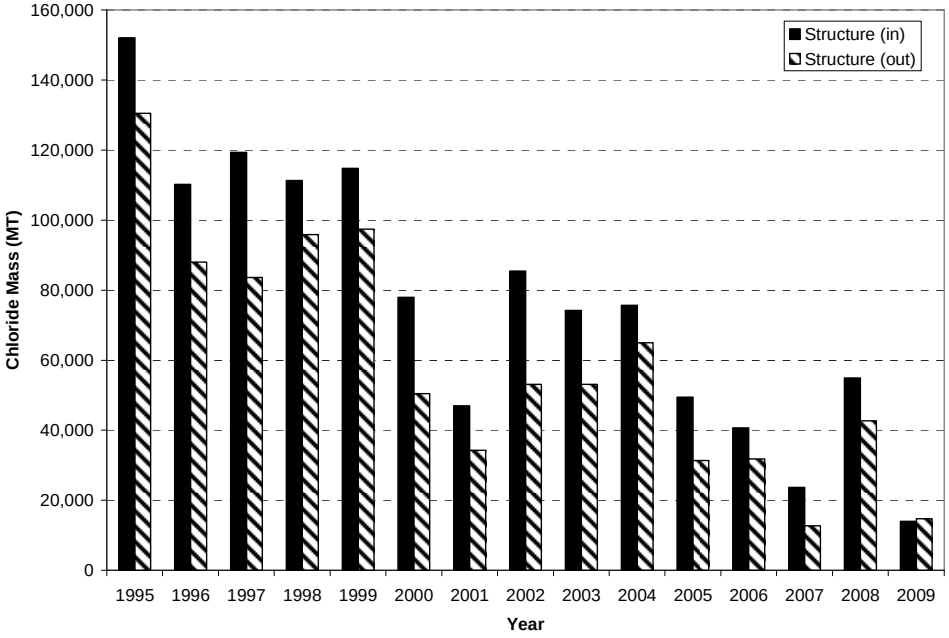

Figure 57 – Yearly chloride inflow and outflow load from perimeter canal structures.

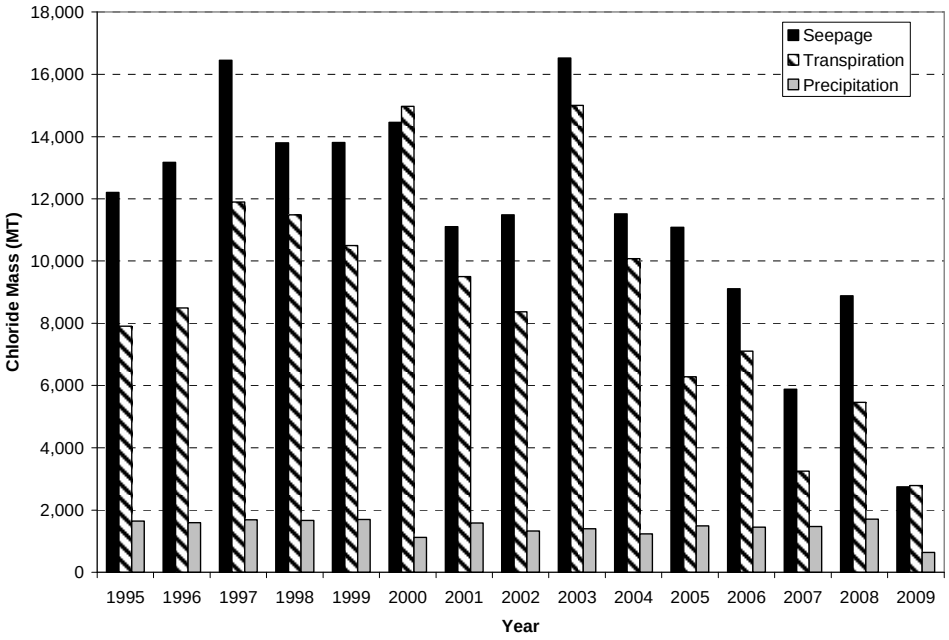

Figure 58 – Yearly chloride accumulated loss to seepage and transpiration; accumulated gain to precipitation.

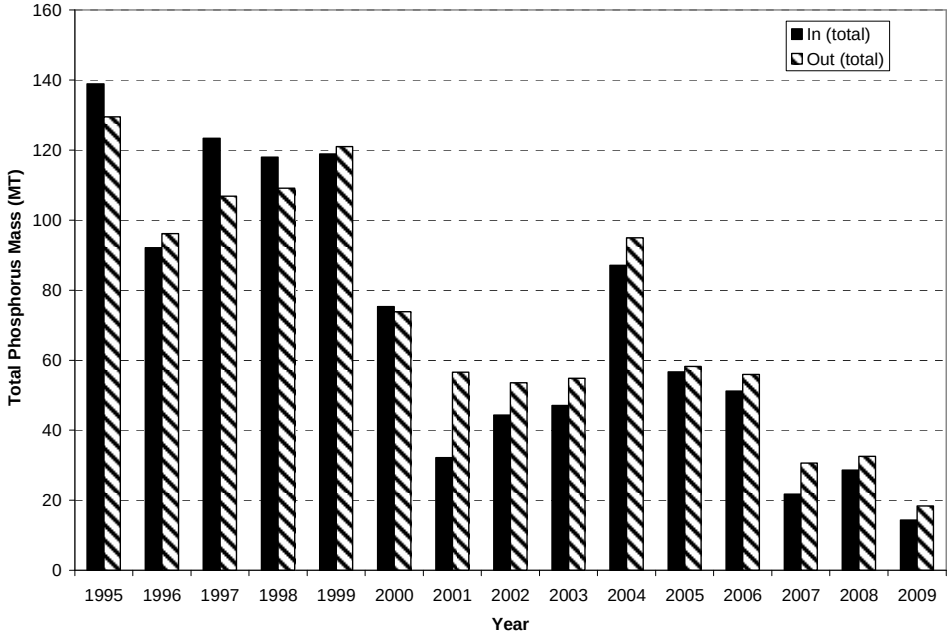

Figure 59 – Total TP (EMG) inflow and outflow accumulation for the data period.

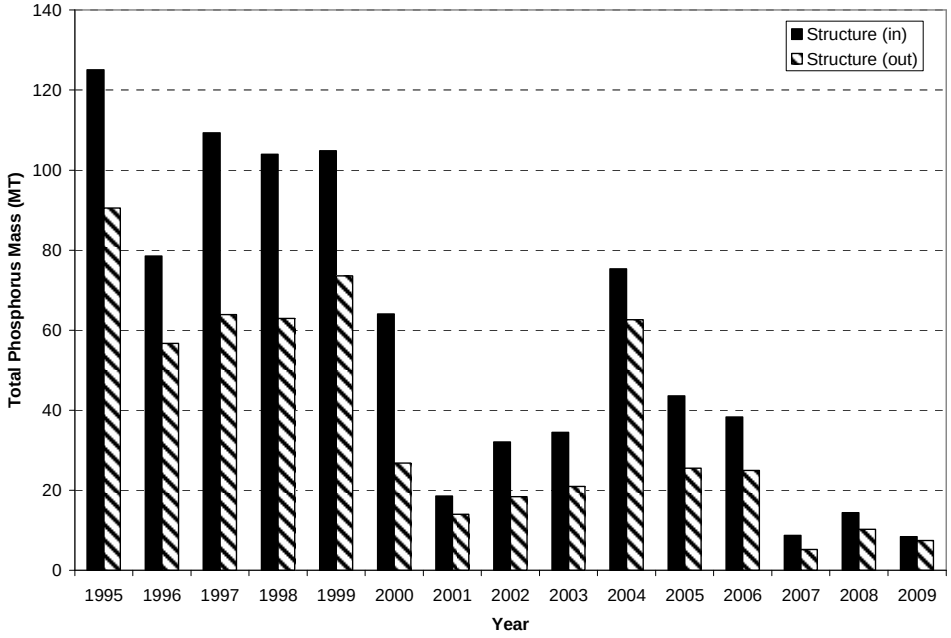

Figure 60 – Yearly TP (EMG) inflow and outflow load from perimeter canal structures.

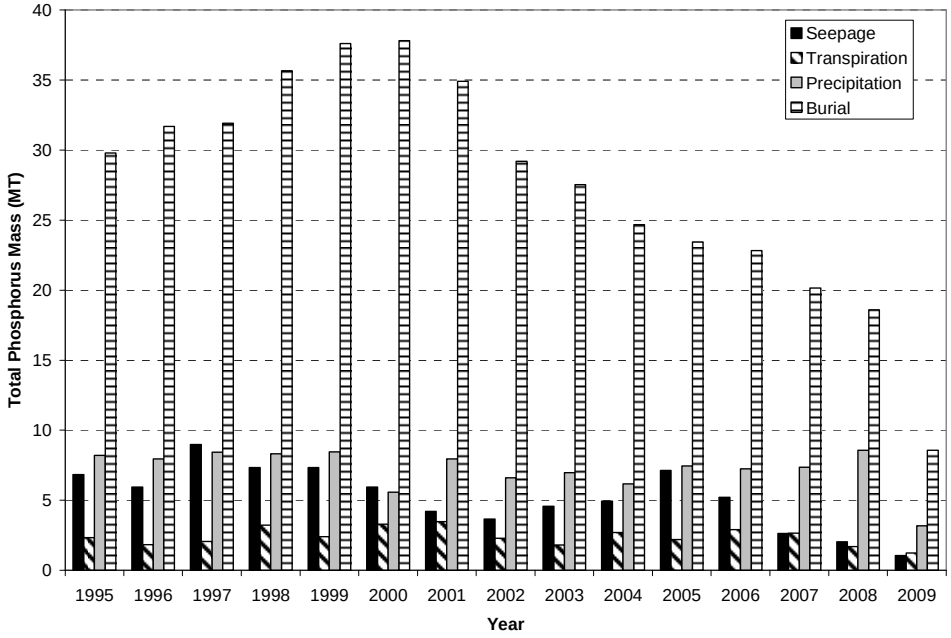

Figure 61 – Yearly TP (EMG) accumulated loss to seepage, transpiration, and burial; accumulated gain to precipitation.

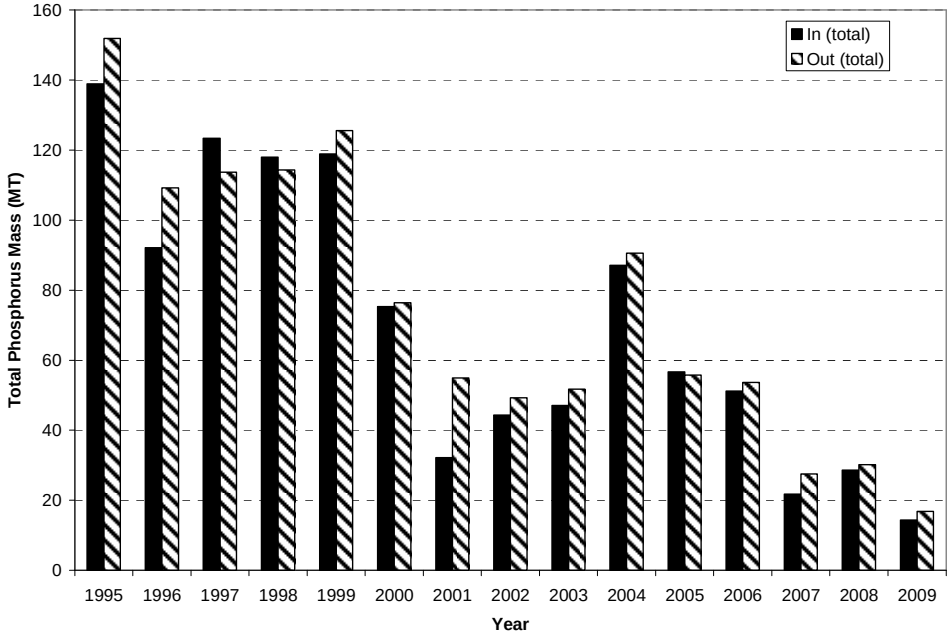

Figure 62 – Total TP (PEW) inflow and outflow accumulation for the data period.

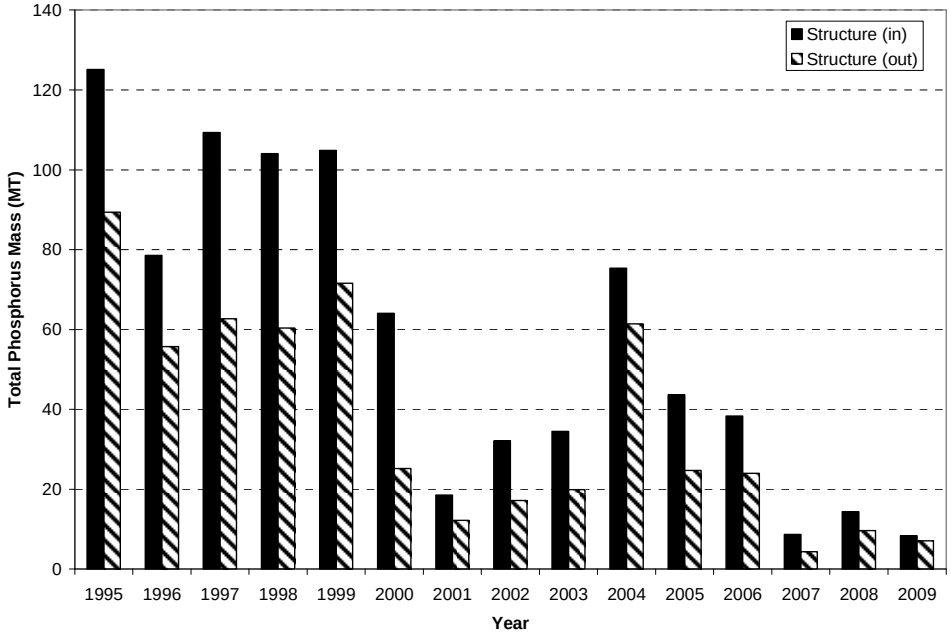

Figure 63 – Yearly TP (PEW) inflow and outflow load from perimeter canal structures.

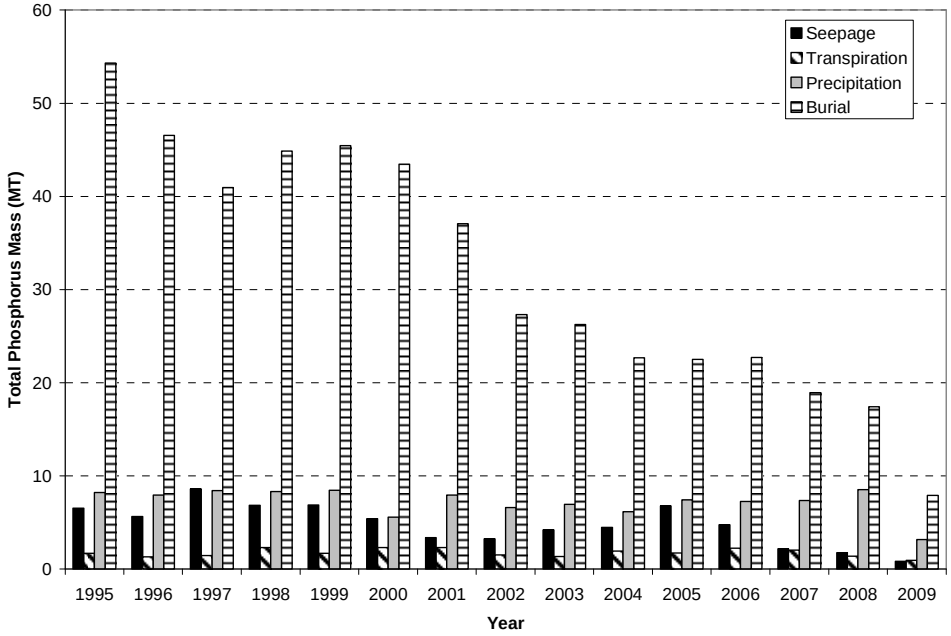

Figure 64 – Yearly TP (PEW) accumulated loss to seepage, transpiration, and burial; accumulated gain to precipitation.

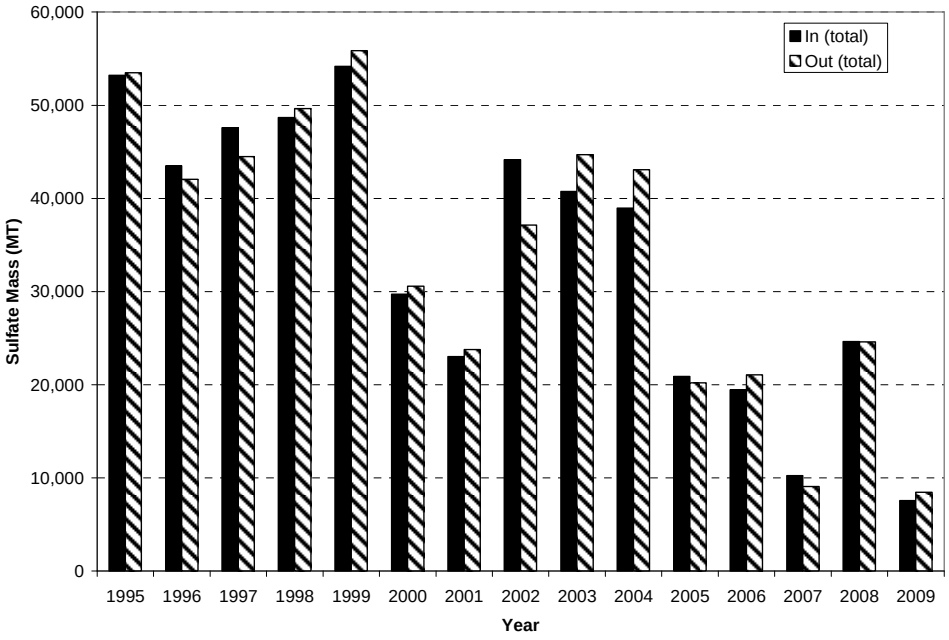

Figure 65 – Total SO4 inflow and outflow accumulation for the data period.

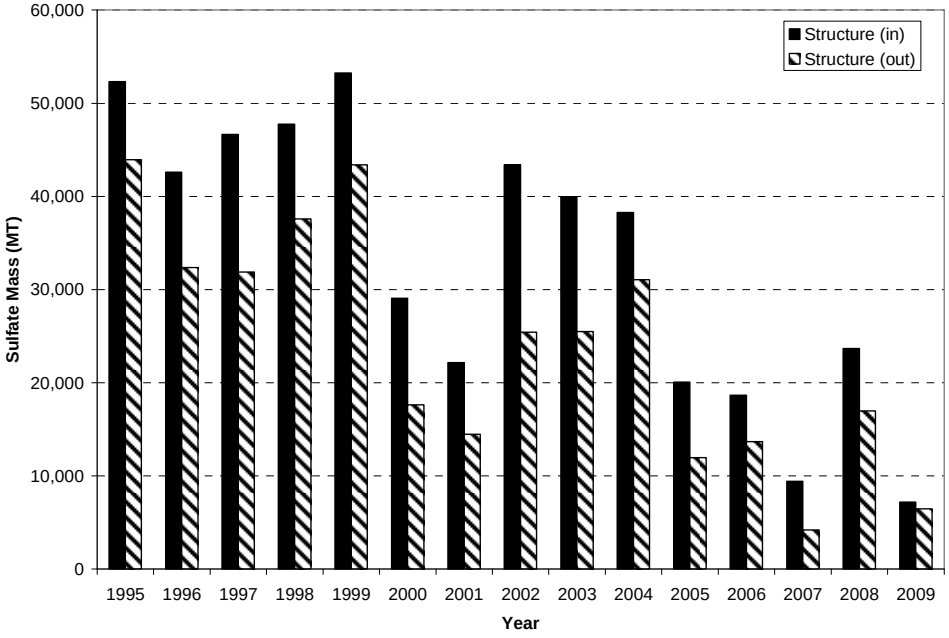

Figure 66 – Yearly SO4 inflow and outflow load from perimeter canal structures.

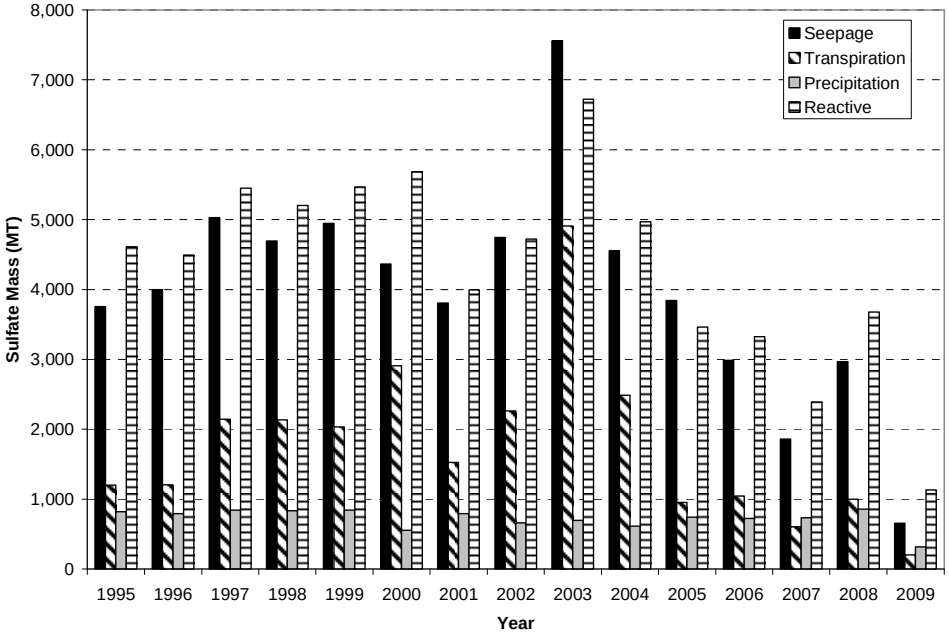

Figure 67 – Yearly SO4 accumulated loss to seepage, transpiration, and reaction; accumulated gain to precipitation.

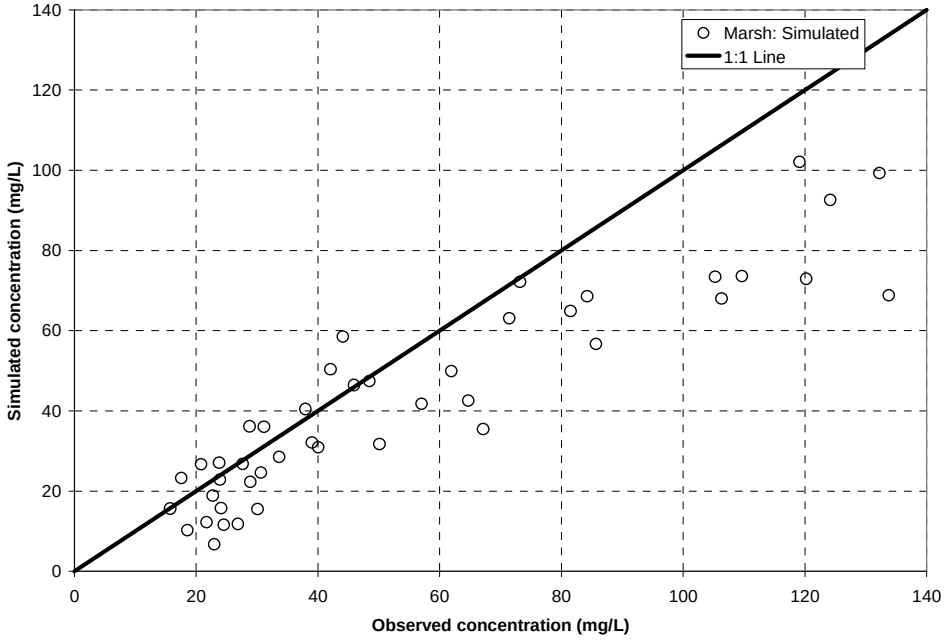

Figure 68 – Yearly average marsh chloride comparison.

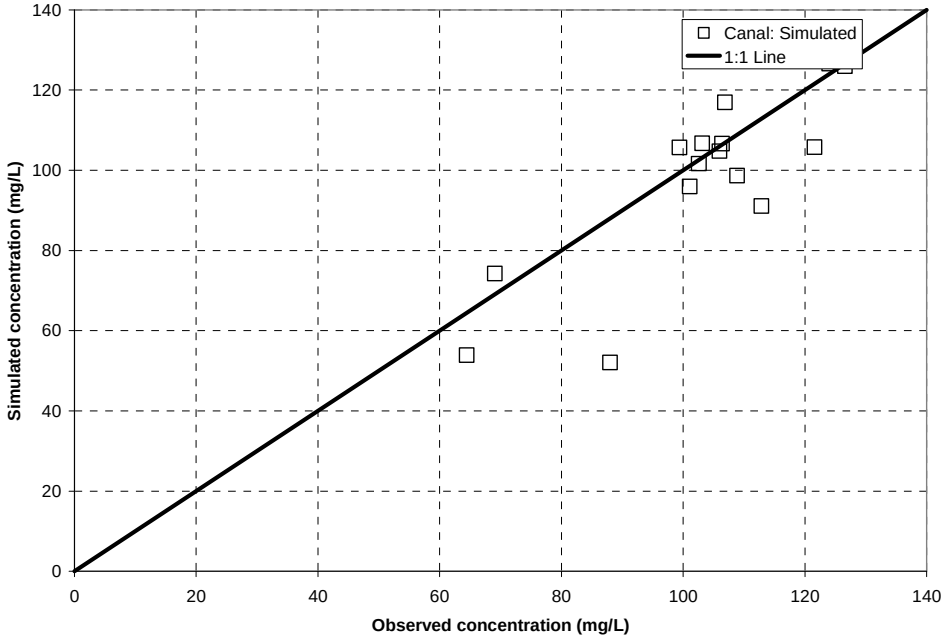

Figure 69 – Yearly average canal chloride comparison.

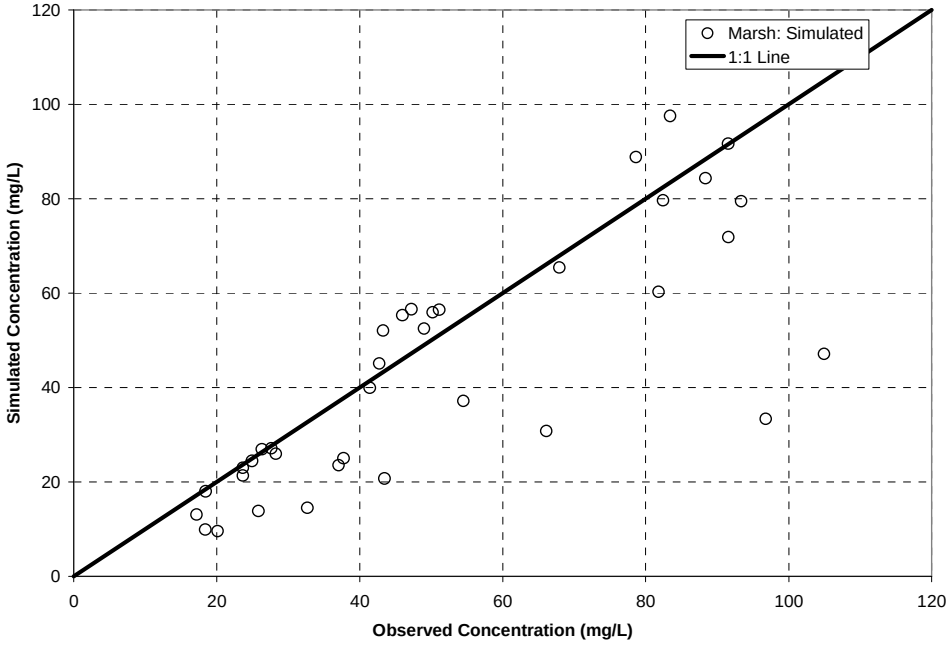

Figure 70 – Monthly average marsh chloride comparison.

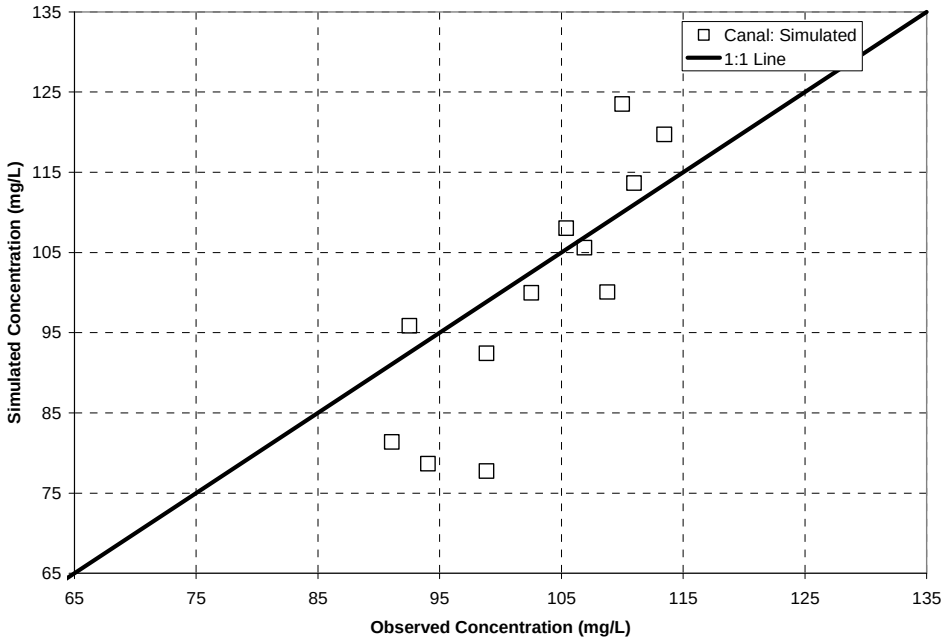

Figure 71 – Monthly average canal chloride comparison.

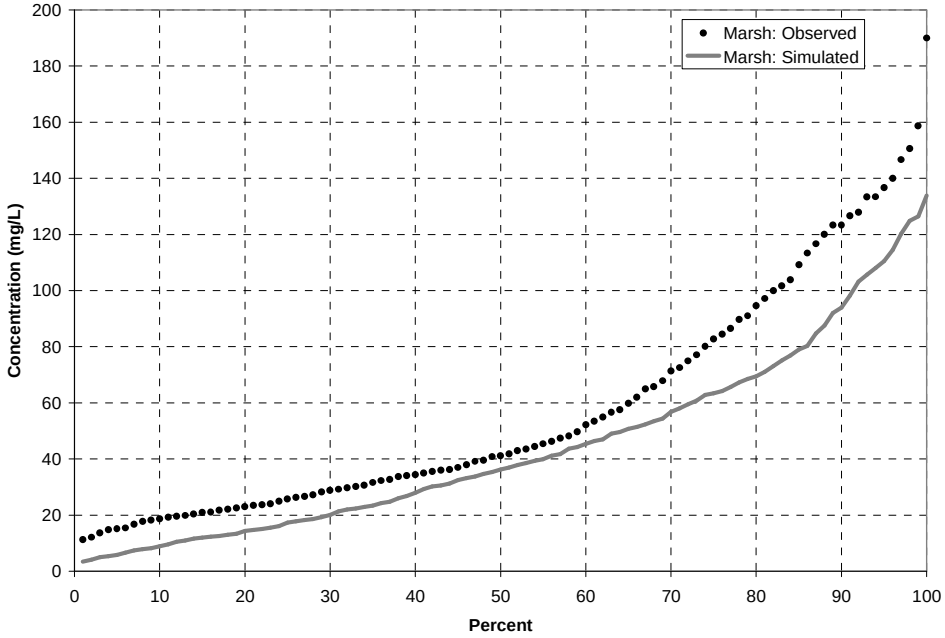

Figure 72 – Percent distribution of chloride in the marsh.

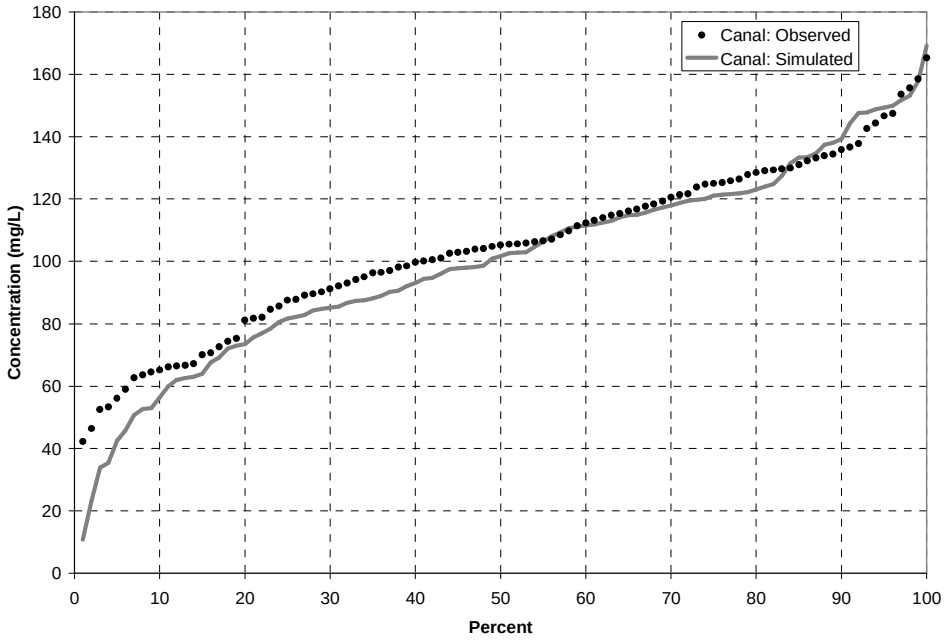

Figure 73 – Percent distribution of chloride in the canal.

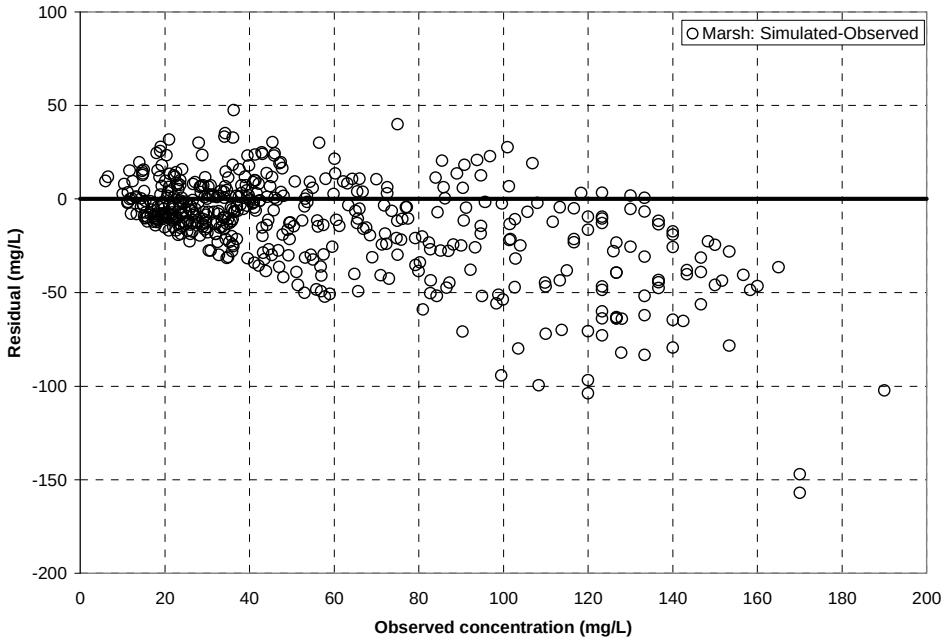

Figure 74 – Residual chloride concentration in the marsh.

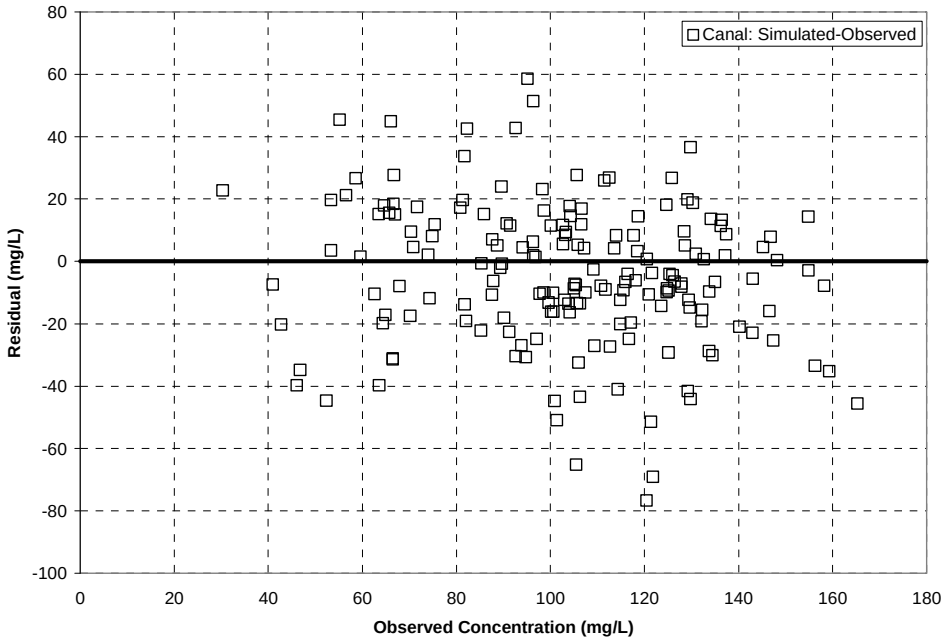

Figure 75 – Residual chloride concentration in the canal.

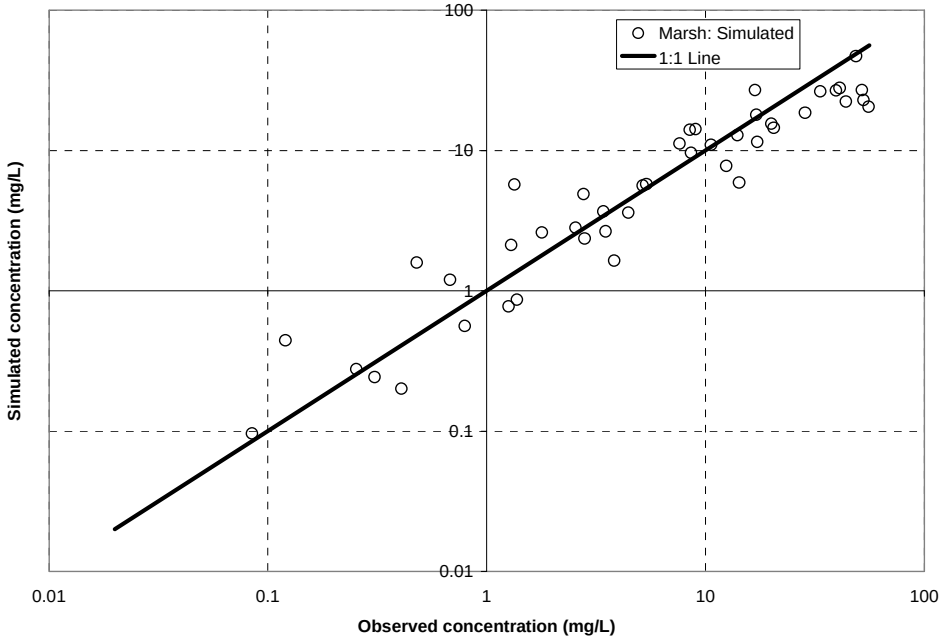

Figure 76 – Yearly average marsh sulfate comparison.

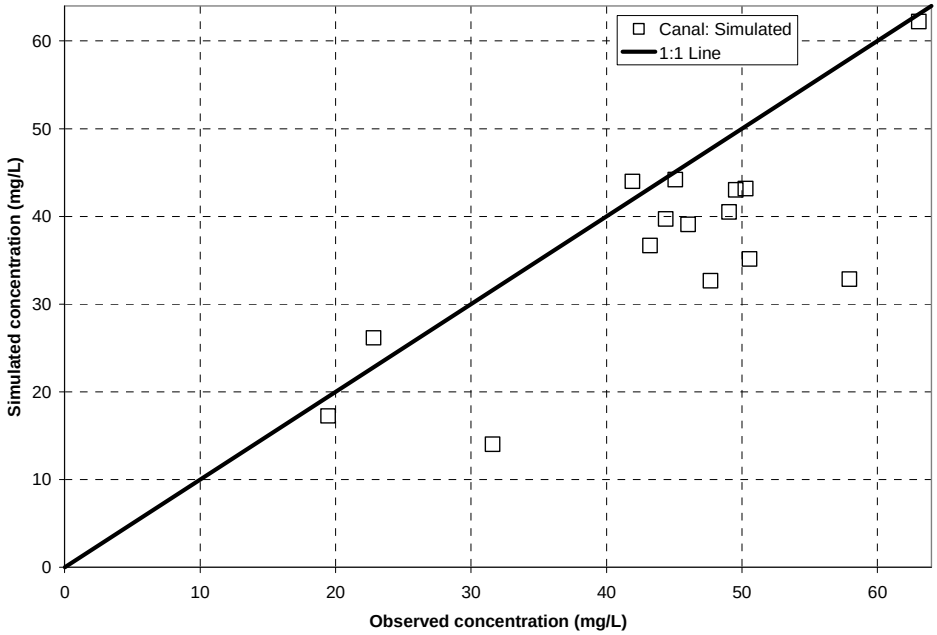

Figure 77 – Yearly average canal sulfate comparison.

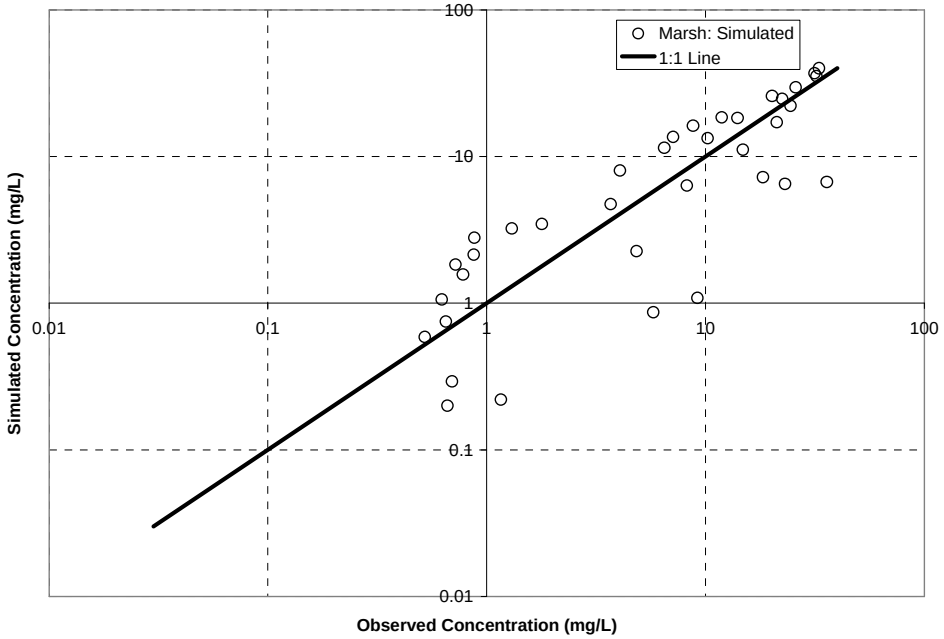

Figure 78 – Monthly average marsh sulfate comparison.

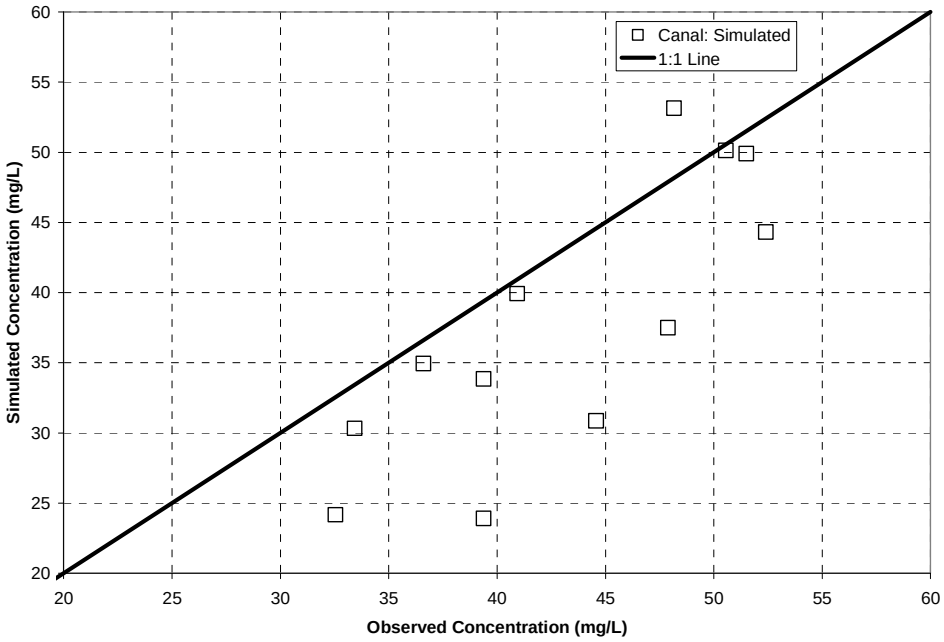

Figure 79 – Monthly average canal sulfate comparison.

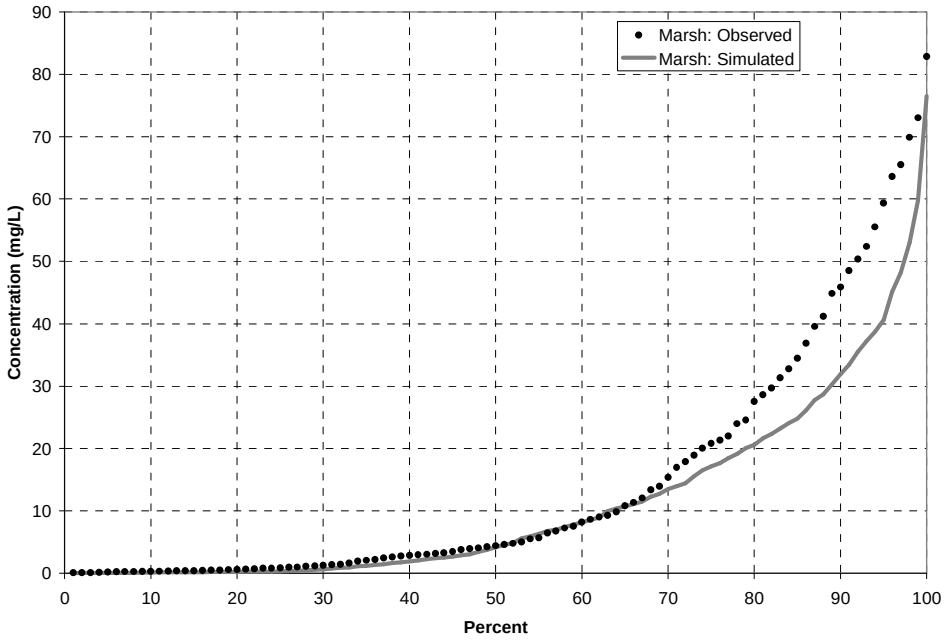

Figure 80 – Percent distribution of sulfate in the marsh.

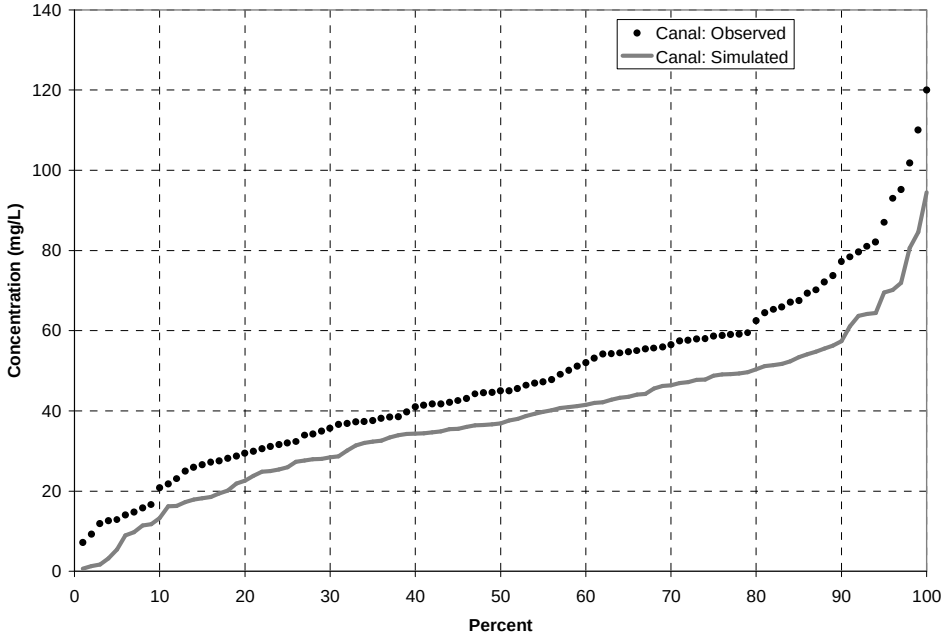

Figure 81 – Percent distribution of sulfate in the canal.

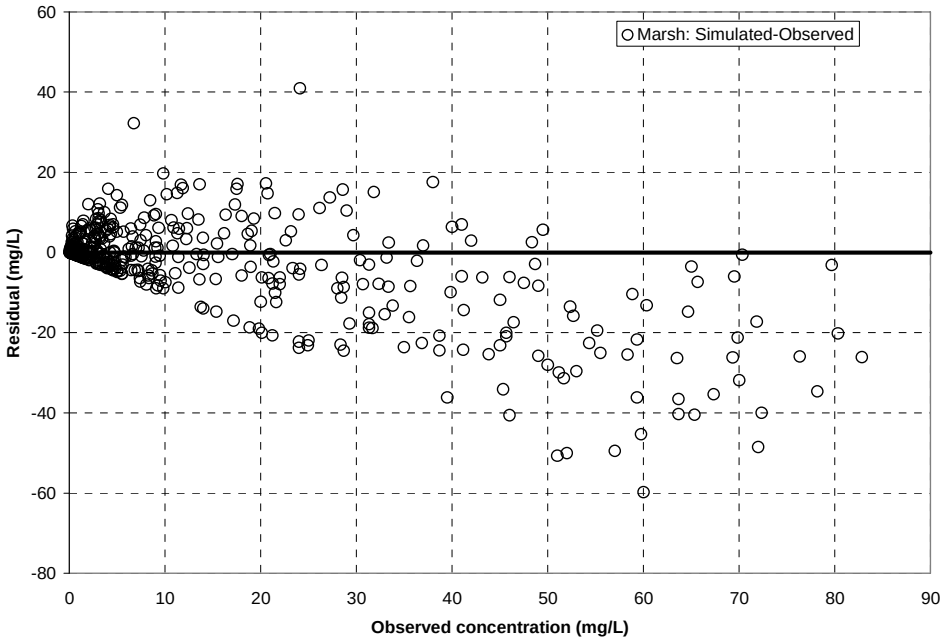

Figure 82 – Residual sulfate concentration in the marsh.

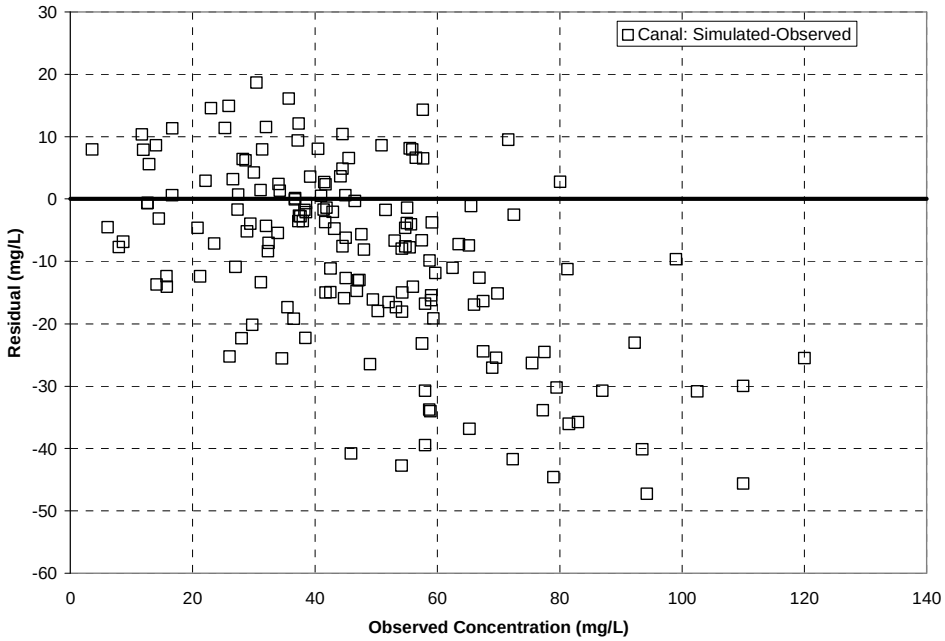

Figure 83 – Residual sulfate concentration in the canal.

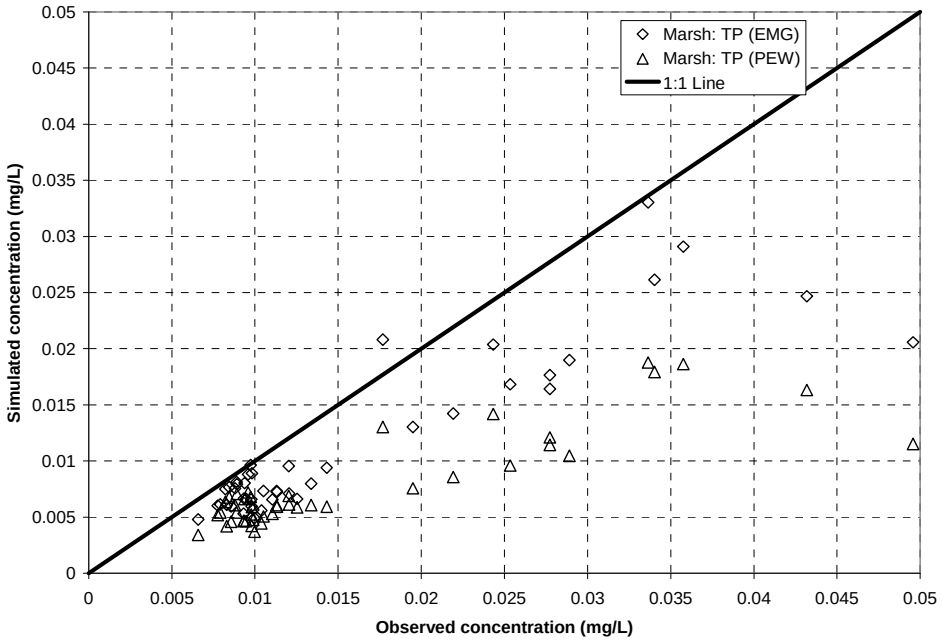

Figure 84 – Yearly average total phosphorus marsh comparison.

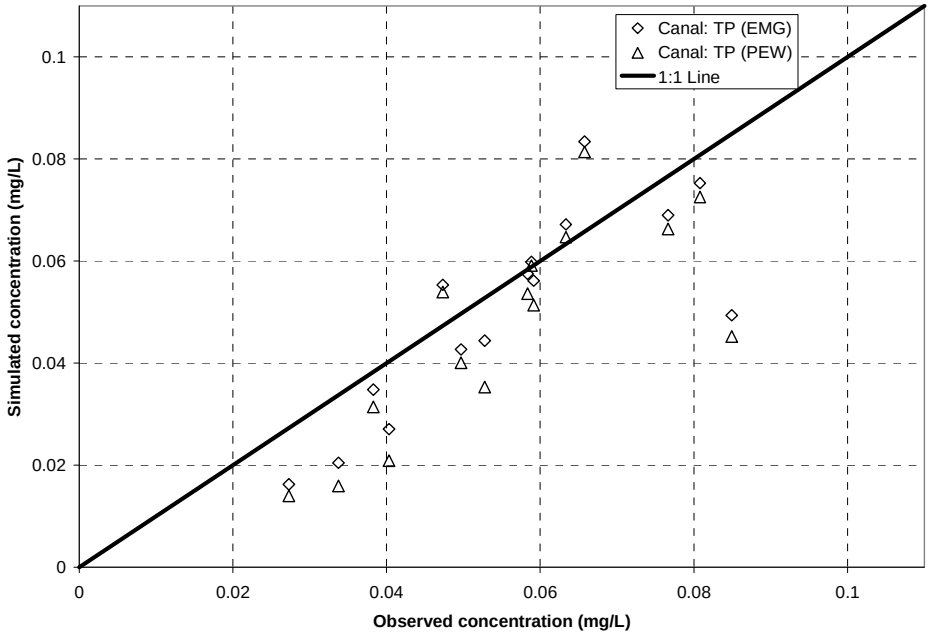

Figure 85 – Yearly average total phosphorus canal comparison.

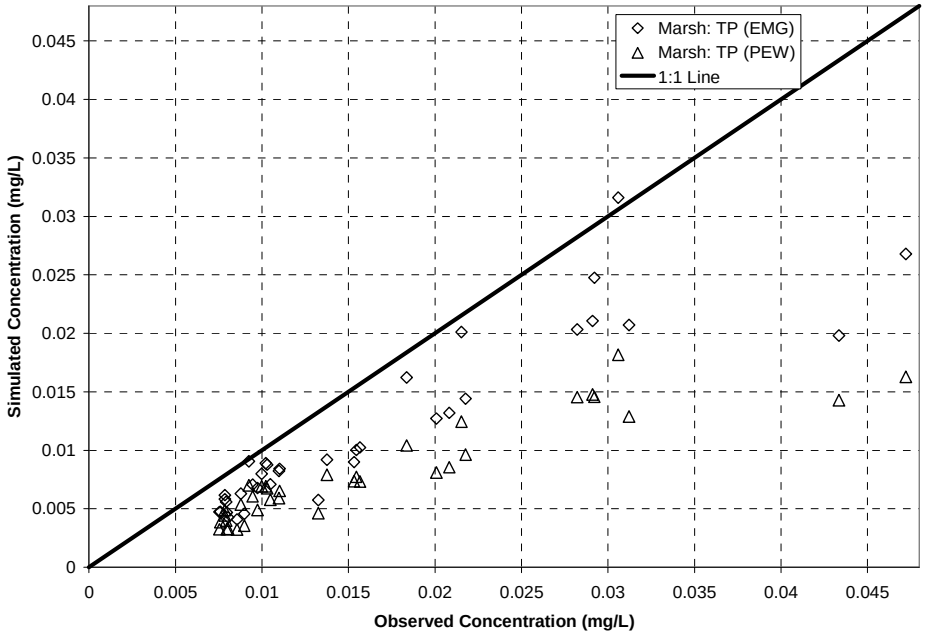

Figure 86 – Monthly average total phosphorus marsh comparison.

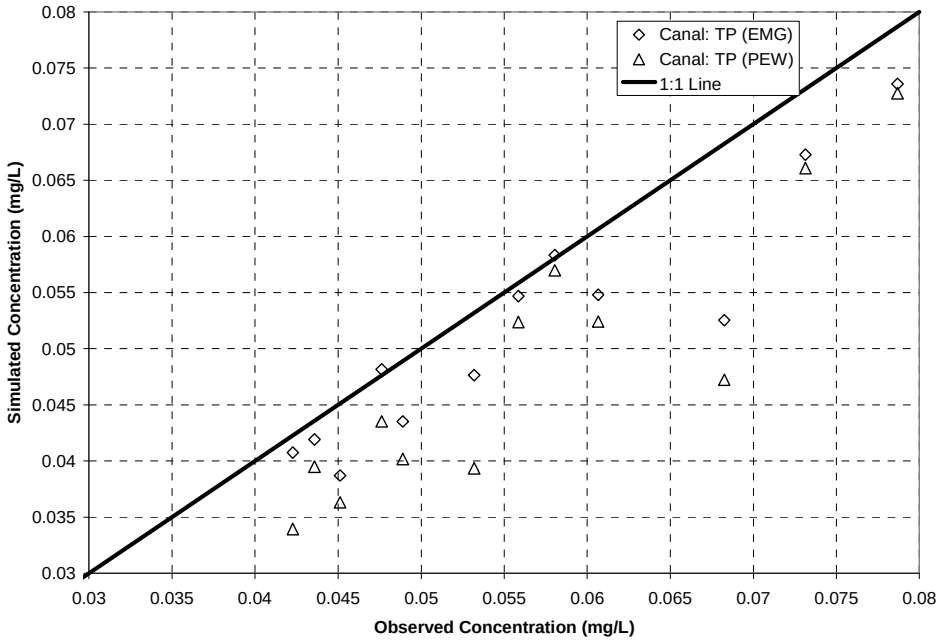

Figure 87 – Monthly average total phosphorus canal comparison.

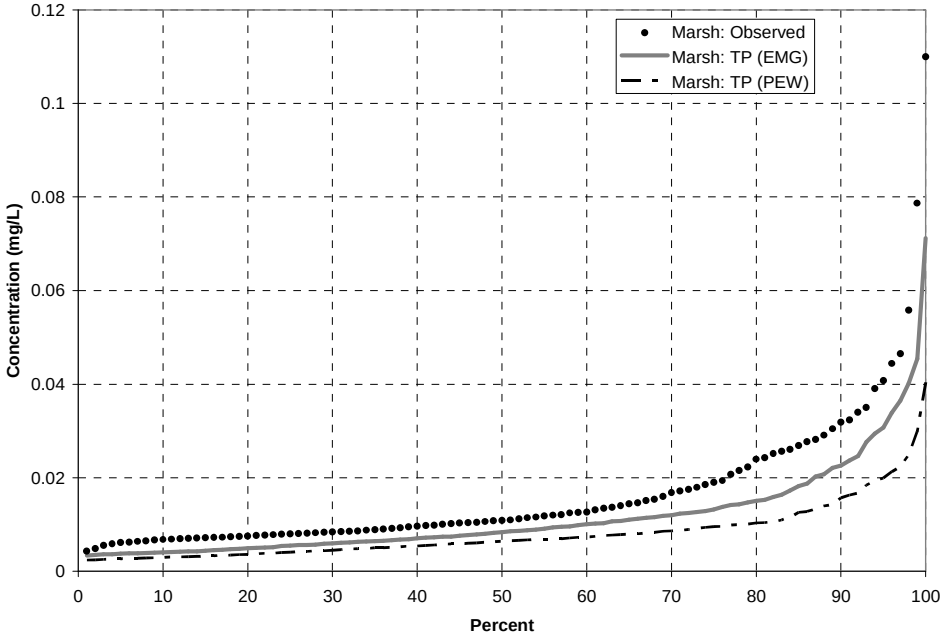

Figure 88 – Percent distribution of total phosphorus in the marsh.

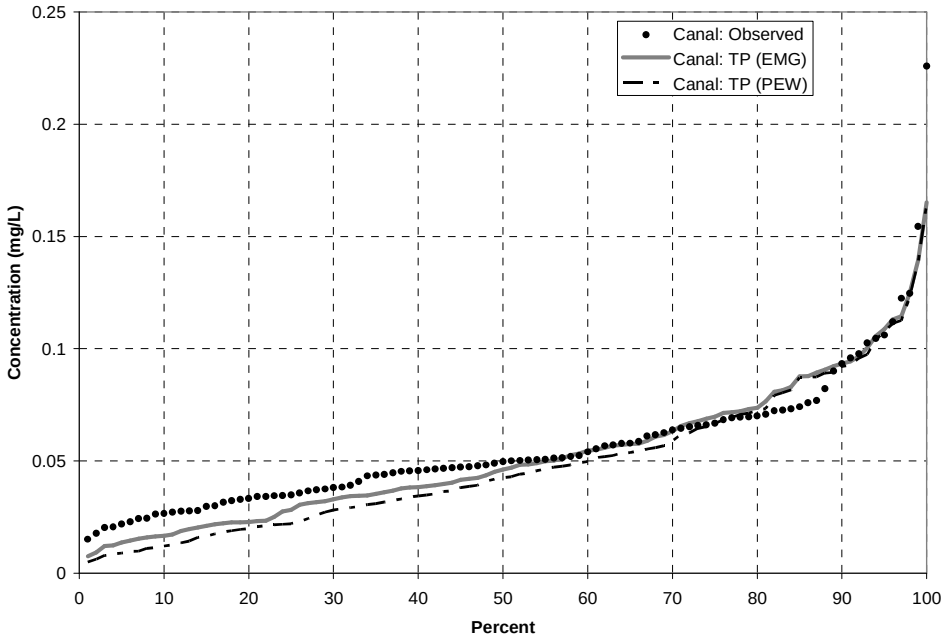

Figure 89 – Percent distribution of total phosphorus in the canal.

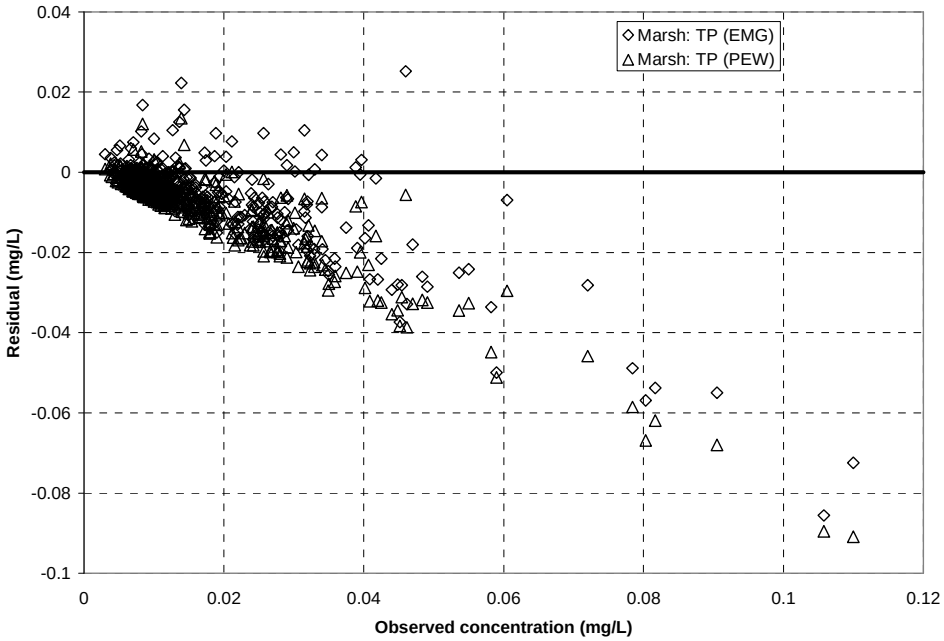

Figure 90 – Residual total phosphorus concentration in the marsh.

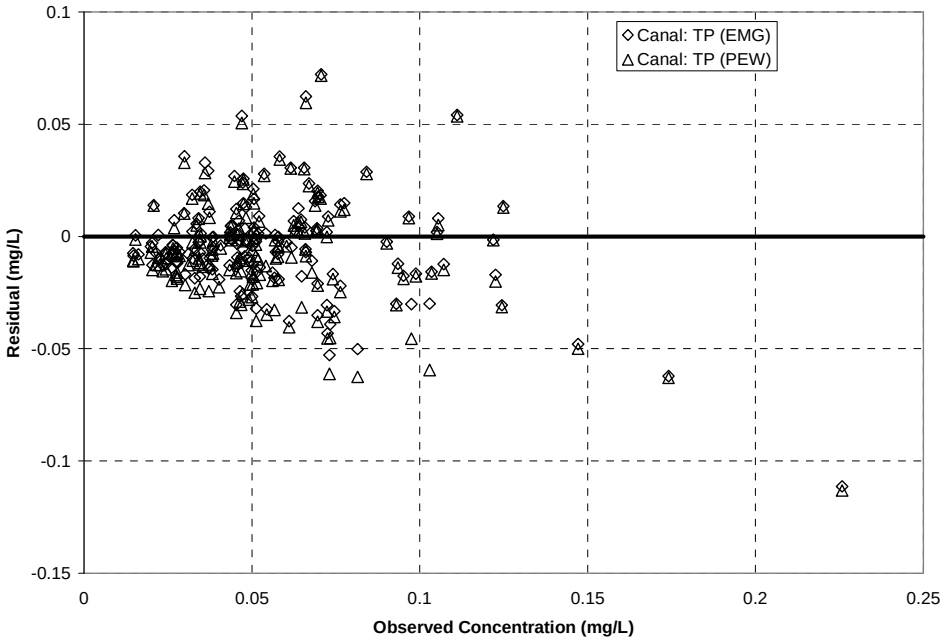

Figure 91 – Residual total phosphorus concentration in the canal.

Structure			Operational Dates for Data Period			Total Inflow (hm3)	Total outflow (hm3)
Name	Type	Flow	Start	End	Total Days		
S-39	Spillway	Outflow	1/1/1995	6/30/2009	5295	0.00	1799.88
G-94A	Culvert	Outflow	1/1/1995	6/30/2009	5295	0.00	114.16
G-94B	Culvert	Outflow	1/1/1995	6/30/2009	5295	0.00	37.44
G-94C	Culvert	Bidirectional	1/1/1995	6/30/2009	5295	3.55	245.60
ACME2	Pump Station	Inflow	1/1/1995	12/31/2007	4748	213.80	0.00
ACME1	Pump Station	Inflow	1/1/1995	12/31/2007	4748	231.18	0.00
S-362	Pump Station	Inflow	9/21/2004	6/30/2009	1744	571.87	0.00
G-300	Spillway	Bidirectional	8/26/1999	6/30/2009	3597	187.61	203.61
S-5AS	Spillway	Bidirectional	1/1/1995	6/7/1999	1619	30.78	477.69
S-5A	Pump Station	Inflow	1/1/1995	8/26/1999	1699	1628.55	0.00
G-301	Spillway	Bidirectional	8/26/1999	6/30/2009	3597	198.00	293.96
G-310	Pump Station	Inflow	7/7/2000	6/30/2009	3281	2397.43	0.00
G-251	Pump Station	Inflow	1/1/1995	6/30/2009	5295	1164.82	0.00
S-6	Pump Station	Inflow	1/1/1995	5/15/2001	2327	2284.71	0.00
G-338	Culvert	Outflow	1/1/1995	5/15/2001	2327	0.13	2.65
S-10E	Culvert	Outflow	1/1/1995	6/30/2005	3834	0.00	298.87
S-10D	Spillway	Outflow	1/1/1995	6/30/2009	5295	0.00	1956.42
S-10C	Spillway	Outflow	1/1/1995	6/30/2009	5295	0.00	1566.02
S-10A	Spillway	Outflow	1/1/1995	6/30/2009	5295	0.00	1531.77

Table 1 – Hydraulic structures operation schedule and total flow values (hm^3).

Measurement Site		Grab			ACF
Flow	Concentration	TP (µg/L)	CL (mg/L)	SO4 (mg/L)	TP (µg/L)
ACME 1	ACME1DS	70.3	89.3	25.9	
G-251	ENR012	38.6	148.2	54.3	43.5
G-300	G300	124.1	99.7	26.1	
G-301	G301	130.9	106.1	**67.1**	
G-310	G310	52.6	145.3	61.8	65.3
G-94B	G94B	76.8	74.5	27.5	
G-94D	G94D	100.4	62.5	25.0	
S-10A	S10A	35.0	82.6	32.6	
S-10C	S10C	45.3	100.4	42.5	
S-10D	S10D	61.1	112.9	50.7	
S-10E	S10E	67.7	128.1	52.7	
S-362	S362	47.7	148.2	40.2	50.0
S-39	S39	32.2	86.6	32.6	83.0
S-5A	S5A	128.4	129.3	**67.1**	146.3
S-5AS	S5AS	108.1	104.2	53.8	
S-6	S6	69.4	140.0	63.4	85.5

Table 2 – Canal structure concentration sites with average concentration values for the data period.

Year	Chloride			
	In	Out	Difference	% Retained or lost
1995	152,253	136,864	15,389	10%
1996	110,060	87,358	22,702	21%
1997	119,740	70,855	48,885	41%
1998	111,173	80,549	30,624	28%
1999	114,721	94,466	20,255	18%
2000	77,873	42,634	35,239	45%
2001	46,948	33,098	13,851	30%
2002	85,867	60,484	25,383	30%
2003	73,737	56,778	16,959	23%
2004	75,750	45,957	29,793	39%
2005	49,434	23,380	26,054	53%
2006	40,664	27,185	13,480	33%
2007	23,614	11,014	12,600	53%
2008	54,900	37,076	17,824	32%
2009	14,288	19,616	-5,328	37%

Table 3 – Chloride loading in metric tons for the Refuge during the data period.

Year	Total Phosphorus			
	In	Out	Difference	% Retained or lost
1995	125.2	94.8	30.3	24%
1996	78.5	45.5	32.9	42%
1997	109.5	37.7	71.8	66%
1998	103.9	49.8	54.1	52%
1999	104.8	76.9	28.0	27%
2000	64.0	21.8	42.2	66%
2001	18.6	14.9	3.7	20%
2002	32.2	19.9	12.3	38%
2003	34.3	20.0	14.2	42%
2004	75.4	50.2	25.2	33%
2005	43.6	22.2	21.3	49%
2006	38.3	16.1	22.2	58%
2007	8.7	5.0	3.7	43%
2008	14.4	23.7	-9.3	65%
2009	8.6	5.8	2.7	32%

Table 4 – Total phosphorus loading in metric tons for the Refuge during the data period.

Year	Sulfate			
	In	Out	Difference	% Retained or lost
1995	52,798	84,183	-31,386	59%
1996	42,539	31,607	10,932	26%
1997	46,777	32,001	14,776	32%
1998	47,670	34,987	12,683	27%
1999	53,257	50,407	2,850	5%
2000	29,034	15,790	13,244	46%
2001	22,154	14,320	7,834	35%
2002	43,661	26,078	17,583	40%
2003	39,687	25,793	13,893	35%
2004	38,296	19,393	18,904	49%
2005	20,044	12,081	7,963	40%
2006	18,667	11,846	6,821	37%
2007	9,433	4,251	5,183	55%
2008	23,686	15,504	8,182	35%
2009	7,364	9,184	-1,820	25%

Table 5 – Sulfate loading in metric tons for the Refuge during the data period.

Station	Year						Total	Available	Missing		
	1995	1996	1997	1998	1999	2000-2009			Number	Percent	Consecutive
S-39							5295	5096	199	4%	32
S-5A							5295	5295	0	0%	0
S-6							5295	5295	0	0%	0
STA1W							5295	5294	1	0%	1
WCA1ME							4888	4215	673	14%	359
LOXWS							4931	4703	228	5%	85
Gage 6							4564	4318	246	5%	6
Gage 8							4564	4321	243	5%	6
Gage 10							3378	3136	242	7%	6

Table 6 – Schedule of available precipitation data for the data period.

Gage	Year							Total	Available	Missing		
	1995	1996	1997	1998	1999	2000	2001-2009			Number	Percent	Consecutive
1-7								5295	5295	0	0.0%	0
1-8C								5295	5207	88	1.7%	88
1-8T								5295	5278	17	0.3%	6
1-9								5295	5295	0	0.0%	0
North								2927	2854	73	2.5%	36
South								2973	2902	71	2.4%	11

Table 7 – Schedule of available data for all water level stations in the Refuge.

Monitoring Type	Year												Dates	
	1995	1996	1997	1998	1999	2000	2001	2002	2003	2004-2007	2008	2009	First	Last
ENHANCED													6/8/2004	6/11/2009
EVPA													1/11/1995	6/2/2009
Structure													1/5/1995	6/17/2009
XYZ													4/26/1996	9/11/2007

Table 8 – Schedule of available data for all water quality data in the Refuge.

Constituent	Station	Maximum	Minimum	Average
Chloride (mg/L)	ENHANCED	184	8.3	52.5
	EVPA	170	0.2	30.9
	Structure	197.4	13.21	97.9
	XYZ	240	8.9	86
Total Phosphorus (mg/L)	ENHANCED	0.653	0.002	0.025
	EVPA	0.08	0.001	0.009
	Structure	0.515	0.006	0.052
	XYZ	0.29	0.004	0.025
Sulfate (mg/L)	ENHANCED	107	0.02	12.7
	EVPA	110	0.05	3.9
	Structure	99.2	1.42	39.4
	XYZ	120	0.2	28.1

Table 9 – Summary of chloride, total phosphorus, and sulfate data for the data period.

Station	TP	CL	SO4
X0	0.058	125.9	54.6
X1	0.039	119.8	48.9
X2	0.016	91.5	29.1
X3	0.012	71.5	18.5
X4	0.014	45.8	4.7
Y4	0.011	48.5	6.9
Z0	0.059	125.7	54.1
Z1	0.039	120.3	47.2
Z2	0.016	97.1	29.4
Z3	0.011	61.3	11.9
Z4	0.010	41.3	4.2

Table 10 – Summary of the average concentrations for total phosphorus, chloride, and sulfate at each of the XYZ stations.

Compartment	Area (km^2)	Flow Weight
1	89.36	1.00
2	224.1	0.84
3	246.6	0.44
Marsh Total	560.06	

Table 11 – Water quality model marsh compartment areas and flow weighting coefficients.

Value	Chloride	TP (EMG)	TP (PEW)	SO4
Wet Deposition (mg/L)	2	0.01	0.01	1
Dry Deposition (mg/m2-yr)	1136	10	10	138.2
Initial Concentration_1 (mg/L)	71.5	0.0065	0.0065	19.55
Initial Concentration_2 (mg/L)	30	0.01438	0.01438	6.18
Initial Concentration_3 (mg/L)	12.19	0.01329	0.01329	1.21
Initial Concentration_4 (mg/L)	89.55	0.05	0.05	35.68
Initial Storage_1 (g/m2)		0.5	0.5	
Initial Storage_2,3 (g/m2)		0.1	0.1	
k_{half} (g/m3)				1
R_{max} (mg/m2-yr)				14.4
k_1 (m3/mg-yr)		0.1064	0.221	
k_2 (m2/mg-yr)		0.002	0.0042	
k_3 (1/yr)		0.3192	0.6631	

Table 12 – Initial values and constants used in SRSM water quality equations.

Statistics	Canal	Marsh
Bias (m)	-0.026	-0.030
Average Observed (m)	4.959	5.003
Average Modeled (m)	4.936	4.973
RMSE (m)	0.121	0.089
SD Observed (m)	0.252	0.146
SD Model (m)	0.256	0.191
SD Error (m)	0.118	0.084
n, sample #	5207	5295
Variance Reduction	78%	67%
R (Correlation Coefficient)	0.892	0.911
R^2 (Coefficient of Determination)	0.796	0.830
Nash-Sutcliffe Efficiency	0.770	0.627

Table 13 – Statistics for canal and marsh stage performance.

Volume (hm^3)	Simulation Total	Yearly Average
In (total)	19826.2	1367.3
Out (total)	19993.1	1378.8
Difference (IN-OUT)	-166.9	-11.5
Structure (in)	8985.16	619.7
Structure (out)	8448.83	582.7
Precipitation	10841.1	747.7
Evapotranspiration	9171.52	632.5
Seepage	2372.79	163.6

Table 14 – Cumulative water volumes for the simulation period and yearly simulation average values.

Budget (hm^3)	Water Volume
Initial (canal)	8.07
Initial (marsh)	339.26
Initial (combined)	347.33
Final (canal)	6.81
Final (marsh)	173.64
Final (combined)	180.44
Closing Value	-0.041
% of Cumulative	0.0002%

Table 15 – Budget values for the model simulation period.

Statistics: Chloride	Canal	Marsh
Bias (mg/L)	-4.33	-13.02
Average Observed (mg/L)	103.67	56.97
Average Modeled (mg/L)	99.34	43.95
RMSE (mg/L)	23.17	28.53
SD Observed (mg/L)	27.55	40.22
SD Model (mg/L)	32.43	32.90
SD Error (mg/L)	22.76	25.38
n, sample #	174	484
Variance Reduction	32%	60%
R (Correlation Coefficient)	0.723	0.777
R^2 (Coefficient of Determination)	0.523	0.604
Nash-Sutcliffe Efficiency	0.293	0.497

Table 16 – Statistics for chloride performance.

Jan95-Jun09 Sulfate		Marsh	Canal
Simulated	Maximum	84.10	106.63
	Minimum	0.0095	0.0139
	Average	10.88	37.50
	Number	15885	5295
	Days at minimum	3	1
	# Below average	10529	2746
	Percent below average	66%	52%
Observed	Maximum	110	120
	Minimum	0.0165	1.42
	Average	9.87	42.66
	Number	4125	903
	Days at minimum	3	1
	# Below average	3100	472
	Percent below average	75%	52%

Table 17 – Sulfate data variation for the period of simulation.

Statistics: Sulfate	Canal	Marsh
Bias (mg/L)	-9.11	-2.95
Average Observed (mg/L)	47.28	14.13
Average Modeled (mg/L)	38.17	11.18
RMSE (mg/L)	17.16	12.05
SD Observed (mg/L)	22.15	19.29
SD Model (mg/L)	18.31	14.63
SD Error (mg/L)	14.53	11.68
n, sample #	161	484
Variance Reduction	57%	63%
R (Correlation Coefficient)	0.758	0.797
R^2 (Coefficient of Determination)	0.575	0.635
Nash-Sutcliffe Efficiency	0.400	0.610

Table 18 - Statistics for sulfate performance.

Statistics: TP	*Emergent Marsh (EMG)*		*Pre-existent Wetland (PEW)*	
	Canal	Marsh	Canal	Marsh
Bias (mg/L)	-0.004	-0.006	-0.007	-0.009
Average Observed (mg/L)	0.055	0.016	0.055	0.016
Average Modeled (mg/L)	0.052	0.011	0.048	0.007
RMSE (mg/L)	0.022	0.013	0.024	0.016
SD Observed (mg/L)	0.029	0.016	0.029	0.016
SD Model (mg/L)	0.031	0.008	0.032	0.005
SD Error (mg/L)	0.021	0.011	0.023	0.013
n, sample #	174	489	174	489
Variance Reduction	46%	45%	40%	31%
R (Correlation Coefficient)	0.744	0.690	0.726	0.627
R2 (Coefficient of Determination)	0.553	0.476	0.527	0.393
Nash-Sutcliffe Efficiency	0.449	0.318	0.345	-0.021

Table 19 – Statistics for total phosphorus performance.

Cumulative Values (MT)	CL	TP (EMG)	TP (PEW)	SO4
In (total)	1181660	1049.79	1049.79	506469
Out (total)	1189970	1091.91	1121.46	508193
Difference (IN-OUT)	-8313.22	-42.1192	-71.67	-1724.51
Seepage	172217	77.7682	71.5107	59772.5
Burial		414.406	478.31	
Reactive				65313.4
Evapotranspiration	133079	36.0362	26.2637	26623.4
Aerial (wet+dry)	30969.5	190.166	190.166	11970.9
Precipitation	21682.1	108.411	108.411	10841.1
Structure (in)	1150690	859.623	859.623	494498
Structure (out)	884673	563.698	545.374	356484

Table 20 – Accumulation of constituent mass for the simulation data period.

Yearly Average Accumulation (MT)	CL	TP (EMG)	TP (PEW)	SO4
In (total)	81493.79	72.40	72.40	34928.90
Out (total)	82066.90	75.30	77.34	35047.79
Difference (IN-OUT)	-573.33	-2.90	-4.94	-118.93
Seepage	11877.03	5.36	4.93	4122.24
Burial		28.58	32.99	
Reactive				4504.37
Evapotranspiration	9177.86	2.49	1.81	1836.10
Aerial (wet+dry)	2135.83	13.11	13.11	825.58
Precipitation	1495.32	7.48	7.48	747.66
Structure (in)	79357.93	59.28	59.28	34103.31
Structure (out)	61011.93	38.88	37.61	24585.10

Table 21 – Yearly average accumulation of constituent mass for the simulation period.

Budget (MT)	CL	TP (EMG)	TP (PEW)	SO4
Initial (marsh)	9764.08	96.03	96.03	2078.03
Initial (canal)	722.40	0.12	0.12	287.83
Initial (combined)	10486.50	96.16	96.16	2365.86
Final (marsh)	1600.88	54.02	24.47	366.60
Final (canal)	576.90	0.30	0.30	277.30
Final (combined)	2177.78	54.32	24.77	643.90
Closing Value	-4.52	-0.29	-0.29	-2.54
% of Cumulative	0.0004%	0.0274%	0.0275%	0.0005%

Table 22 – Constituent budget initial, final, and closing mass values.

Difference		Compartment			
		1	2	3	4
CL	Maximum (mg/L)	7.31	1.52	0.54	16.61
	Minimum (mg/L)	-6.27	-5.14	-4.98	-19.34
	Average (mg/L)	-0.42	-0.61	-0.56	0.19
	Standard Deviation (mg/L)	1.34	0.74	0.86	1.76
SO4	Maximum (mg/L)	4.79	0.31	0.02	7.75
	Minimum (mg/L)	-3.93	-3.30	-2.54	-3.65
	Average (mg/L)	-0.17	-0.23	-0.13	0.04
	Standard Deviation (mg/L)	0.66	0.39	0.41	0.66
TP	Maximum (µg/L)	5.12	0.86	0.29	36.65
	Minimum (µg/L)	-9.24	-0.92	-0.14	-21.93
	Average (µg/L)	-0.06	0.01	0.03	0.55
	Standard Deviation (µg/L)	0.51	0.10	0.05	1.88
Storage	Maximum (mg/m^2)	1.90	0.02	0.00	
	Minimum (mg/m^2)	-14.22	-1.73	-0.32	
	Average (mg/m^2)	-4.09	-0.69	-0.15	
	Standard Deviation (mg/m^2)	4.58	0.60	0.12	

Table 23 – Difference calculated for chloride, sulfate, and total phosphorus water column concentration and total phosphorus storage in each model compartment.

Collection Type	Station	Date	Total	Constituent
Grab	ENR012	6/1/1999	2	TP
Grab	ENR012	7/6/1999	2	TP
Grab	ENR012	9/7/1999	2	TP
Grab	ENR012	9/16/1999	2	TP
Grab	ENR012	1/18/2000	2	TP
Grab	S5AS	5/28/1998	2	TP
Grab	S6	3/14/2000	2	TP
Grab	S6	3/27/2000	2	TP
Grab	S6	4/11/2000	2	TP
Grab	ENR012	11/2/1999	3	TP
Grab	S5A	3/19/2009	3	TP
Grab	S5A	6/11/2009	3	TP
Grab	G310	6/1/2000	4	TP
Grab	G310	6/8/2000	5	TP
Grab	S5AS	5/28/1998	2	CL
Grab	S5A	3/19/2009	3	CL
Grab	S5A	6/11/2009	3	CL
Grab	S5A	3/19/2009	3	SO4
Grab	S5A	6/11/2009	3	SO4

Table 24 – Canal stations with multiple readings on the same day.

Collection Type	Station	Date	Constituent	Value (mg/L)	Conductivity (µS)	Predicted (mg/L)	Multiplier
Grab	S6	7/8/1997	CL	755.96	1247	161	0.129
Grab	S6	10/11/1999	CL	-0.1	1333	172	0.129
Grab	ENR012	7/12/1999	CL	830.67	940	137	0.146
Grab	S6	7/8/1997	SO4	460.685	*Eliminated based on the above CL observations.*		
Grab	S6	10/11/1999	SO4	-0.1			
Grab	ENR012	7/12/1999	SO4	231.22			

Table 25 – Boundary data days with extreme values.

Roth, William B. Bachelor of Science, University of Louisiana at Lafayette, Fall 2007;
Master of Science, University of Louisiana at Lafayette, Fall 2009
Major: Engineering, Civil Engineering option
Title of Thesis: The Development of a Screening Model for the Arthur R. Marshall Loxahatchee National Wildlife Refuge
Thesis Director: Dr. Ehab Meselhe
Pages in Thesis: 189; Words in Abstract: 198

ABSTRACT

Arthur R. Marshall Loxahatchee National Wildlife Refuge (Refuge) exists as the only soft-water remnant (58,275 ha) of the Northern Everglades. Alterations in the water quality, quantity, and timing have resulted in myriad impacts to the Refuge. Therefore, it is paramount to develop an effective means to study the impact of the hydrodynamic and water quality changes.

The Simple Refuge Screening Model (SRSM) version 4 is implemented using the ordinary differential equations solver Berkeley Madonna (www.berkeleymadonna.com). The compartment size and arrangement are identical to an earlier version of this model, whereas the constituent modeling approach has become more refined. Concentrations are calculated for chloride as a conservative tracer, sulfate using a Monod relationship, and total phosphorus dynamics as described by Walker and Kadlec (2008) in the Dynamic Model for Everglades Stormwater Treatment Areas (DMSTA).

Stage and constituent concentrations modeled by the SRSM are in good agreement with the observed data for the marsh and canal areas of the Refuge. However, such a generalized scheme only allows for average assessments of these areas as a whole. Therefore, the

SRSM has been developed as a component in a suite of models used for various applications concerned with Refuge restoration and management.

Biographical Sketch

William Benjamin Roth was born on March 19, 1984, in Metairie, Louisiana to Randall C. and Barbara S. Roth. After graduating from Brother Martin High School in New Orleans, Louisiana, he attended the University of Louisiana at Lafayette. There, William earned a Bachelor of Science degree in Civil Engineering. He began undergraduate research work for Dr. Ehab Meselhe in the summer of 2007 and continued this effort through the fall of 2009. William entered the Graduate School in January 2008 and is expected to graduate with a Master of Science degree in Engineering, Civil Engineering option, in December 2009. He is married to Stephanie Perrin of Henry, Louisiana and resides in Lafayette, Louisiana.